NTNU

Norwegian University of
Science and Technology

Reliability-based Derating Approach for Interconnectors

Kjetil Koldingsnes

Master of Energy and Environmental Engineering
Submission date: June 2017
Supervisor: Vijay Vadlamudi, IEL

Norwegian University of Science and Technology
Department of Electric Power Engineering

Abstract

This Masters project work has its genesis in the preliminary findings of a research collaboration in 2016 between the Department of Electric Power Engineering, NTNU, and Statnett (the Norwegian Transmission System Operator). As its overarching goal, the research proposition centred on developing a foundation for a suitable theoretical framework for one issue related to cross-border capacity auctions: interconnector adequacy. The motivation itself for such an undertaking stemmed from the divergent recommended approaches for estimating the capacity that the prospective Norway-GB interconnector (North-Sea Link) is allowed to bid into the GB Capacity Market.

Capacity made available through an interconnector for an area with a capacity mechanism in place, should be eligible to participate in the auctions to prevent market distortion and to ensure that correct investment signals are sent. There is also a need for a transparent and robust method to calculate the proportion of the rated interconnector capacity allowed to participate in market auctions. Such a methodology should consider and remunerate the interconnector's contribution to improved system adequacy in the importing area. In the NTNU-Statnett project, a unique reliability metric – Interconnector Effective Load Carrying Capability (IELCC) was conceptualized for the purpose of probabilistic interconnector de-rating; preliminary results were demonstrated on a very simple interconnected test system with a simple load profile. IELCC was founded on Loss-of-Load Expectation (LOLE) quantification in the interconnected system, addressing the need for a reliability-based de-rating procedure, as opposed to other existing approaches that focused on empirical considerations such as price differentials.

This thesis examines the NTNU-Statnett project claim that obtaining the de-rated interconnector capacity using a probabilistic reliability framework is a well-argued approach. To corroborate the effectiveness of the IELCC metric, larger interconnected test systems (Roy Billinton Test Systems and IEEE Reliability Test Systems) with detailed load profiles have been deployed, and relevant sensitivity analyses have been conducted. Further, a new variant of IELCC, founded on Expected Energy Not Served (EENS) quantification in the interconnected system is posited, the results demonstrated on the aforementioned test systems and the implications investigated.

In a report by The Joint Research Centre of the European Commission from 2016, appropriate generation- and system adequacy standards for the internal electricity market in Europe were identified. One of the recommendations of the study was to "*. . . establish EENS as a preferred metric as it alone proves appropriate for the calculation of socially optimal levels of reserve*". In light of this, the proposed EENS-based IELCC in this thesis is deemed to have significant application potential in cross-border capacity markets.

Sammendrag

Denne masteravhandlingen har sin opprinnelse i resultatene fra et forskingssamarbeid i 2016 mellom Institutt for elkraftteknikk ved NTNU, og Statnett. Arbeidet hadde som sitt overordnede mål å bygge et solid teoretisk grunnlag for å besvare et sentralt spørsmål innen kapasitetsmarkedsauksjoner: Hvor mye av sin maksimale overføringskapasitet skal forbindelser mellom ulike kraftmarkeder bli tillatt å by inn i en kapasitetsauksjon? Motivasjonen bak dette arbeidet kom som et resultat av at de hittil foreslåtte metodene for å fastsette denne kapasiteten for den planlagte forbindelsen mellom Norge og England (North-Sea Link) i svært liten grad baserer seg på pålitelighetskonsepter.

Kapasitet som gjøres tilgjengelig for et område med et kapasitetsmarked, gjennom en forbindelse, bør være berettiget til å delta i auksjonene for å sikre at korrekte investeringssignaler blir sendt. I tillegg vil kapasiteten som blir gjort tilgjengelig gjennom slike forbindelser styrke leveringspåliteligheten til det importerende kraftsystemet. Det er derfor et behov for en transparent metodikk for kapasitetsreduksjon, for å avgjøre hvor mye forbindelsene kan delta med i et kapasitetsmarked. En slik metodikk bør godtgjøre forbindelsen basert på dens bidrag til økt leveringspåliteligheten i det importerende kraftsystemet. Forskningssamarbeidet mellom NTNU og Statnett resulterte i en ny Capacity Credit, kalt Interconnector Effective Load Carrying Capability (IELCC), som kan brukes til dette formålet. Denne kvantifiserer den delen av kapasiteten til en forbindelse som kan regnes som pålitelig, og er basert på anvendelse av velkjente probabilistiske konsepter som Loss-of-Load Expectation (LOLE). Denne metodikken skiller seg derfor ut fra en del andre foreslåtte metoder, som baserer seg på empiriske betraktninger rundt for eksempel prisdifferensialer.

Denne avhandlingen undersøker påstanden fra NTNU/Statnett-prosjektet om at det er velbegrunnet å basere en metodikk for kapasitetsreduksjon på probabilistisk pålitelighetsteori. For å undersøke dette, har metodikken blir anvendt på større testsystemer (Roy Billinton Test Systems og IEEE Reliability Test Systems) med detaljerte lastprofiler, og relevante sensitivitetsanalyser har blitt utført. I tillegg legger denne avhandlingen frem et forslag til en ny variant av IELCC basert på Expected Energy Not Served (EENS) i stedet for LOLE. Denne varianten blir også undersøkt og demonstrert for testsystemene nevnt ovenfor.

I en rapport fra EU-kommisjonen sitt felles forskningssenter (Joint Research Centre) fra 2016 ble det undersøkt hvilke pålitelighetsstandarder som er egnet for Det indre elektrisitetsmarkedet i Europa. En av anbefalingene fra denne rapporten var å "*... establish EENS as a preferred metric as it alone proves appropriate for the calculation of socially optimal levels of reserve*". På bakgrunn av dette vurderes den EENS-baserte IELCC-metodikken som blir foreslått i denne avhandlingen til å ha et betydelig anvendelsespotensial i kapasitetsmarkeder der forbindelser fra andre kraftmarkeder deltar.

Preface

This Master's Thesis concludes my Master of Science (MSc) degree in Energy and Environmental Engineering with the Department of Electric Power Engineering at the Norwegian University of Science and Technology (NTNU). The thesis treats concepts related to Power System Reliability (PSR), and is written under the supervision of associate Professor Vijay Venu Vadlamudi with the Department of Electric Power Engineering NTNU.

Without having conducted any pre-work in the form of a specialization project, and with limited knowledge on PSR, the thesis work proved to be challenging. However, over the course of the five months that the work was conducted, I have built a solid foundation for potential future work within the areas of PSR in particular, and research in general. The knowledge that I have gained is in large parts owed to my supervisor, associate Professor Vijay Venu Vadlamudi. My sincerest gratitude goes out to him for always being available and willing to answer my questions, share his knowledge and embark on lengthy discussions on the theoretical concepts that constitute this thesis. I have benefited greatly from standing on his shoulders, and from his outstanding talent for providing pedagogical clarity. I would also like to extend my gratitude to my brother, Jostein Koldingsnes, for helping with the tedious work of proofreading.

Trondheim, June 2017

Kjetil Koldingsnes

Contents

Abbreviations

AC	Alternating Current
AIC	Aggregated Import Capacity
CAP	Capacity Adequate Portfolio
CC	Capacity Credits
CEAU	Constrained Equivalent Assisting Unit
CEER	Council of European Energy Regulators
CIGRE	The International Council on Large Electric Systems
CM	Capacity Mechanism
COPT	Capacity Outage Probability Table
CRM	Capacity Remuneration Mechanism
CYPL	Constant Yearly Peak Load
DBF	Diversity Benefit Factor
DECC	Department of Energy & Climate Change

DPL Daily Peak Load

DRF De-Rating Factor

DSR Demand Side Response

EAU Equivalent Assisting Unit

EC European Commission

ECC Equivalent Conventional Capacity

EDNS Expected Demand Not Served

EEAG Environmental and Energy State Aid Guidelines

EENS Expected Energy Not Served

EEU Expected Energy Unserved

EFC Equivalent Firm Capacity

EFORd Equivalent Demand Forced Outage Rate

EIC Effective Interconnector Capacity

ELCC Effective Load Carrying Capability

EMDF External Market De-rating Factor

ESS Electric Energy Storage

EU European Union

EUE Expected Unserved Energy

FOR Forced Outage Rate

HL Hierarchical level

HPL	Hourly Peak Load
HVDC	High Voltage Direct Current
I-SEM	Integrated Single Electricity Market
IEEE-RTS	IEEE-Reliability Test System
IELCC	Interconnector Effective Load Carrying Capability
LDC	Load Duration Curve
LOEE	Loss-of-Energy Expectation
LOEP	Loss-of-Energy Probability
LOLE	Loss-of-Load Expectation
LOLP	Loss-of-Load Probability
MCS	Monte Carlo Simulation
NG	National Grid
NTNU	Norwegian University of Science and Technology
PA	Probability Array
PJM	Pennsylvania—New Jersey—Maryland
PSR	Power System Reliability
PTE	Panel of Technical Experts
PV	Photovoltaic
RBTS	Roy Billinton Test System
SEM	Single Electricity Market

SoS	Security of Supply
System B	Assisting system
System A	Assisted system
TSO	Transmission System Operator
UCAP	Unforced Capacity
USE	Expected Unserved Energy (Normalized)

Nomenclature

x_j	Capacity on outage in outage state j
$P(X \geq x_j)$	Cumulative probability of capacity outage $\geq x_j$
$p(X)$	Individual probability of event X
C	Total installed capacity
j	Running index of outage-/assistance states
p_{up}	Probability of generator being available
p_{down}	Probability of generator not being available
p_i	Probability of generator unit being in derated state i
$P^{old}(X)$	Cumulative probability of event X before adding a new generator to the COPT
g	Capacity of generator being added to COPT as a two-state model
$P^{new}(X)$	Updated cumulative probability of event X after adding a new generator to the COPT
i	Running index of derated states for a generator

g_i	Capacity of derated state i for a generator being added to COPT as a multi-state unit
t	Running index of time inrements in a load model
L_t	Load level in time increment t
ΔT	Duration of the time increments being considered
E	An intermediate to unserved energy
T	Total number of time increments
O	Superscript used to denote various properties of the *original* system in ELCC calculations
N	Superscript used to denote various properties of the *altered* system in ELCC calculations
c^A	Nameplate capacity of unit being added to the system in ELCC calculations
$L_t^{'}$	Scaled load level in time increment t
$L_{max}^{'}$	Maximum load level in scaled load/time-series
L_{max}	Maximum load level in original load/time-series
k	Running index of interconnector capacity states
IC_k	Capacity of interconnector in state k
p_k	Probability of interconnector being in capacity state k
R_t^B	Reserve in System B in time increment t
C^B	Installed capacity in System B

L_t^B	Load level in System B in time increment t
$LOLP_{t,k}^U$	LOLP in time increment t for System A when assisted by System B through an interconnector in state k
A, B, EAU, $CEAU$, U	Superscripts pointing to assisted system, assisting system, EAU, CEAU and Unified system, respectively. The superscripts are used by a variety of symbols
$COPT_{t,k}^{Sup.}$	COPT for the system/unit referred to by $^{Sup.}$ for time increment t and interconnector state k
$x_{t,j,k}^{Sup.}$	Outage capacity for the system/unit referred to by $^{Sup.}$ for time increment t, outage state j and interconnector state k
$a_{t,j,k}^{Sup.}$	Assistance capacity for the system/unit referred to by $^{Sup.}$ for time increment t, outage state j and interconnector state k
$LOLE^U$	LOLE for System A when assisted by System B
R^U	Reserve in System A when assisted by System B
$IELCC_{LOLE}$	IELCC with LOLE as guiding index
$IELCC_{EENS}$	IELCC with EENS as guiding index
$\|\epsilon\|$	Absolute value of the percentage difference between benchmark results and obtained results

List of Figures

List of Tables

Chapter 1

Introduction

1.1 Background

The European electricity sector is in a state of transition, with liberalization and decarbonization as the key drivers in the pursuit of a more sustainable and affordable electricity market. Electricity generation from renewable energy sources increased in the European Union's (EU) member countries from 8.4% in 2005 to 15% in 2014 [1]. Especially generation from wind and photovoltaic (PV) are showing large growth rates. In the same period, there has also been a reduction in wholesale electricity prices. These developments are in accordance with two of the main objectives defined by the EU as drivers for its energy policies [2]: *sustainable energy consumption* and *affordable prices* for homes, businesses and industry. *Security of Supply* (SoS), which is the last main objective, however, is suffering under this development. Conventional thermal generation technologies, such as gas and coal, have larger operational costs than PV and wind. This, combined with lower prices and a lowered demand, has led to a reduced profitability for these technologies. There is a growing concern that this development will reduce the incentives for maintaining or building new, conventional generation capacity to such an extent that the generation mix will not be able to meet demand at all times. Although this can be deemed a positive development from a decarbonization point-of-view, conventional generation still plays an important role as a provider of flexibility to

an energy system with larger shares of intermittent renewables. Capacity mechanisms are therefore being considered by several European countries to produce investment signals that will create capacity investments sufficient to maintain SoS in the future. An example is the Capacity Market introduced in GB for the provision of generation capacity from 2018. The remainder of the work in this thesis deals with a specific design question that arises when introducing capacity mechanisms. As such, the thesis will not look further into the motivation for introducing such mechanisms, but rather assume that they are in place.

The International Council on Large Electric Systems (CIGRE) defines a Capacity Mechanism (CM) as follows [3]: "*Capacity mechanisms are defined as an arrangement that is part of the market design, meant to provide revenues to capacity providers (generation and demand resources) in addition to the revenues from selling energy in the day-ahead, intraday and possibly other physical markets.*" Such mechanisms can be designed in a variety of ways. EU member states are subject to Environmental and Energy State Aid Guidelines (EEAG), which include guidelines on aid for generation adequacy [4]. These guidelines generally seek to avert negative effects on competition and trade, and state that the CM should be designed in such a way that it is possible for any capacity, including interconnectors[1], which can contribute to better generation adequacy, to participate. An important design question is therefore how participation in CMs from foreign capacity through interconnectors should be handled. Not considering the possibility of completely neglecting interconnectors, as this would result in an overcapacity[2], there are two main approaches:

1. *Implicit participation*, does not allow the interconnector to participate in the CM auction, but its expected capacity contribution is subtracted when deciding the total level of capacity to be procured in the CM. This approach was used in the first auction of the GB CM (2014 T-4), but it can potentially lead to suboptimal investment in foreign capacity and interconnectors, as it only remunerates domestic capacity, and is therefore not encouraged by the EEAG.

[1]The term *interconnector* will in this thesis refer to all means of interconnection between two different power systems or areas, i.e., the term encompasses both cables and overhead lines, whether they use AC (Alternating Current) or HVDC (High Voltage Direct Current).

[2]Overcapacity denotes a situation in a market where supply exceeds demand, meaning that the market fails to allocate resources efficiently.

2. The EEAG require *explicit cross-border participation*, which is also emphasized by the Council of European Energy Regulators (CEER) as the favourable approach [5]. Three different models are possible: (1) *pure interconnector model*, (2) *pure foreign capacity provider model* and (3) *revenue sharing model*. In (3), the foreign capacity providers participate in the CM, but revenue is shared between the interconnector operator and the foreign capacity operator. This is deemed the most likely to be successful by CEER in terms of providing the most correct investment signals, but it is also considered to be very complex to implement. The European Commission (EC) also seems to be leaning in favour of this model, judging by the *high level approach* for explicit cross-border participation suggested in Annex 2 of [6]. For models (1) and (2) respectively, the interconnector operator or foreign capacity operator participate in the CM and receives the remuneration. Especially model (1) is considered less complex to implement than (3), and it was the chosen approach in the second and third Four-Year Ahead Auctions (2015 T-4 & 2016 T-4) in the GB CM. A key issue with this model is to assure sufficient capacity for export. For certain circumstances, e.g., when the interconnector is the scarce resource, this can be the overall preferable model because it is less complex, and because it doesn't necessarily send wrong investment signals in such a situation.

Regardless of the model chosen, an essential element of a CM with explicit cross-border participation, is an interconnector capacity calculation methodology that maximizes the available capacity of the interconnector, while taking network constraints and the possibility of a simultaneous scarcity[3] situation into account. A proposed solution is to base the capacity evaluation of the interconnector on de-rating methodologies which seek to account for the risk of simultaneous scarcity by only allowing a reduced, or *de-rated*, value of the total technical capacity of the interconnector to enter the CM auction. A probabilistic calculation procedure for the de-rating of interconnector capacity will therefore be the focus for the remainder of this thesis.

[3] A *scarcity situation* will henceforth refer to a situation where available capacity in an area is not able to meet load demand, leading to the risk of shedding load to keep the system balanced. *Simultaneous scarcity* in this context, is therefore a situation where the area that sold the capacity in the CM is experiencing a scarcity situation at the same time as the area that bought it through the CM is in a state of scarcity.

1.2 Scope

As a continuation of research work done earlier, at the Department of Electrical Power Engineering, NTNU [7], this thesis will investigate the de-rating procedure for interconnectors developed in that work, and subsequently utilize it for more extensive testing as a means of critically examining the procedure. The focus will be on the de-rating procedure itself and the concepts it consists of. Consequently, market issues will not be treated beyond what is discussed in Section 1.1.

The probabilistic methodology developed is based on well-established concepts from the field of Reliability of Electric Power Systems such as Loss-of-Load Probability (LOLP), Loss-of-Load Expectation (LOLE), Expected Energy Not Served (EENS) and Effective Load Carrying Capability (ELCC). In its consideration of power system reliability, the thesis only conducts HL1-studies (i.e., generation adequacy). Several scripts were developed in MATLAB as an essential part of the project work. All testing of the methodology itself, testing of underlying concepts and sensitivity analysis were conducted with these scripts.

The focus of the thesis work is to examine the methodology and its underlying concepts in detail, and to present it in a transparent manner. Therefore, the thesis does not look into best practices for obtaining precise input data, nor does it present results from real-life power systems. The results presented are obtained from testing on the Roy Billinton Test System (RBTS), the IEEE-Reliability Test System (IEEE-RTS), from an illustrative two bus test system and from the interconnected versions of these three systems.

The issues addressed in this thesis are mostly motivated by the several procedures proposed to estimate the capacity that interconnectors are allowed to bid into the GB Capacity Market. However, the proposed methodology is relevant for all instances where a CM is in place and foreign capacity is allowed to participate through an interconnector. Hence, further discussions will not be based specifically on the GB CM and its interconnectors.

Contributions

1. The thesis examines the NTNU-Statnett project claim that obtaining the de-rated interconnector capacity using a probabilistic reliability framework is a well-argued approach.

2. Necessary models and tools have been created to establish a conceptual framework from which de-rated interconnector capacities can be computed for large scale systems. The LOLE based Interconnector Effective Load Carrying Capability (IELCC) metric has been supplemented with a newly conceived EENS based IELCC metric. These metrics are put forward as instruments for decision making in interconnector auctions in Capacity Markets.

    a) In the course of realizing the framework, this thesis also contributes to identifying the nuances of obtaining adequacy indices for interconnected systems, which otherwise are seemingly cryptic in their presentation in literature.

    b) Where deemed necessary, the narrative of the thesis has been strengthened with essential pedagogical treatment of procedural steps. Potential special cases that ought to be dealt with additional care within the generic framework of LOLE and EENS for interconnected systems have been highlighted.

3. Scripts have been developed in MATLAB to implement the proposed algorithms on large-scale interconnected systems. These scripts are released for further internal use and research at the Department of Electric Power Engineering.

1.3 Report Structure

Chapter 1 - *Introduction*, provides the background for the thesis work conducted and introduces the reader to some of the concepts that are discussed in the thesis.

Chapter 2 - *Previous work on de-rating*, gives a non-exhaustive summary of current practices for de-rating of both generation sources and interconnectors.

Chapter 3 - *Generation adequacy*, presents the underlying reliability concepts that constitute the proposed IELCC. The various concepts are explained through the use of illustrative examples.

Chapter 4 - *Interconnector Effective Load Carrying Capability*, puts forward the proposed de-rating methodology for interconnectors, and illustrates it through a simple example.

Chapter 5 - *Case study*, applies the IELCC-procedure to demonstrate its use, by presenting and discussing results from several test cases. IELCC is calculated for several test systems, and sensitivity analysis is conducted.

Chapter 6 - *Conclusions*, sums up the results from Chapter 5 before giving some concluding remarks to the work done. Suggestions for future work are also included.

Chapter 2

Previous work on de-rating

A variety of assessment methodologies exist for the evaluation of generation adequacy. One of the simplest is *capacity margin*. This is a deterministic metric that expresses, usually as a ratio, the relation between installed nameplate capacity and the peak demand in the system. However, it is a too simplistic metric, as it does not consider the fact that all sources of capacity will have some level of unavailability due to issues such as maintenance, failures or unfavourable weather conditions for intermittent renewables, etc. The practice of *de-rating* seeks to take into account these periods of time where the source is unavailable for delivering capacity. This is done by assigning an expected average capacity contribution to the various sources, preferably based on probabilistic considerations. For example Markov modelling of the generator can be used to predict the amount of time it will be unavailable to deliver capacity because of random failures. An alternative is to estimate the time the generator is unavailable by using historical data. These unavailabilities are taken into account to produce a de-rated capacity, which is the net capacity of the source that is deemed to be dependable at all times. Sections 2.1 and 2.2 present existing practices on de-rating of generators and interconnectors.

2.1 De-rating of generation capacity

2.1.1 The United Kingdom

In GB, de-rating of conventional generators, i.e., hydro-, nuclear- and fossil fuel based power plants, is done by the Transmission System Operator (TSO). De-rating is also done for Demand Side Response (DSR) units. Resulting De-Rating Factors (DRFs) are used for assessing the generation adequacy of the power system, and as an extension of this, to help decide the capacity volume that should be secured in the CM. The factors are presented as percentage values of the total nameplate capacity of the generator type as shown in Table 2.1, and are based on historical delivery data from high demand periods for the previous seven winters [8]. For example Hydro is de-rated to 86%, which means that a given hydro generator with a nameplate capacity of 100MW will be assumed to be able to deliver 86MW, averaged over time. This factor will be applied to hydro generators regardless of potential individual differences like size of reservoir or inflow. The effect of DRFs is illustrated in [9] where the aforementioned capacity margin in Great Britain year 2013 is calculated to be 34% using nameplate capacity, called *gross capacity margin*, whereas using DRFs for generation leads to a de-rated capacity margin of 7%.

Table 2.1: De-rating factors used in the GB CM, adapted from [8].

Generation type	Availability/De-rating factor [%]
Oil-fired steam generators	85.44
Open Cycle Gas Turbine (OCGT)	94.17
Nuclear	84.36
Hydro	86.16
Storage	96.29
Combined Cycle Gas Turbine (CCGT)	87.60
Combined Heat and Power (CHP)	90.00
Coal/Biomass	86.92
DSR	86.88

2.1.2 The Pennsylvania—New Jersey—Maryland market

In the Pennsylvania—New Jersey—Maryland (PJM) market [10] a variation of de-rating is utilized for conventional generation to yield Unforced Capacity (UCAP), which represents the amount of capacity that is expected to be available at times of demand. UCAP is obtained by multiplying the nameplate capacity of the generator with the Equivalent Demand Forced Outage Rate (EFORd) for that generator type. EFORd represents the probability of a unit not meeting its generating requirements in periods when there is a demand for generation [11]. As such, EFORd is analogous to the DRFs used in GB in that they are a result of historical performance data from demand periods. The performance data includes forced outage hours, service hours, run times, etc. However, it can be observed in Table 2.2 that EFORd-values for PJM differ from the DRFs for GB. UCAP is used both to evaluate the capacity adequacy of the system and for generators participating in the PJM Capacity Market.

Table 2.2: De-rating factors used in the PJM CM, adapted from [10].

Technology	EFORd	Availability [%]
Combined Cycle	3.3	96.7
Combustion Turbine	5.8	94.2
Diesel	7.1	92.9
Hydroelectric	3.5	96.5
Nuclear	1.9	98.1
Steam	10.0	90.0

2.1.3 Ireland

The Single Electricity Market (SEM), which is the electricity market for the island of Ireland, is currently undergoing significant change in response to EU legislation. The new market, Integrated Single Electricity Market (I-SEM), is planned to be in place by the end of 2017. It will include a CM, named the Capacity Remuneration Mechanism (CRM), for which guidelines and rules are currently being designed. Among these are guidelines for de-rating, both for deciding the overall capacity requirement that is to be procured in the CRM, and

also for deciding the capacity that different capacity providers will be allowed to bid into the market. For this purpose, the CRM will utilize *de-rating curves*, which expands somewhat on the DRF used in GB and PJM system, by having them vary by size (MW of generation) as well as by generation technology [12]. The de-rating curves or DRFs for different capacity intervals are shown in tabular form in Table 2.3. The de-rating curves are obtained through a comprehensive process, taking into account forced outage rates, scheduled outage rates[1], ambient outage rates[2] as well as projected demand. Figure 2.1 summarizes the process.

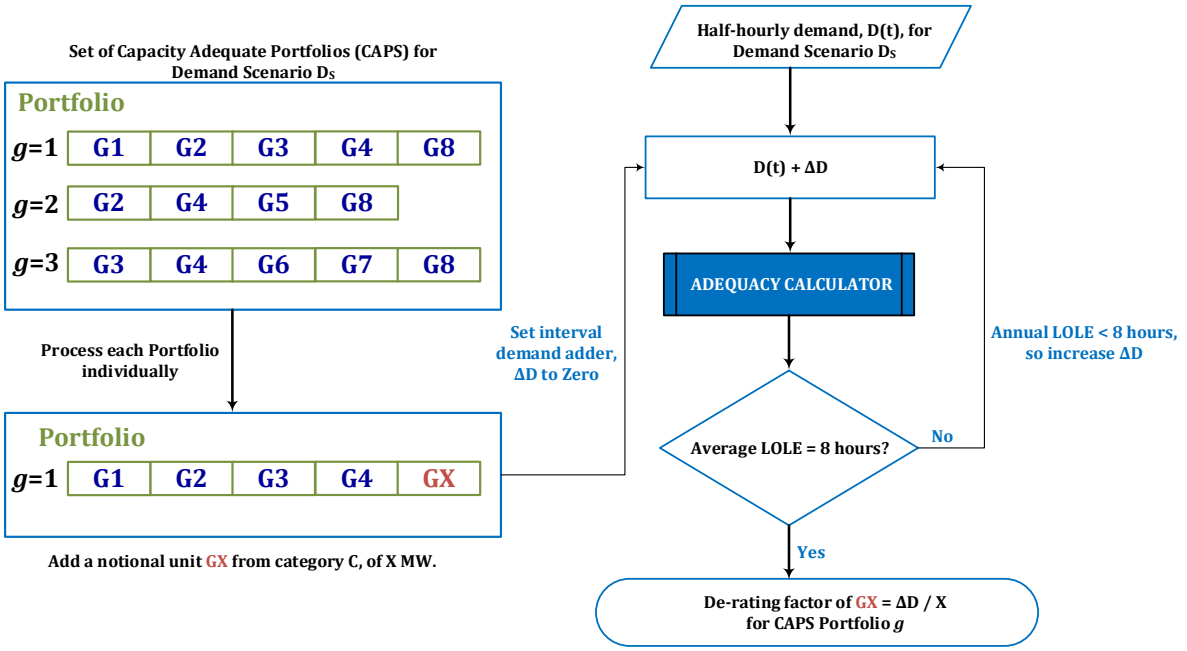

Figure 2.1: Flowchart showing the I-SEM de-rating procedure, adapted from [13].

1. For a year, *x*, a set of *Capacity Adequate Portfolios* (CAPs) are simulated by randomly picking a subset of generators from all capacity market units that were operational in the on the last day of the preceding year, *x-1*. Enough units are picked so that the capacity portfolio combined with a simulated demand scenario, yields an adequate reliability level. In this case, the adequate level is an LOLE of 8 hours/year. LOLE is

[1]Scheduled outage rates are dependent on the amount of time the capacity source is on planned outage, e.g., because of maintenance. This does not significantly influence DRFs as such outages are scheduled to occur at times of low demand.

[2]Ambient outage rates are applied to gas fired power plants, for which the output power is somewhat dependent on ambient temperature

presented in detail in Section 3.1.4. In short, the three types of outage rates (i.e., forced-, scheduled- and ambient outage rates) are used to generate a probability distribution of all possible permutations of outages in a given hour. Together with load demand, simulated by the demand scenario, this gives a probability of having a capacity deficit, i.e., load larger than generation, in that given hour. The sum of these probabilities for all hours of a year yields the LOLE in *hours/year*. Several demand scenarios are considered, and five CAPs are randomly generated for each demand scenario.

2. Each CAP is evaluated individually together with its demand scenario to obtain the de-rating factor. This is done by adding a single notional unit belonging to a specific technology and size category to each CAP, resulting in a lower LOLE (more reliable system). Further, the demand in each hour is incrementally increased, i.e., making the system less reliable, until the LOLE again just satisfies the standard of 8 hours/year. The ratio of the final demand increase to the capacity of the notional unit added gives the marginal de-rating factor. De-rating curves are obtained by averaging the results from the different CAPs and repeating the procedure for notional units of different sizes and technology types.

Table 2.3: Indicative de-ratings for different technologies and size classes for the I-SEM CRM, adapted from [12].

Size [MW]	Gas Turbine	Steam Turbine	Hydro	Storage	Demand Side Units
1-100	95.8	91.8	95.4	86.0	73.0
101-200	95.0	90.3	94.6	82.7	68.8
200-300	94.0	88.3	93.4	74.4	64.1
301-400	92.6	85.9	92.0	64.3	59.3
401-500	91.1	83.1	90.3	54.2	54.4

2.2 De-rating of interconnectors

An interconnector can be a source of capacity from an assisting system; therefore, the amount of capacity allowed to participate in a CM can also be based on a de-rated capacity. As the

availability of any capacity resource is based on stochastic processes, the de-rating methodology should be probabilistic. In the search for such a methodology there are two main issues that need to be addressed:

- The probability that the interconnector will be technically available to deliver capacity at times of scarcity for the area procuring the capacity in the CM, i.e., that the interconnector is not on any kind of outage when capacity is needed from it.
- The probability that the capacity needed in the area of the CM at its times of scarcity is available for import from the interconnected area, i.e., there are no simultaneous scarcity events in the interconnected areas limiting the possibility of exporting capacity through the interconnector.

Technical interconnector availability can be evaluated by examining historical outage data, analogous to how de-rating of conventional generators is performed. Determining the capacity available for import at times of stress is more problematic. Incorporated in this issue of available foreign capacity, is the question of how the actual power flows will turn out. There are uncertainties surrounding what market mechanisms will determine the actual flow in times of simultaneous stress events on both sides of the interconnector [14].

2.2.1 The United Kingdom

In GB, several separate processes have been carried out with the goal of obtaining precise DRFs for the interconnectors that can participate in the CM. The TSO, National Grid (NG), commissioned two separate consultancy-firms to calculate the factors, since NG as interconnector-owner is in a conflict of interest. One of the firms came up with DRFs for each of the interconnectors that were fairly low, and the other firm came up with a set of higher DRFs. These two sets of DRFs defined the low and high ends of the proposed ranges for the DRFs of each interconnector. NG delivered these proposed ranges to the Department of Energy & Climate Change (DECC), from which the Secretary of State chooses the final

DRFs. Proposed ranges from NG, and final DRFs for the 2020/21 T-4 auction are shown in Table 2.4.

Table 2.4: Proposed ranges and final decision for interconnector DRFs for the 2020/21 T-4 auction, adapted from [8] and [15], respectively.

Interconnector	Proposed range [%]	Final DRF [%]
IFA (France)	45-88	60
IFA2 (France)	45-88	62
Eleclink (France)	45-88	65
BritNED (Netherlands)	70-82	74
NEMO (Belgium)	65-92	77
Moyle and EWIC (Ireland)	25-90	26
NSL (Norway)	76-92	78

The de-rating procedure, which yielded the low end of the DRF-ranges, was based on historical relationships of price differentials and flows. For existing interconnectors, data for the top 50% of peak demand periods for winter business days from 2009 to 2015 was used. Out of these peak demand periods, DRFs were constructed by counting the time periods where GB was expected to be importing capacity, defined as the time periods when: a) price differentials were positive, b) GB was importing, c) when both price differentials were positive and GB was importing [16]. For new interconnectors, DRFs were calculated as the percentage of time of the high demand periods where price differentials were positive. However, there has been a large increase in price-flow correlation over the last two years, following the introduction of market coupling[3]. The procedure has therefore received some criticism, e.g., from the Panel of Technical Experts (PTE), commissioned by DECC to impartially scrutinize and quality assure the analysis carried out by NG, as it produces too conservative DRFs for Norway, Belgium, Netherlands and France when taking into account data for the last seven years [14].

The high end of the DRF-ranges were calculated through the use of a pan-European wholesale electricity model. The model models interconnector flows to be driven by the prices in each country, and assumes efficient market coupling. Flows were modelled for four different

[3]Market coupling is a market construction that allows for players from different energy markets in different areas to participate in one integrated market. This market coupling mechanism also decides how the cross-border power flow through interconnectors will be [17].

demand- and weather scenarios, and average flows as a percentage of interconnector capacity were calculated for times where the GB capacity margin was simulated to be less than or equal to zero. Averaged values of the four scenarios defined the high end of the recommended DRF-ranges [8].

In addition to the results provided by consultancy firms, NG on suggestion from the PTE, conducted a study to estimate the benefits in 2019/20 delivered through interconnection [16, 18]. The study considered two interconnected areas, where one was to be assisted by the other. The assisted system was stochastically modelled to meet the GB reliability standard of LOLE=3 hours/year, considering no interconnection. Further, the systems were modelled with a given interconnection capacity, and the improved LOLE was calculated. The difference in LOLE for the stand-alone and interconnected systems was used to calculate what was called *Diversity Benefit Factor* (DBF), expressed as a percentage of the interconnector capacity. DBF aims to quantify the reliability benefit that arises from demand and generation outages in the two areas not being correlated. However, results from this analysis do not seem to have made an impact on the DRF-ranges in spite of recommendation in NG's Electricity Market Reform National Capcity report 2015 [16] that DRFs should ideally be set based on stochastic modelling taking LOLE into account.

2.2.2 The Pennsylvania—New Jersey—Maryland market

For the sake of consistency it will be mentioned that the PJM-market does not employ de-rating for interconnectors in their CM. They utilize an external participation model similar to the EC's pure foreign capacity provider model, with external generators bidding directly into the CM auction. Admission to do so is secured by fulfilling a series of demands, including demonstration of firm transmission service from the capacity-providing unit to the border of the PJM-area [10].

2.2.3 Ireland

Design of the Irish CRM also includes the development of a de-rating procedure for interconnectors. In Ireland, it has been deemed problematic to use historical flows and price differentials to determine the availability and direction of interconnector power flow during times of scarcity in Ireland. An argument for this is the substantial market differences between the SEM, for which price and flow data exists, and the I-SEM. Similarly, it is argued that the GB market has undergone significant changes that affect the data used [19]. As a result, it was chosen to use historic data unaffected by market change, including temperature, wind, demand, and outage data. This historic data is coupled with forecasts for demand and plant mix to create several scenarios for the forecast years. It is assumed that the scarcity pricing system that will be implemented in the I-SEM will provide sufficient incentives for the power to flow into Ireland at times of scarcity.

The scenarios form a basis from which 500,000 winter working days are simulated through Monte Carlo Simulation[4] (MCS). Demand and generation portfolios with possible outages, wind- and solar production are simulated in both Ireland and GB for half-hourly periods. This is used to estimate the probabilities of scarcity in the I-SEM and GB for each half-hour period. Conditional probability is then used to find the probability of coincident scarcity in the two systems. Also used is the probability of capacity being unavailable for import when needed, $P(Capacity\ unavailable\ when\ needed)$. An External Market De-rating Factor (EMDF) is then defined as shown in Equation (2.1).

$$EMDF = 1 - P(Capacity\ unavailable\ when\ needed) \tag{2.1}$$

The EMDF is computed for all interconnectors that connect I-SEM and external markets. Effective Interconnector Capacity (EIC) for an interconnector is obtained when EMDF is multiplied by the Aggregated Import Capacity (AIC) of the interconnector, which is the maximum possible capacity the interconnector can import at optimal conditions. Inter-

[4]Monte Carlo Simulation is a widely used simulation technique that employs sampling of the outcome of random processes, to estimate a probability distribution.

connectors are then inserted into the marginal de-rating methodology used for conventional generation, explained in Section 2.1.3, with the EIC used the same way as nameplate capacity for the generators.

Chapter 3

Generation Adequacy: Indices and evaluation methods

The de-rating methodology presented in this thesis has its theoretical basis in Power System Reliability (PSR). PSR studies are categorized into two domains [20]: *Adequacy* and *Security*. Power system adequacy is defined by CIGRE as [21] "*The ability of the power system to supply the aggregate electric power and energy requirements of the customers at all times, taking into account scheduled and unscheduled outages of the system components.*" Adequacy is associated with static conditions and relates to the existence of sufficient facilities in the system to satisfy consumer demand. Security on the other hand relates to the systems ability to respond to dynamic and transient disturbances.

PSR studies are also categorized in terms of what segment of the power system they are addressing. Figure 3.1 shows the functional zones: Generation, Transmission and Distribution as well as the Hierarchical levels (HL): HLI, HLII and HLIII. The concepts treated in this thesis are almost solely related to generation adequacy. As such, dynamic security, HLII- and HLIII-issues are not treated in this thesis.

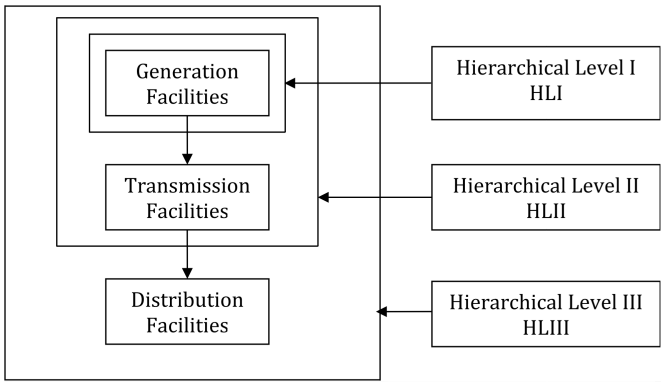

Figure 3.1: Hierarchical levels and functional zones of a power system, adapted from [20].

Measurement of generation adequacy is done through the use of some appropriate index which quantifies the performance of the system. A system's performance is evaluated by calculating a given index and comparing it to a criterion, which is based on acceptable values for that particular adequacy index. At least one basic index, e.g., a probability, and one severity index, e.g., EENS, are needed for detailed information on reliability. For the calculation of indices, probabilistic methodologies are preferred over deterministic ones [22]. Probabilistic metrics require a suitable model and methodology. Further, the adequacy indices can be evaluated using either analytical or simulation approaches. Analytical techniques use mathematical equations and seek direct numerical solutions, while simulation techniques like MCS estimate the indices by simulating the processes and random behaviour of the system.

According to [20], there are two main types of adequacy indices. The first type is used for comparing the adequacy of different systems, and is called *annualized* indices. These indices only consider the maximum yearly load, i.e., the worst case load in a year is applied to the entire year. This separates it from the other type of indices, which is called *annual* indices. These indices utilize a chronological load model where specified time increments are represented by their own load levels (e.g., day 4 can have a different, but not necessarily larger, load level than day 5). Annual indices are used for investigating where a system can be strengthened and as a design criterion, whereas annualized indices are used for comparing the adequacy of two different systems.

3.1 Loss-of-Load-based Indices

The most commonly used indices for evaluating generation adequacy have their basis in Loss-of-Load Probability (LOLP). Loss-of-load Expectation (LOLE) is closely related to LOLP and is considered the most widely used metric [20, 22, 23]. Both indices require the combination of load- and generation models of the system. The load models vary in relation to which time period is being considered and the desired accuracy, while the generation model commonly used is the Capacity Outage Probability Table (COPT)). Other generation models can be found in literature, e.g., the Cumulant Method based model presented in [24], which reduces computation time compared to the COPT, but also imposes a loss of accuracy. COPT is the generation model of choice for this thesis.

3.1.1 Load model

A load model describes the system load for a defined period of time, e.g., a year, for which some adequacy metric will be calculated. The overall time period is further divided into increments of equal duration, where each increment is represented by its duration and a load value. For the large part, variations between the different load models revolve around the duration of the time increments that the overall period is divided into. A simple model to consider is the Constant Yearly Peak Load (CYPL) model, where the entire year is represented by one load increment with a single load level equal to the maximum load for that year. This is a very pessimistic approximation, and as a result, it is more common to divide the year into daily or hourly increments. Figure 3.2a shows how the load models are increasingly pessimistic as the number of time increments used in the model decreases, i.e., fewer load levels that have a longer time duration. The load levels in Figure 3.2a are also sorted in descending order, leading to the hourly peak load curve here being equivalent to the Load Duration Curve (LDC) for the system. Another common variation of the load models is to have a chronological representation of the load levels, where a specified time interval, e.g., hour 45, of a year is represented by a specific load level. This is illustrated in Figure 3.2b.

Load models are predictions of future load that are based on historical data. There are ways to include uncertainty in these load forecasts [20], but such techniques are not treated in this thesis.

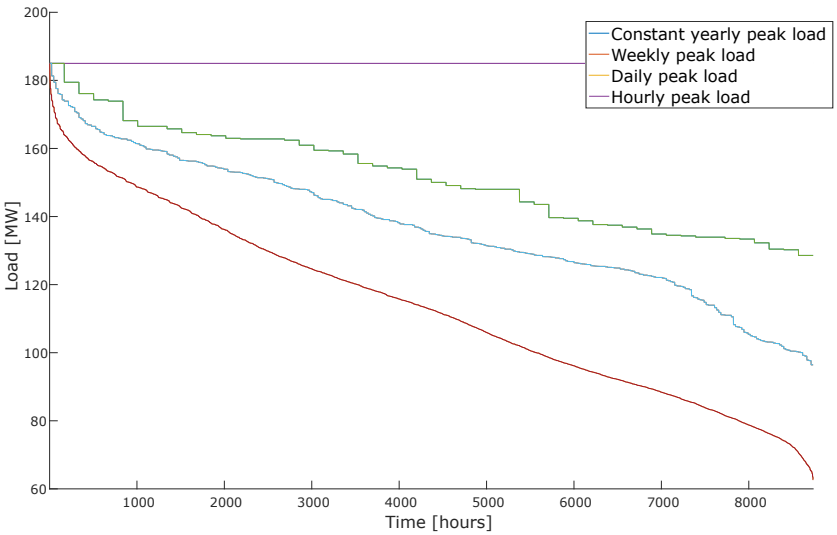

(a) LDCs for overall period of one year with different load increments. The curves are for the RBTS with a maximum load of 185MW.

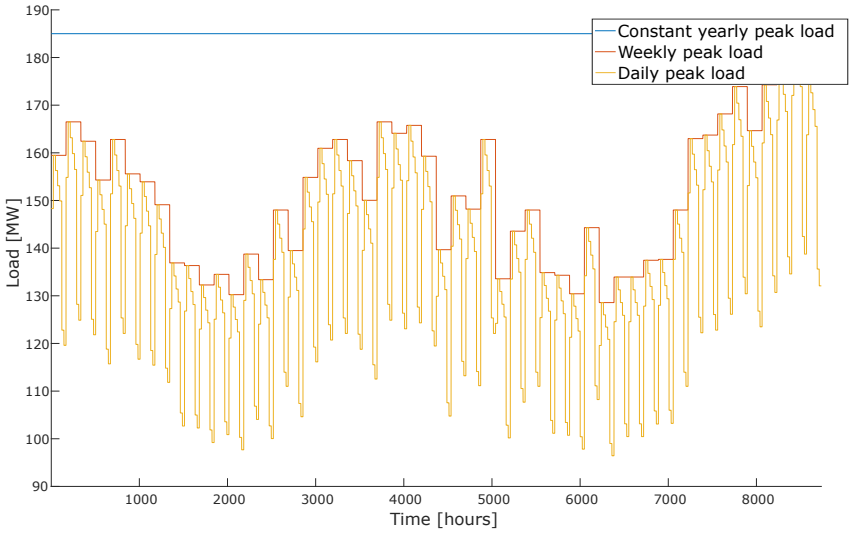

(b) Chronological load level-curves for overall period of one year with different load increments. The curves are for the RBTS with a maximum load of 185MW.

Figure 3.2: Illustration of different load models.

3.1.2 Generation model: Capacity Outage Probability Table

There are some small variations, but most commonly the COPT is represented by a table containing the possible outage states of a generation system. Each state is represented by a given number of MWs on outage, x_j, as well as the corresponding cumulative probability $P(X \geq x_j)$ of having an outage greater than or equal to x_j, which can be represented mathematically by Equation (3.1). Individual probability, $p(X)$ is summed to C, which represents the total installed capacity in the system. Table 3.1b shows an example COPT for a system composed of four 10MW generators and one 20MW generator, for a total of 60MW of installed capacity. The table also includes a column that shows the individual probability of being in outage state, j, with associated outage capacity x_j. In literature, variations to the COPT-layout can be found that show capacity "innage" instead of outage, or that present the cumulative probability as $P(X > x_j)$ instead of $P(X \geq x_j)$. The probabilities shown in Table 3.1b are truncated at a probability of 1×10^{-8}.

$$P(X \geq x_j) = \sum_{X=x_j}^{C} p(X) \tag{3.1}$$

The probability entries in the COPT originate from the generators being represented by two or more states. A two-state model is the simplest, where each generator is modelled as being fully available or fully unavailable, with associated probabilities p_{up} andp_{down}, respectively. p_{down} is most commonly referred to as the Forced Outage Rate (FOR), which is defined as the probability of finding the unit on forced outage some distant time in the future [20]. The multi-state approach allows for partial availabilities/partial outages whose probabilities will be denoted by p_i. It is common to refer to the various states of a multi-state model as *derated states*. This must not be confused with the process of de-rating, or de-rating factors. Ideally speaking, the probability attributes of a generator need to be computed from appropriate reliability models, e.g., Markov modelling of the generator. An alternative is to estimate the required attributes from field data, i.e., historical availability. A multiplicative combination of the probabilities representing each generator's availability yields an individual probability

Table 3.1: Generator unit data (a) and resulting example COPT (b), adapted from [20].

(a)

Unit cap.[1] [MW]	Unit FOR
10	0.02
10	0.02
10	0.02
10	0.02
20	0.02

(b)

State j	Cap. outage x_j [MW]	Individual prob. $p(X = x_j)$	Cum. prob.[2] $P(X \geq x_j)$
1	0	0.90392080	1.00000000
2	10	0.07378945	0.09607920
3	20	0.02070622	0.02228975
4	30	0.00153664	0.00158353
5	40	0.00004626	0.00004689
6	50	0.00000063	0.00000063
7	60	0.00000000	0.00000000

of the system being in that particular configuration. Further, the individual probability associated with a distinct outage state can be the sum of the probabilities of several system configurations that results in the same amount of capacity outage. Since the generating units are added in discrete sizes of capacity, the resulting outage states will represent discrete megawatts on outage. Therefore the COPT models the system as having possible outage states described by a discrete probability function, $P(X \geq x_j)$.

When constructing the COPT, the generators are added one by one, convolving the capacity states of each unit with the outage states already added to the COPT. This can be done systematically by utilizing a recursive algorithm [20, 25] that allows for direct calculation of the cumulative probability without having to calculate the individual probabilities for each state first. When utilized for a system with only two-state generator representation, the algorithm is represented mathematically by Equation (3.4). Assuming some units are added to the COPT already, yielding a discrete cumulative probability distribution represented by $P^{old}(X)$, the addition of a two-state generator with capacity, g, and unavailability, p_{down}, the new discrete cumulative probability distribution $P^{new}(X)$ is given by

[1] Cap. is an abbreviation for capacity.
[2] Cum. prob. is an abbreviation for cumulative probability.

$$P^{new}(X \geq x_j) = (1 - p_{down}) \cdot P^{old}(X \geq x_j) + p_{down} \cdot P^{old}(X \geq x_j - g). \tag{3.2}$$

All existing capacity outages, x_j, in the old COPT, as well as new possible outage states caused by the addition of the new unit are evaluated by Equation (3.2), updating the cumulative probability of the outage states in the COPT. It can be observed that there are cases where the argument for the cumulative probability function can become zero or negative. This is handled by the defintion in Equation (3.3). For a more detailed example of how COPT is obtained, or for more explanation of the two terms in Equation (3.2), the reader is referred to [20] or [25], respectively.

$$P^{old}(X \geq x_j) = 1 \text{ for } \begin{cases} x_j \leq 0 \\ x_j - g \leq 0 \end{cases} \tag{3.3}$$

The recursive algorithm can be expanded to handle multi-state representation of generation units as well. Addition of a unit with i states, where p_i denotes the probability of the unit being in state i and having capacity g_i, is done with Equation (3.4).

$$P^{new}(X \geq x_j) = \sum_{i=1}^{n} p_i \cdot P^{old}(X \geq x_j - g_i) \tag{3.4}$$

When executing the algorithm, a new COPT is created each time a new unit is added to the probability distribution, updating all previous outage states as well as adding new ones. The cumulative probabilities demanded by $P^{old}(X \geq x_j)$ are found by looking up the corresponding value from the COPT as it were before the addition of the current unit. When doing this, it is also possible to get arguments to the cumulative probability function that do not represent an existing outage state that can be looked up from the current COPT, as $x_j - g$ might fall between two existing states. Since the probability distribution deals with cumulative probabilities, the probability value for the next state larger than $x_j - g$ will be used in the when there are no outage states in the current COPT with outage equal to $x_j - g$.

3.1.3 LOLP

LOLP is a probabilistic approach that examines the probability of occurrence of a loss-of-load situation in the system in a given period of time. A loss-of-load situation can occur if the system experiences that load exceeds the available generation, either caused by generation unit outages or unexpected increase in demand. This index can be calculated by combining the load model and the COPT. The system will have a loss-of-load situation for any given instance where the sum of system load and the total capacity outage is larger than the installed capacity. LOLP can be represented as shown in Equation (3.5).

$$LOLP_t = P(X > C - L_t) \tag{3.5}$$

The t-subscript is included to highlight that LOLP denotes the probability of having a loss-of-load situation in the particular time increment, t, for which LOLP is calculated, when the system load is L_t. C is the total installed capacity in the system which is not on scheduled outage. C can vary depending on which time increment is evaluated, because there can be generator units on scheduled outage during the overall time period. Such situations will, however, not be considered in this thesis.

As LOLP is a probability, it is a unitless quantity; however, it can also be interpreted as the proportion of time of a considered time period when load is not met. If a CYPL model is used, equivalent to the blue curve in Figures 3.2a-3.2b, evaluating the LOLP for the overall time period of one year would result in a probability value. This value can also be interpreted as having a loss-of-load situation for Y years ($Y \leq 1$) out of the overall period of one year. As an example, consider a CYPL of 35MW in the system defined by the COPT in Table 3.1b. This results in $P(X > C - L) = P(X > 25MW) = 0.00158353$, i.e., the probability of losing load is 0.00158353. Alternatively, it can be interpreted as follows: 0.00158353 years out of the year that is evaluated, it is expected that the system will lose load. By using the proper unit conversions (365 days/year or 8760 hours/year), this quantity can be expressed as the number of days or hours of a year the system is expected to lose load. These conversions are

permissible only when just a single load increment is considered, e.g., when using the CYPL model. This is because for this particular instance, the LOLP equals the LOLE, a notion which will be more thoroughly explained in Section 3.1.4.

3.1.4 LOLE

There are several misconceptions surrounding LOLP and LOLE in literature, and the terms are often, but wrongfully, used interchangeably [26]. Especially LOLE is often mistakenly referred to as LOLP. In practice, it is the loss-of-load *expecation* that is most used by power system planners and operators, while the loss-of-load *probability* is not widely used in itself, but serves as a constituent part of the LOLE-calculation procedure. Where LOLP describes the probability of not being able to meet load for particular system conditions in a given time increment, LOLE can provide the number of time units in an overall time period where loss-of-load events are expected to occur. Serving to increase the confusion between LOLP and LOLE, the former can be re-engineered from the latter by dividing LOLE by the total number of time units in the overall time period considered, i.e., 365 days or 8760 hours for one year. This can provide an LOLP for say a whole year, which is based on a load model considering more than one load level through the year. Although not explicitly stated, examples of this practice can be encountered in literature, for example in Table IV in [27]. This version of LOLP will be briefly encountered later in the thesis, then referred to as LOLP'.

Even though LOLE quantifies the number of time units where loss-of-load situations are expected to occur, LOLE should not be interpreted as the amount of time in a year there will be blackouts. Following the interpretation in [18]: *"A loss of load is not equivalent to blackout; rather, it represents the number of hours that the market has not met demand and when National Grid needs to use its reserves and tools to balance the system (the very last option being customer disconnection)."* Most of the time, the system operator (National Grid in the interpretation above) is able to perform mitigating actions such that a loss-of-load event does not lead to blackouts or power cuts.

It is common to calculate LOLE in terms of *days/year* or *hours/year*, usually represented by Equation (3.6) and Equation (3.7), respectively. The unit days/year is the convention used, but this is actually a shortened form of daily peaks/year.

$$LOLE = \sum_{t=1}^{365} P(X > C - L_t)\Delta T \quad [\frac{days}{year}] \tag{3.6}$$

$$LOLE = \sum_{t=1}^{8760} P(X > C - L_t)\Delta T \quad [\frac{hours}{year}] \tag{3.7}$$

Equations (3.6)-(3.7) can be recognized as probabilistic expectations, consisting of summations of individual increments of time weighted with a probability value. $P(X > C - L_t)$ can also be recognized as LOLP, and the equations can be rewritten as in Equations (3.8)-(3.9).

$$LOLE = \sum_{t=1}^{365} LOLP_t \cdot \Delta T \quad [\frac{days}{year}] \tag{3.8}$$

$$LOLE = \sum_{t=1}^{8760} LOLP_t \cdot \Delta T \quad [\frac{hours}{year}] \tag{3.9}$$

For most applications, the duration of the time increment, ΔT, is 1 day when a Daily Peak Load (DPL) model is used, and is 1 hour when an Hourly Peak Load (HPL) model is used. Hence, the LOLE calculation simplifies to summing the LOLP-values from each time increment in the overall time period evaluated. It is important to be aware of which type of load model is being used when computing LOLE, as LOLE calculated with a DPL-model will differ from the LOLE calculated for the same system using a HPL-model. The only exception is the unrealistic case where all 24 hours in each day have the exact same load as the corresponding daily load in the DPL-model. It is therefore not correct to convert from LOLE in hours/year to LOLE in days/year by using a conversion factor of 24 hours/day [28]. A LOLE of 1 days/year calculated using a DPL-model does not equate to 1 day/year$\times$24 hours/day= 24 hours/year.

A much used criterion in adequacy planning is the "1 day in 10 years" standard, which equates to LOLE=0.1 days/year. This standard, which has been widely adopted by industry, dates back to the 1950s [29], which was the actual LOLE of a specific real-life system at that time. The performance and reliability of this system was deemed acceptable, and the standard stems from this. As mentioned in the previous paragraph, it is not correct to convert an LOLE of 0.1 days/year to 2.4 hours/year. This mistake is often encountered in literature as it is now more common to calculate LOLE using an HPL-model, even though there is no industry-standard reliability level for LOLE in hours/year. However, some countries in western Europe have defined their own LOLE standard as shown in Table 3.2.

Table 3.2: Selected countries with defined LOLE standards in hours/year, adapted from [30].

Country	LOLE standard [hours/year]
Belgium	3
France	3
Great Britain	3
Ireland	8
The Netherlands	4

3.1.5 EENS

Despite its near universal use in adequacy studies, LOLE is sometimes criticized as a measure of system reliability, as it does not provide any information about the severity of an outage [31, 32]. Equally long capacity deficits of 10MW and 100MW are not treated differently in LOLE calculations; both cases yield the same LOLP, since the loss-of-load situation occurs as soon as there is a capacity deficit larger than zero MW. It can be argued that the 100MW outage should be weighted more, as it would cause a ten times larger energy deficit. The adequacy index Expected Energy not Served[3] (EENS) extends on LOLE by also including the size of such capacity shortfalls. In [22], appropriate generation and system adequacy standards for the internal electricity market in Europe were identified. One of the recommendations of

[3]EENS is also often referred to by other names, such as Expected Energy Unserved (EEU) [33], Loss-of-Energy Expectation (LOEE) [31] or Expected Unserved Energy (EUE) [34].

the study was to "*... establish EENS as a preferred metric as it alone proves appropriate for the calculation of socially optimal levels of reserve*". The fact that EENS accounts for the severity of capacity deficits is one of the main arguments for this recommendation.

Just as LOLE, EENS is a probabilistic expectation. For a given capacity outage, x_j, and load, L_t, an intermediate to unserved energy, E, can be represented by Equation (3.10).

$$E = [x_j - (C - L_t)] \cdot p(X = x_j) \tag{3.10}$$

$[x_j - (C - L_t)]$ gives the capacity deficit, which is multiplied with the individual probability of being in the outage state, x_j that is responsible for the capacity deficit. For EENS-calculations it is common and logical to use an HPL-model. For a given hourly load, the unserved energy found in Equation (3.10) is summed over all the outage states that yield a capacity outage, as shown in Equation (3.11).

$$EENS = \sum_{x_j=C-L_t}^{C} [x_j - (C - L_t)] \cdot p(X = x_j) \quad [MWh] \tag{3.11}$$

Equation (3.11) yields EENS for the time increment t. This sum is performed over all hourly loads in the overall time period, usually a year, to get the total EENS for the entire period as in Equation (3.12).

$$EENS = \sum_{t=1}^{8760} \sum_{x_j=C-L_t}^{C} [x_j - (C - L_t)] \cdot p(X = x_j) \quad [MWh/year] \tag{3.12}$$

To illustrate the procedure, the COPT in Table 3.1b has been extended to Table 3.3. The generation model is the same as before, and a single time increment where L_t=45MW is considered. With this load, five out of seven outage states cause a capacity deficit. The size of the deficits are weighted by the individual probabilities of the outage state, resulting in $EENS = 0.1035311 + 0.0230496 + 0.0011565 + 0.0000221 = 0.12775925$. Assuming the

duration of the time increments is one hour, the units will be MWh/hour. This calculation could be done for 8760 hourly time increments in a year, yielding the EENS in MWh/year.

Table 3.3: Extended COPT to illustrate EENS for an example system, adapted from Table 4.2 in [20]

State j	Cap. out.[4] x_j [MW]	Ind. prob.[5] $p(X = x_j)$	Cum. prob. $P(X \geq x_j)$	Capacity deficit $[x_j - (C - L_t)]$	E_j
1	0	0.90392080	1.00000000	0	0
2	10	0.07378945	0.09607920	0	0
3	20	0.02070622	0.02228975	5	5×0.02070622=0.1035311
4	30	0.00153664	0.00158353	15	15×0.00153664=0.0230496
5	40	0.00004626	0.00004689	25	25×0.00004626=0.0011565
6	50	0.00000063	0.00000063	35	35×0.00000063=0.0000221
7	60	0.00000000	0.00000000	45	45×0.00000000=0

EENS is not as frequently used as LOLE as a reliability standard, but the Australian Energy Market Commission's Reliability Panel has defined its standard in terms of Expected Unserved Energy (USE), which is a normalized version of EENS, i.e., EENS is divided by the total yearly energy consumption. Currently, their level of USE is set to 0.002% of the annual energy consumption [35]. Normalized EENS can also be encountered elsewhere in literature [36], but referred to as Loss-of-Energy Probability (LOEP). This index, which is derived from EENS, is often wrongfully referred to being the same as EENS.

While normalized EENS/LOEP is derived from dividing EENS by the total annual energy demand, another index, Expected Demand Not Served (EDNS), can be derived by dividing EENS by the total number of time units in the overall time period considered. This is equivalent to how LOLP' is derived from LOLE. EDNS can be interpreted as the expected average demand that will not be served by the system because of loss-of-load situations [27].

[4]Cap. out. is an abbreviation for capacity outage.
[5]Ind. prob. is an abbreviation for individual probability.

3.2 Capacity Credits: Using Effective Load Carrying Capability to Quantify Generation Adequacy

In generation expansion planning there are two main aspects that, from a reliability perspective, are interesting to evaluate. Firstly, how will an addition of generation to a system, defined by its existing generation fleet and peak load demands, influence the system's overall performance in terms of reliability? This can be examined by using traditional adequacy metrics like LOLE, as adding generation to a system will improve its LOLE if the load requirements remain the same. However, this gives little information beyond the LOLE-improvement in itself, which is hard to interpret into a quantity that can be used for practical applications other than just quantifying the system's reliability level. Therefore, it is also useful to quantify in which proportion the added generation unit can contribute to meeting a future increasing load, while still maintaining the desired reliability level. This information can be obtained from the concept of Capacity Credits (CC). CCs, with Effective Load Carrying Capability (ELCC) as the most recognized variation, are extensions of the basic reliability metrics that seek to give more extensive generation adequacy information. A distinct definition is hard to find, as different types of capacity credits and different computation methods exist. Judging by [37, 38, 39, 40], three of the most commonly used metrics are ELCC, Equivalent Firm Capacity (EFC) and Equivalent Conventional Capacity (ECC). However, the common feature of all these metrics is that they quantify the capacity contribution in terms of MW by taking into account that the reliability level should be the same before and after the addition of generation and load.

3.2.1 Effective Load Carrying Capability

Effective Load Carrying Capability, as described by Garver in [41], was initially used as an aid in generation expansion planning, allowing evaluation of the capacity contribution of added conventional generation units to a system. Lately, the use of ELCC has regained interest

and has been established by many studies as a very dependable metric for quantifying the reliability contribution of wind plants [38, 42, 43]. The use also extends to CC for Electric Energy Storage (ESS) [39, 44] and Demand Side Response (DSR) [32, 37, 40]. Classically, ELCC has used LOLE as its guiding reliability metric, and using the same notation used for LOLP/LOLE, ELCC can be represented by Equations (3.13)-(3.14) [43]

$$LOLE^O = LOLE^N \tag{3.13}$$

where $LOLE^O$ represents the LOLE of the original system and $LOLE^N$ represents the LOLE for the new system configuration with additional generation and load.

$$\sum_{t=1}^{T} P(X^O > C^O - L_t) = \sum_{t=1}^{T} P(X^N > C^N - (L_t + \Delta L)) \tag{3.14}$$

T is the number of time increments evaluated, the superscripts O and N represent the original system configuration and the new configuration, respectively, such that $C^N = C^O + c_A$, where c^A is the nameplate capacity of the generator added. ΔL represent the additional load that can be served for the new system while still satisfying Equation (3.13). It is a constant which is added to the load level, L_t, of every time increment, t. The arguments to the cumulative probability function can be recognized as the same as for LOLP for the original and new systems, which can be obtained from their respective COPTs. Equations (3.13)-(3.14) can be evaluated by increasing ΔL and calculating $LOLE^N$ iteratively until LOLE of the new system equals that of the original system. The ΔL that satisfies this condition quantifies the additional load that can be served at the same reliability level when adding a generator with capacity c_A to the system. ΔL is then the ELCC of that specific generator added to that specific system.

It is important to mention that a specific generator unit with a defined nameplate capacity and FOR can have different ELCC for different systems. Both the pre-existing reliability level and the size of the added unit in relation to installed capacity can influence the ELCC

of an added generator [32, 38]. This can cause some non-intuitive results, such as ELCC of an added conventional generator turning out to be larger than its nameplate capacity. Such results are showcased, but not explained in [45]. Explanations to this have not been found in other literature either, but it will be further investigated in Section 5.3.

The iterative approach represented by Equations (3.13)-(3.14) gives exact solutions for ELCC, but can be computationally intensive for large systems. There are also non-iterative methods, e.g., Garver's approximation as described in [41] or [43], which calculate ELCC by using curve-fitting. This method will not be discussed here, but a very simplified version will be used in this thesis to determine ELCC of systems graphically:

Step 1: A curve is plotted for the original system, showing how its LOLE varies with respect to an increase in load. This is the blue curve in Figure 3.3, which shows the ELCC for an addition of a 10MW generator with FOR=0.03 to the system described by Table 3.1b. All the marked points on the curve correspond to an LOLE value in days/year calculated from a load/time-series, represented on the x-axis by the maximum load in the series. Between peak load/LOLE-points, the curve is approximated as being linear in the semi-logarithmic scale. For large scale systems using DPL- or HPL-models, this approximation does not cause large errors.

Although represented in the plot by a single load value, an entire yearly load/time-series, in this case 365 time increments with corresponding load levels, are used for the LOLE-calculation. The different load/time-series used are obtained by scaling a main series, which belongs to the original system. Each load point, $L_t^{'}$, in the scaled series is obtained by scaling the base case load levels, L_t, with the same factor, as shown in Equation (3.15). $L_{max}^{'}$ is the maximum load in the new load/time-series and L_{max} is the maximum load in the original series. This results in all load-series having the same variability during the overall time period, which is the same variability as shown by the yellow curve in Figure 3.2b.

$$L_t^{'} = L_t \frac{L_{max}^{'}}{L_{max}} \tag{3.15}$$

Step 2: To measure the ELCC of a generator added to the original system, the COPT for the new system with the added capacity is obtained, and LOLE is calculated for the new system for different load/time-series, as in step 1. This data is also plotted, represented by the red curve in Figure 3.3.

Step 3: The ELCC is the horizontal distance in MW between the two curves at a specific level of reliability, measured by the reliability index on the y-axis, which in this case is LOLE. The reliability-level used can be a pre-defined standard, such as the 0.1 days/year standard [46, 47], or more commonly, the reliability-level as it was before the generator addition [42]. The latter is the basis for Equation (3.13). In the illustrative example shown here, LOLE=0.27 days/year is used, as this is the LOLE for the original system with a load/time-series with a maximum load of 40MW.

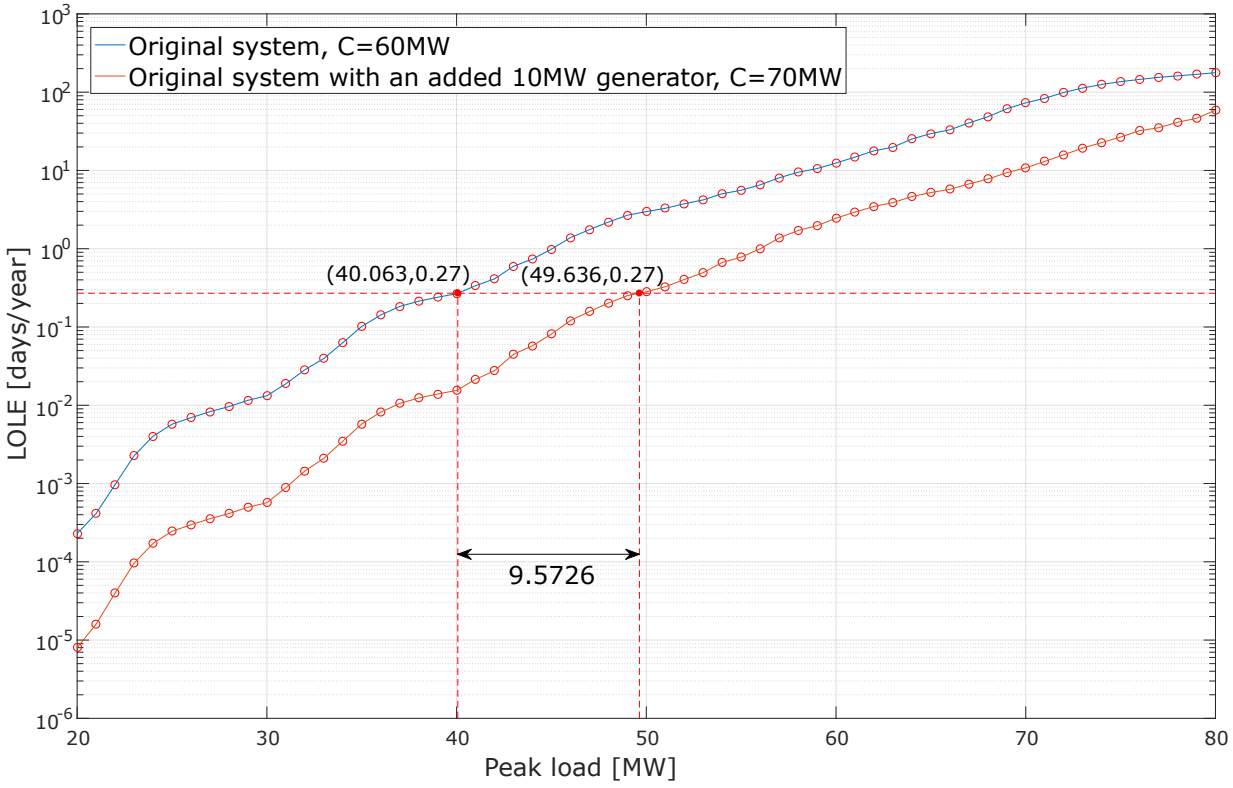

Figure 3.3: Plot showing a graphical approximation to ELCC.

As exemplified through Equations (3.13)-(3.14) and Figure 3.3, LOLE is a common reliability metric used when calculating ELCC. However, as stated in [42]: *"The definition of capacity credit is independent of the risk index used."* This is also supported by [39], where it is stated that *"evaluation of CC metrics is based on evaluating and comparing adequacy levels. These can be quantified by different reliability indices, e.g., loss of load probability, loss of load expectation, EENS, loss of load frequency (LOLF), loss of load duration (LOLD) etc. In fact, different indices address different aspects of system reliability, and therefore the CC metric that uses a specific index indicates the capacity value in terms of the reliability performance that index is measuring."* This simply means that varying system load will be plotted vs. a different index on the y-axis, e.g., EENS, instead of LOLE as in Figure 3.3, and LOLE will be replaced by EENS in Equations (3.13)-(3.14). This notion is utilized in [37, 39] for various CC-calculations. This is a strength of ELCC, as in some cases it might be preferred to use EENS or some other index (e.g., LOLP', LOEP, EDNS) instead of the conventional LOLE.

3.2.2 Equivalent Firm Capacity and Equivalent Conventional Capacity

The other CCs mentioned, EFC and ECC, will also be briefly defined here, but they will not be used further in this thesis. EFC measures the capacity addition of an added generation unit by applying a fictitious 100% reliable unit to the original system. The capacity of this fictitious unit, which achieves the same improvement to the reliability level of the original system as the added real generation unit, is the EFC of the unit added [38, 39].

ECC is very similar to EFC, the only difference being that the fictitious unit considered is a realistic generator with a specified unavailability, and hence the name "conventional". The capacity of an added unit is measured in terms of the capacity of such a conventional unit that gives the same reliability improvement to the original system as the added unit [38, 39].

A description of ELCC, EFC and ECC presented in [48] is included here to summarize and distinguish between the three metrics:

- *"ELCC: If X MW of a power plant result in that the demand can increase with Y MW at the same LOLP, then the capacity credit as ELCC of the X MW power plant is Y MW.*

- *EFC: If X MW of a power gives the same decrease of LOLP as a 100 percent reliable Y MW power plant, then the capacity credit as EFC of the X MW power plant is Y MW.*

- *ECC: If X MW of a power gives the same decrease of LOLP as a conventional, not 100 percent reliable, Y MW power plant, then the capacity credit as ECC of the X MW power plant is Y MW."*

3.3 Interconnected Systems

The rationale behind letting interconnectors or capacity providers in different areas participate in CMs is mainly the system adequacy improvement. Given that occurrences of capacity outages and large loads will be more uncorrelated in different systems, each of the interconnected systems can run at the same level of reliability as when isolated, with less capacity reserves [20]. In addition to installed capacity and load levels, the ability of each system to assist the other will depend on the capacity and technical availability of the interconnector. This ability is also subject to the contractual agreements that are in place between the systems, whereas the probability of simultaneous scarcity in the systems could constrain the assistance. Evaluating the ability of interconnected systems to assist each other and quantifying the reliability contribution of interconnecting systems can be viewed as an integral part of building a probabilistic de-rating methodology for interconnectors. This section will present two HL1 reliability assessment methods for interconnected systems: The Probability Array method and The Equivalent Assisting Unit (EAU) method. The latter will be treated in detail. Both methods assess the interconnected systems in terms of adequacy indices, e.g., LOLE or EENS. Both the probability array method and the EAU-method can be extended to handle multi-area interconnected systems. Interconnections of more than two systems are not treated in this thesis, but would be a natural extension of the work done here.

In this thesis, the focus in both methods is on one system, System A, being assisted by a different system, System B, through an interconnection. Positive capacity reserves in the assisting system will increase reliability of the assisted system. Larger positive reserves in the assisting system will lead to a larger increase in reliability, up to the point where reserve is larger than the interconnector capacity. It is assumed in both methods that System B will assist System A only as long as System B has a positive capacity reserve. Hence, the maximum assistance System B can provide at a given instance, not taking into account interconnector capacity constraint, is equal to its reserve capacity. This assumption might not be valid, depending on what contractual agreements are in place. There can be situations where a system is forced to assist because of contractual obligations/penalties, even though it would cause loss-of-load in its own system. Such situations are not considered here as it would be difficult to cover such market related agreements exhaustively. Further, it is realistic to consider a situation where a system would serve its own loads when needed, rather than providing assistance.

3.3.1 Equivalent Assisting Unit Approach

The EAU-method quantifies the reliability benefits by modelling the assisting system and interconnector as an equivalent multi-state unit [20]. This unit can be added to the COPT of the assisted system by using Equation (3.4). The approach will be explained with the help of an illustrative example gathered from [20], described by Tables 3.4-3.5. The load model used will affect the number of calculations in the overall procedure greatly, as computations for each time increment result in the creation of an Equivalent Assisting Unit from System B and the interconnector. In the following, the approach for obtaining LOLE for a System A, assisted by a System B, by means of the EAU-model will be explained. A chronological load model is assumed. The procedure involves finding an EAU-model for each time increment, t, and uses the model to find the resulting LOLP for System A, when System A is assisted by System B through an interconnector. The approach is summarized in the following steps, and illustrated in a flowchart in Figure 3.4:

Table 3.4: Generation and load data for Systems A and B, adapted from [20].

System	Number of units	Unit cap. [MW]	Unit FOR	Installed cap. [MW]	Daily Peak Load [MW]
A	5	10	0.02	75	50
	1	25	0.02		
B	4	10	0.02	60	40
	1	20	0.02		

Table 3.5: Interconnector data, adapted from [20].

State k	Interconnector cap. IC_k[MW]	Probability p_k
1	0	0.00815217
2	10	0.99184783

Step 1: The first step is to obtain the generation models for each of the systems by building $COPT^A$ and $COPT^B$, as explained in Section 3.1.2. COPTs are shown in Table 3.6.

Step 2: LOLP is to be found for each time increment, t, out of the total number of increments, T. A time increment is represented by a load-level, L_t, as well as its duration. For L_t, reserve in the assisting system is R_t^B=C^B−L_t^B, which is the maximum assistance from an assisting system with installed capacity equal to C^B. Maximum assistance can be provided only by State 1, i.e., when none of the units in System B is on outage. Other levels of assistance, $a_{t,j}^{EAU}$ can be obtained by subtracting the capacity on outage in each state in $COPT^B$ from the reserve, $a_{t,j}^{EAU} = R_t^B - x_j^B$. It can be seen in Table 3.7a that for outage states where the outage capacity exceeds the reserve, $x_j^B \geq R_t^B$, there is zero available assistance capacity from System B. Outage states yielding zero assistance, $j = 3$ to $j = 7$ for the example, are merged into one assistance state. The sum of the individual probabilities of these outage states gives the probability of zero assistance in the assistance probability table, as shown in Table 3.7b.

For the time increment evaluated in the example, the load is 40MW so that System

Table 3.6: COPT for Systems A and B.

System A				System B			
State j	Cap. out x_j^A[MW]	Ind. prob. $p(X = x_j^A)$	Cum. prob. $P(X \geq x_j^A)$	State j	Cap. out x_j^B [MW]	Ind. prob. $p(X = x_j^B)$	Cum. prob. $P(X \geq x_j^B)$
1	0	0.88584238	1.00000000	1	0	0.90392080	1.00000000
2	10	0.09039207	0.11415762	2	10	0.07378945	0.09607920
3	20	0.00368947	0.02376555	3	20	0.02070622	0.02228975
4	25	0.01807841	0.02007608	4	30	0.00153664	0.00158353
5	30	0.00007530	0.00199767	5	40	0.00004626	0.00004689
6	35	0.00184474	0.00192237	6	50	0.00000063	0.00000063
7	40	0.00000077	0.00007763	7	60	0.00000000	0.00000000
8	45	0.00007530	0.00007686				
9	50	0.00000000	0.00000156				
10	55	0.00000154	0.00000156				
11	65	0.00000002	0.00000002				
12	75	0.00000000	0.00000000				

B has a reserve of 20MW, which is the maximum assistance that can be provided from System B. The assistance states are shown in Table 3.7b, which can be easily translated into an EAU-model showing outage capacity states instead of assistance capacity states as shown in Table 3.7c, by using that $x_{t,j}^{EAU} = a_{t,j=1}^{EAU} - a_{t,j}^{EAU}$, where $j = 1$ is the index of the maximum assistance state.

Step 3: With the EAU-model for System B in place, the next step is to combine it with the model for the interconnector, resulting in a Constrained Equivalent Assisting Unit (CEAU) model. As in the case of generators, interconnectors have unavailability and can be represented by either a two-state model or a multi-state model. A two-state model, i.e., either fully up or fully down, can be relevant for AC interconnectors, while HVDC interconnectors might very well have derated states, requiring a multi-state model [49].

Depending on the characteristics of the interconnector model, i.e., interconnector-capacity, -FOR and number of derated states, various alterations have to be made to the EAU-model. Potential cases that can arise are listed as follows:

Table 3.7: Transforming $COPT^B$ into an EAU-model.

(a) Intermediate EAU-assistance probability table.

State j	Cap. out x_j^B[MW]	Assistance $a_{t,j}^{EAU}$ [MW]	Ind. prob. $p(X = x_j^B)$
1	0	20	0.90392080
2	10	10	0.07378945
3	20	0	0.02070622
4	30	0	0.00153664
5	40	0	0.00004626
6	50	0	0.00000063
7	60	0	0.00000000

(b) Assistance probability table for the EAU.

State j	Assistance $a_{t,j}^{EAU}$[MW]	Ind. prob. $p(X = a_{t,j}^{EAU})$
1	20	0.90392080
2	10	0.07378945
3	0	0.02228975

(c) EAU-model of System B.

State j	Cap. out. $x_{t,j}^{EAU}$ [MW]	Ind. prob. $p(X = x_{t,j}^{EAU})$
1	0	0.90392080
2	10	0.07378945
3	20	0.02228975

a) Interconnector capacity is larger than maximum assistance capacity from the assisting system:

   i) Interconnector represented by a two-state model.

   ii) Interconnector represented by a multi-state model.

b) Interconnector capacity is smaller than maximum assistance capacity from the assisting system:

   i) Interconnector represented by a two-state model.

   ii) Interconnector represented by a multi-state model.

For a hypothetical case where the interconnector is 100% reliable and has a capacity larger than the maximum assistance from System B, i.e., a variation of case a)-(i), no convolving with the interconnector model is needed, and the EAU-model can be added directly to $COPT^A$ as a multi-state unit by using Equation (3.4). The COPT resulting from the addition of the (C)EAU-model to $COPT^A$, is called $COPT^U$

(U stands for *unified*)[6]. Taking unavailability or multiple interconnector states into consideration, however, results in alterations of the EAU-model when obtaining the CEAU-model. Probabilities of different derated states of interconnector capacity, p_k, can be incorporated directly when transforming the EAU-model to the CEAU-model. However, this approach requires application of a slightly different logic depending on which of the cases mentioned above comes into play. As a result, the procedure is not easily generalized or illustrated. An alternative approach, and the one explained here, is to obtain a CEAU-model and the corresponding unified LOLP for System A assisted by System B, $LOLP^U_{t,k}$, for every state of the interconnector.

When obtaining the CEAU-model for each interconnector capacity state, IC_k, the interconnector is modelled as being able to transfer the capacity of that state with 100% availability. Subsequently, $LOLP^U_{t,k}$ is calculated and weighted with the probability p_k of the interconnector being in state IC_k, and Bayes theorem of conditional probability can be applied. With this approach, the procedure employs the same logic no matter which of the aforementioned cases arise when transforming the EAU-model into a CEAU-model. A drawback to this procedure is that it does not produce one unique $COPT^U_t$ that comprehensively models the generation in System A when assisted through multiple states of the interconnector. Several $COPT^U_{t,k}$ are produced, which are mere intermediate models. For LOLP/LOLE-calculations, this approach yields correct results. Calculating EENS for interconnected systems however, requires a single unique $COPT^U_t$ because each outage state leading to a capacity deficiency has to be evaluated from a unique COPT when calculating EENS; this warrants an alternative approach. $COPT^U_t$ can be obtained by considering the probabilities of the interconnector states directly when going from a EAU-model to a CEAU-model. This approach is also applicable to LOLE-calculations, and will be referred to as the "direct CEAU approach". More on this is explained in Section 3.3.1.1.

[6] A, B, EAU, $CEAU$, U are used as superscripts pointing to assisted system, assisting system, EAU, CEAU and unified system, respectively. The superscripts are used by a variety of other symbols in the form $COPT^{Sup.}_{t,k}$, $x^{Sup.}_{t,j,k}$, $a^{Sup.}_{t,j,k}$, etc. The subscript t is only used for symbols that describe something that is dependent on the time increment that is being considered. Similarly, k is only used for symbols that describe something dependent on which state the interconnector is in.

The interconnector in the example (Table 3.5) has two capacity states. First, $IC^{7}_{k=2}$, which has a capacity of 10MW, will be evaluated. Maximum assistance from the CEAU is in this case constrained to 10MW, which can be achieved from any of the two first outage states in $COPT_t^{EAU}$: $x_{t,j=1}^{EAU}$ and $x_{t,j=2}^{EAU}$. The probability of having 10MW assistance, or equivalently 0MW on outage, in $COPT_{t,k=2}^{CEAU}$ is therefore the sum of the probabilities of these two states, as shown in Table 3.8. Notice that the COPT for the CEAU-model differs slightly from COPTs shown earlier for generators, in that only the individual probability is shown, not the cumulative probability. This is because the CEAU will be added to the COPT of System A as a multi-state generator, so the cumulative probability is not needed.

Table 3.8: Transforming the EAU-model into a CEAU-model for a 10MW interconnector.

(a) Intermediate CEAU-assistance probability table.

State j	Cap. out. $x_{t,j}^{EAU}$ [MW]	Assistance $a_{t,j,k=2}^{CEAU}$ [MW]	Ind. prob. $p(X = x_{t,j,k=2}^{CEAU})$
1	0	10	0.90392080
2	10	10	0.07378945
3	20	0	0.02228975

(b) Assistance probability table for the CEAU.

State j	Assistance $a_{t,j,k=2}^{CEAU}$[MW]	Ind. prob. $p(X = a_{t,j,k=2}^{CEAU})$
1	10	0.97771025
2	0	0.02228975

(c) CEAU-model, $COPT_{t,k=2}^{CEAU}$.

State j	Cap. outage $x_{t,j,k=2}^{CEAU}$[MW]	Ind. prob. $p(X = x_{t,j,k=2}^{CEAU})$
1	0	0.97771025
2	10	0.02228975

If the interconnector capacity is 15MW instead, the resulting $COPT_{t,k=2}^{CEAU}$ would be as shown in Table 3.9. As opposed to the case of Table 3.8, $x_{t,j=1}^{EAU}$ and $x_{t,j=2}^{EAU}$ cannot be merged into one assistance state in the CEAU-model, as each of these result in a distinct state. Outage states in the CEAU-model are defined from the point of view of the maximum possible assistance in the CEAU-model. In this specific case, the interconnector capacity is smaller than the largest assistance state in the EAU-model,

$a^{EAU}_{t,j=1}$. The maximum outage state, $x^{CEAU}_{t,j=J,k=2}$, in $COPT^{CEAU}_{t,k=2}$ is therefore constrained to 15MW, i.e., the interconnector capacity. Since the other CEAU-outage states are defined with reference to the maximum CEAU-outage state, the 10MW outage state in the EAU-model, $x^{EAU}_{t,j=2}$, translates to a 5MW outage state in the CEAU-model, $x^{CEAU}_{t,j=2,k=2}$. This is because $x^{EAU}_{t,j=2} = 10MW$ supplies 10MW of assistance out of a maximum of 15MW that can be achieved from the CEAU-model in this specific case.

Table 3.9: Transforming the EAU-model into a CEAU-model for a 15MW interconnector.

(a) Intermediate CEAU-assistance probability table.

State j	Cap. out. $x^{EAU}_{t,j}$ [MW]	Assistance $a^{CEAU}_{t,j,k=2}$ [MW]	Ind. prob. $p(X = a^{CEAU}_{t,j,k=2})$
1	0	15	0.90392080
2	10	10	0.07378945
3	20	0	0.02228975

(b) Assistance probability table for the CEAU.

State j	Assistance $a^{CEAU}_{t,j,k=2}$[MW]	Ind. prob. $p(X = a^{CEAU}_{t,j,k=2})$
1	15	0.90392080
2	10	0.07378945
3	0	0.02228975

(c) CEAU-model, $COPT^{CEAU}_{t,k=2}$.

State j	Cap. outage $x^{CEAU}_{t,j,k=2}$[MW]	Ind. prob. $p(X = x^{CEAU}_{t,j,k=2})$
1	0	0.90392080
2	5	0.07378945
3	15	0.02228975

Step 4: Each $COPT^{CEAU}_{t,k}$ is added to $COPT^{A}$ as a multi-state unit by using Equation (3.4). This yields $COPT^{U}_{t,k}$. An $LOLP^{U}_{t,k}$ can then be calculated for each interconnector state, k. Since the interconnector only can be in one of its multiple states at a given time, the events are mutually exclusive, and Bayes theorem of conditional probabilities can be used. The conditional probability rule states that: if the occurrence of an event A is dependent on a number, n, of events, B_s, which are mutually exclusive, then:

$$P(A) = \sum_{s=1}^{n} P(A|B_s) \cdot P(B_s) \tag{3.16}$$

Event $P(A)$ in Equation (3.16) corresponds to $LOLP_t^U$, $P(A|B_s)$ to $LOLP_{t,k}^A$ and $P(B_s)$ to p_k. Equation (3.16) shows that intermediate LOLPs are weighted by the probabilities of corresponding interconnector states as shown in Equation (3.17).

$$LOLP_t^U = \sum_{k=1}^{K} LOLP_{t,k}^U \cdot p_k \tag{3.17}$$

Adding the two-state unit represented by $COPT_{t,k=2}^{CEAU}$ to $COPT^A$ results in $COPT_{t,k=2}^U$ shown in Table 3.10.

Table 3.10: $COPT_{t,k=2}^U$ for LOLE-calculations.

State j	Cap. out. $x_{t,j,k=2}^U$[MW]	Ind. prob $p(X = x_{t,j,k=2}^U)$	Cum. prob. $P(X \geq x_{t,j,k=2}^U)$
1	0	0.86609718	1.00000000
2	10	0.10812247	0.13390282
3	20	0.00562205	0.02578036
4	25	0.01767545	0.02015830
5	30	0.00015585	0.00248285
6	35	0.00220658	0.00232699
7	40	0.00000242	0.00012042
8	45	0.00011474	0.00011799
9	50	0.00000002	0.00000325
10	55	0.00000318	0.00000323
11	60	0.00000000	0.00000005
12	65	0.00000004	0.00000005
13	75	0.00000000	0.00000000
14	85	0.00000000	0.00000000

With L_t^A =50MW, $LOLP_{t,k=2}^U$ can be found from Table 3.10, by using Equation (3.5): $LOLP_{t,k=2}^U$ =0.00012042.

$LOLP_{t,k=1}^U$, representing the LOLP in System A when the interconnector is down, can be found from $COPT^A$ in Table 3.6, as this interconnector state is equal to System A being isolated from System B: $LOLP_{t,k=1}^U$ =0.00199767.

Using Equation (3.17) now gives:

$$LOLP_t^U = LOLP_{t,k=1}^U \cdot p_{k=1} + LOLP_{t,k=2}^U \cdot p_{k=2}$$
$$= 0.00199767 \cdot 0.00815217 + 0.00012042 \cdot 0.99184783 = 0.00013572$$

Step 5: Steps 1-4 have shown how to calculate the LOLP for System A when assisted by System B, for one time increment, i.e., $LOLP_t^U$. These steps must be executed for every time increment in the load model used, and the LOLPs can be summed up to give $LOLE^U$, as in Equations (3.8)-(3.9).

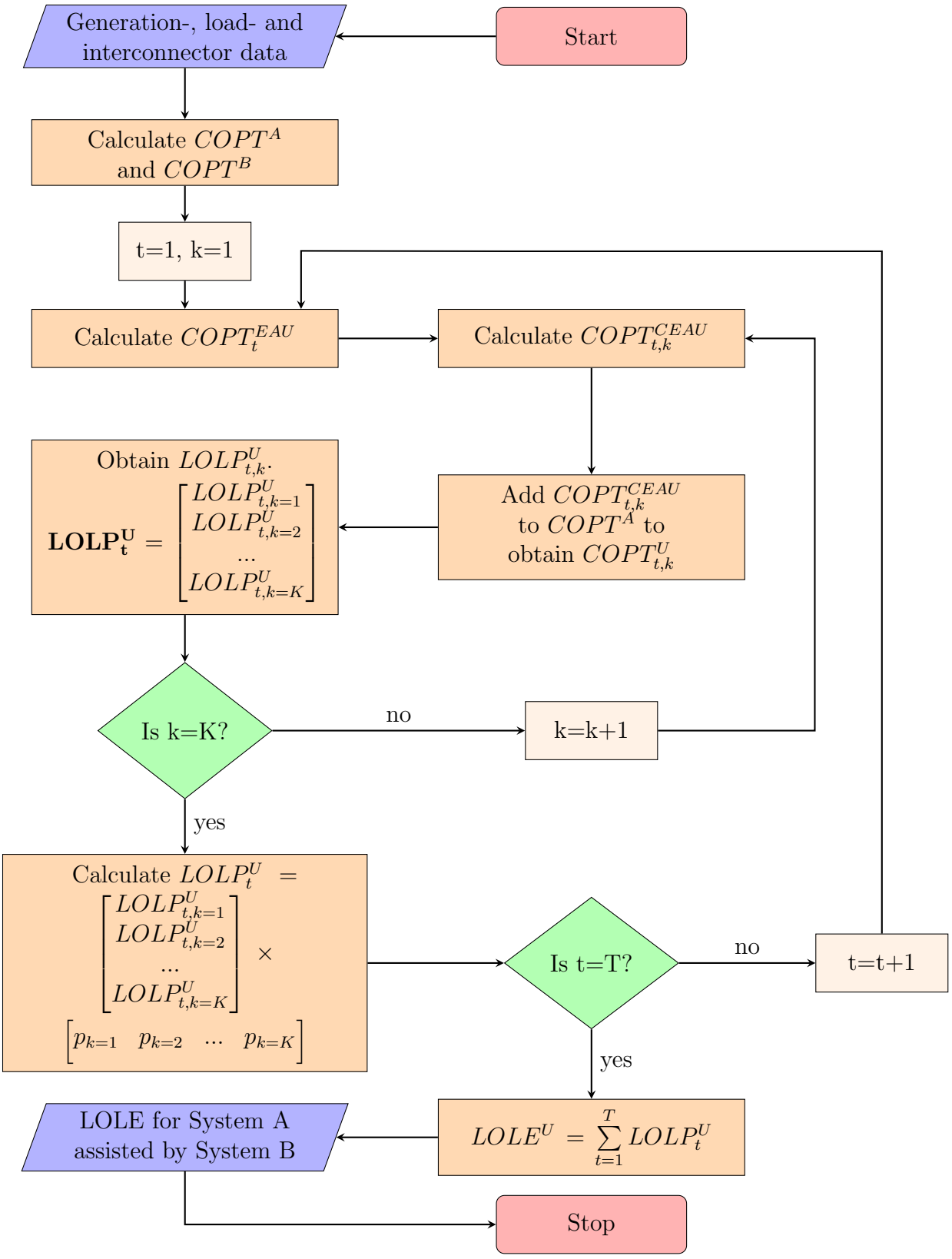

Figure 3.4: Flowchart showing the EAU-approach for obtainment of LOLE for two interconnected systems.

3.3.1.1 Direct CEAU approach

The EAU-procedure described above was for calculating LOLE, but it can also be adjusted to calculate EENS for interconnected systems. These EENS-calculations require direct incorporation of interconnector state probabilities into the CEAU-model in Step, i.e., the use of the "direct CEAU approach". As mentioned above, this approach is needed because calculating EENS for interconnected systems requires a single unique $COPT_t^U$ for each time increment because each outage state leading to a capacity deficiency has to be evaluated from a unique COPT when calculating EENS. The direct CEAU approach provides the needed unique $COPT_t^{CEAU}$ for each time increment, on which the EENS-procedure in Equation (3.11) can be applied. The direct CEAU approach can also be applied when performing LOLE-calculations for interconnected systems, i.e., LOLE-calculations utilizing the direct CEAU approach will yield the same results as those obtained in Section 3.3.1 using Bayes theorem of conditional probabilities to handle interconnector capacity state probabilities. Both methods have been implemented in MATLAB, and it was verified that they yield the same results.

The direct CEAU approach is described in Algorithm 4 in Appendix C, and illustrated here by continuing with the same example as for the LOLE-calculations. The EAU-tables in Tables 3.7b-3.7c have to be transformed into a CEAU-model by taking into account the interconnector state probabilities. For the 10MW interconnector from Table 3.5, the possible CEAU-states will be the same as in Tables 3.8b-3.8c, but with different probabilities. Two separate events can cause zero assistance from the CEAU, $a_{t,j=J}^{CEAU}$=0: If the interconnector is down, $IC_{k=1}$, there will be zero assistance from the CEAU regardless of the EAU; and if zero assistance is provided by the EAU, $a_{t,j=J}^{EAU}$, there will be zero assistance from the CEAU regardless of which state the interconnector is in. The probability of having zero assistance in the CEAU-model is therefore the sum of the probabilities of the interconnector being down and the conditional probability of zero assistance being provided from the EAU-model, given that the line is up: $p(X = a_{t,j=J}^{CEAU}) = p_{k=1} + p(X = a_{t,j=J}^{EAU}) \times p_{k=2}$.

For assistance of 10MW from the CEAU-model to be possible, the interconnector must be

up, and either 10MW or 20MW must be supplied from the EAU-model. The probability of having 10MW assistance from the CEAU-model is therefore obtained by $p(X = a^{CEAU}_{t,j=1}) = p_{k=2}[p(X = a^{EAU}_{t,j=1}) + (p(X = a^{EAU}_{t,j=2}))]$. The CEAU assistance probability table (a) and CEAU-model (b) are shown in Table 3.11. Comparing these tables with Tables 3.8a-3.8b shows the differences in probability values for the CEAU-model that is to be added to $COPT^A$: since interconnector state probabilities are already weighted when using the approach explained in this paragraph, the probability of having zero assistance/maximum outage is larger, as it is factored in that the interconnector can be down. In the approach explained for LOLE, the conditional probability approach, the probability of the interconnector being down is included by weighting the $LOLP^U_{t,k}$ by $p_{k=1}$. Adding the CEAU-model as a multi-state generator to $COPT^A$ results in $COPT^U_t$, shown in Table 3.12.

Table 3.11: Transforming an EAU-model into a CEAU-model for EENS-calculations.

(a) Assistance probability table for CEAU.

State j	Assistance $a^{CEAU}_{t,j}$[MW]	Ind. prob. $p(X = a^{CEAU}_{t,j})$
1	10	0.96973979
2	0	0.03026021

(b) CEAU-model, $COPT^{CEAU}_t$.

State j	Cap. outage $x^{CEAU}_{t,j}$[MW]	Ind. prob. $p(X = x^{CEAU}_{t,j})$
1	0	0.96973979
2	10	0.03026021

For $L^A_t = 50MW$, the reserve in the assisted System A is 35MW. It follows that outage states $x^U_{t,j=7}$ to $x^U_{t,j=14}$ yield a capacity deficit. Individual probabilities of outage states 11, 13 and 14 is rounded to zero, and Equation (3.11) yields:

$$\begin{aligned} EENS^U_t &= 5 \cdot 0.00000302 + 10 \cdot 0.00012884 + 15 \cdot 0.00000003 + 20 \cdot 0.00000377 + 30 \cdot 0.00000006 \\ &= 0.00138115 \end{aligned}$$

The calculated $EENS^U_t$ is for the time-increment, t, with duration of one hour. $EENS^U$ for this time increment is therefore 0.00138115MWh. EENS can be calculated for each time increment, and Equation (3.12) can be used to give the annual EENS in MWh/year.

The direct CEAU approach also includes all possible states of the interconnector in a single CEAU-model. For a case with an interconnector with three possible capacity states as shown

Table 3.12: $COPT_t^U$ for EENS-calculations.

State j	Cap. out. $x_{t,j}^U$[MW]	Ind. prob $p(X = x_{t,j}^U)$	Cum. prob. $P(X \geq x_{t,j}^U)$
1	0	0.85903660	1.00000000
2	10	0.11446258	0.14096340
3	20	0.00631311	0.02650082
4	25	0.01753136	0.02018771
5	30	0.00018466	0.00265635
6	35	0.00233597	0.00247169
7	40	0.00000302	0.00013572
8	45	0.00012884	0.00013270
9	50	0.00000003	0.00000386
10	55	0.00000377	0.00000383
11	60	0.00000000	0.00000006
12	65	0.00000006	0.00000006
13	75	0.00000000	0.00000000
14	85	0.00000000	0.00000000

in Table 3.14, the interconnector capacity states alone would yield three distinct states in the CEAU-model. Potential assistance states from the EAU-model, which have assistance levels that fall between the capacity states from the interconnector, i.e., $IC_k \leq a_{t,j}^{EAU} \leq IC_{k+1}$ will also create distinct states in the CEAU-model. Continuing with the EAU-model in Tables 3.7b-3.7c, $a_{t,j=2}^{EAU}$ will create a distinct assistance state in the CEAU-model with probability $p(X = a_{t,j=2}^{EAU}) \cdot [p_{k=2} + p_{k=3}]$. In Table 3.13a, it is shown how the assistance states in the EAU-model and capacity states for the interconnector are combined to yield the different resulting assistance states in the CEAU-model. The nine cells in Table 3.13a each represent such combinations. Each cell has two entries: the top one indicates the assistance in megawatts for the combination; and the bottom one indicates the individual probability of the particular combination of interconnector capacity state and EAU-model assistance state. Several combinations can result in the same assistance state in the CEAU-model, and the probabilities of these combinations must be added to get the total probability of the particular CEAU-model assistance state.

Table 3.13: Transforming the EAU-model into a CEAU-model for a multi-state, 20MW interconnector.

(a) Combining a multi-state interconnector with an EAU-model to create a CEAU-model.

		Interconnector cap. states, IC_k [MW]		
		0	15	20
Cap. out. states of EAU-model $a_{t,j}^{EAU}$ [MW]	0	0 0.00000148	0 0.00036046	0 0.02192781
	10	0 0.00000490	10 0.00119328	10 0.07259127
	20	0 0.00006007	15 0.01461769	20 0.88924303

(b) Assistance probability table for the CEAU.

State j	Assistance $a_{t,j}^{CEAU}$[MW]	Individual prob. $p(X = a_{t,j}^{CEAU})$
1	20	0.88924303
2	15	0.01461769
3	10	0.07378455
4	0	0.02235472

(c) CEAU-model, $COPT_t^{CEAU}$.

State j	Cap. outage $x_{t,j}^{CEAU}$[MW]	Individual prob. $p(X = x_{t,j}^{CEAU})$
1	0	0.88924303
2	5	0.01461769
3	10	0.07378455
4	20	0.02235472

Table 3.14: Multi-state interconnector data for EENS-example.

State k	Interconnector cap. IC_k [MW]	Prob. p_k
1	0	0.00006646
2	15	0.01617143
3	20	0.98376211

3.3.2 Alternative method for adequacy of interconnected systems: The Probability Array method

The Probability Array (PA) method model combines the two COPTs for the systems into a two-dimensional array, containing probabilities of all possible capacity outage combinations [20]. Each cell in the array has two values: the probability of the event of X MW outage in System A at the same time as Y MW outage in System B; and the corresponding capacity deficit in System A when taking into account potential assistance from System B. To compute the capacity deficit, the load level L_t for the time increment under evaluation is used, as well as the assumption that the interconnector can deliver its capacity, IC_k, with 100% reliability. The probabilities of all resulting loss-of-load situations in System A are summed up to obtain the LOLP for the 100% reliable interconnector state, k, for time increment t. As for the EAU-method, the LOLPs are weighted by interconnector state probabilities to obtain the unified LOLP, and LOLP for all time increments are summed up to give LOLE. The PA method is considered more computationally intensive and less flexible than the EAU-approach [26], and has not been used in this thesis.

Chapter 4

Proposed de-rating approach: Interconnector Effective Load Carrying Capability

As mentioned in the introduction, this thesis builds on the work done in [7], regarding a proposal for a new de-rating approach for interconnectors participating in CMs. In [7], Interconnector Effective Load Carrying Capability was conceptualized for the purpose of probabilistic interconnector de-rating; the IELCC metric was founded on LOLE quantification in the interconnected system. Further, preliminary results were demonstrated on a very simple interconnected test system with a constant load profile. However, to corroborate the effectiveness and applicability of the IELCC metric for large scale systems with chronological variations in load profiles, a clear algorithmic approach with modularity in design is warranted. The proposition in this chapter caters to this identified need; several well-established PSR-concepts that were presented in Chapter 3 are embedded into the proposed approach, using a distinct nomenclature.

In light of the recommendations in [22], a procedure for obtaining IELCC with EENS as the guiding adequacy metric is also presented in this chapter, thus expanding the framework for

probabilistic interconnector de-rating. Illustration of the proposition is limited to IELCC with LOLE for a two bus interconnected system in this chapter. However, the developed framework is applied to larger interconnected test systems in the next chapter, where both LOLE and EENS are used as the guiding reliability index for the IELCC.

4.1 Methodology for obtaining IELCC using LOLE

It is postulated in [7] that using an adapted form of ELCC will be a fitting metric to quantify an interconnector's impact on the reliability of an assisted system. This is justified by ELCC's proven robustness for de-rating of wind generators [47], and the fact that it can be expanded to take into account the characteristics of the assisted system. This is done through the utilization of the Equivalent Assisting Unit method for the calculation of LOLE, which was the reliability index used for the ELCC-calculations in [7]. The proposed procedure is referred to as Interconnector Effective Load Carrying Capability (IELCC), and it is summarized in the following steps:

Step 1: Use either of the two approaches that were explained in Sections 3.3.1 and 3.3.1.1 to obtain LOLE for the system receiving assistance through the interconnector[1].

a) Obtain COPT of System A and System B, $COPT^A$ and $COPT^B$, respectively.

b) For time increment, t:

i) Merge $COPT^B$ and the interconnector model to get $COPT_t^{CEAU}$.

ii) Add $COPT_t^{CEAU}$ to $COPT^A$ as a multi-state unit to get $COPT_t^U$.

iii) Use $COPT_t^U$ and the load-model for System A to compute $LOLP_t^U$.

c) Repeat steps a) and b) for all time increments in the load model for System A to calculate $LOLE^U$ when assisted by System B through the interconnector.

[1]The IELCC-procedure is only described for use of the direct method from Section 3.3.1.1; however, only some adjustments to Step 1 have to be done if the approach from Section 3.3.1 is preferred.

Step 2: Plot the peak load vs. LOLE curves for both the original isolated System A and for the assisted System A to calculate the ELCC as described in Section 3.2.1.

a) Create time/load-series for System A, represented by its peak load, by scaling the original time/load-series.

b) Calculate LOLE-values for the stand-alone system for the time/load-series, and plot the peak load vs. $LOLE^A$ curve showing the relation between the peak load in the time/load-series and LOLE values.

c) Repeat entire Step 1 for each time/load-series and plot the peak load vs. $LOLE^U$ curve showing the relation between the peak load in the series and LOLE values for the assisted System A.

d) Obtain ELCC for the chosen reliability level. This level can either be a predefined reliability standard, e.g., LOLE of 0.1 days/year, or it can be the reliability level as it was in the original System A, before scaling of loads or interconnection. The ELCC is obtained as the horizontal distance between the two intersections of the chosen reliability level and the peak load vs. LOLE curves. This horizontal distance, representing the additional load that can be served in System A as a result of the interconnection, is the Interconnector Effective Load Carrying Capability (IELCC). The obtained IELCC serves as the de-rated capacity of the interconnector.

The methodology is illustrated by means of the same simple example that was used in Section 3.3.1: The two systems in Table 4.1 interconnected by the interconnector in Table 4.2. For the purpose of illustration, a CYPL-model is used, considering a constant peak load of 50MW and 40MW throughout the year for Systems A and B, respectively. By use of the EAU-approach, $COPT^U$ is obtained and showed in Table 4.3a. For results from intermediate steps, i.e., Steps 1.a)-c) of the IELCC-approach, the reader is referred to Section 3.3.1. Since the CYPL-model is used, LOLP and LOLE values will be the same, and the LOLE-values can be read directly from $COPT^U$. The units will be *yearly peaks/year*, as it describes the expected number of yearly peaks which will be lost because of capacity outages.

Table 4.1: Generation and load data for Systems A and B.

System	Number of units	Unit cap. [MW]	Unit FOR	Installed cap. [MW]	Daily peak load [MW]
A	5	10	0.02	75	50
	1	25	0.02		
B	4	10	0.02	60	40
	1	20	0.02		

Table 4.2: Interconnector data for the two bus test system.

State k	Interconnector cap. IC_k[MW]	Probability p^k
1	0	0.00815217
2	10	0.99184783

The peak load vs. LOLE curves/IELCC-plot for the stand-alone case (blue curve) and the interconnected case (red curve) are shown in Figure 4.1. The LOLE of the stand-alone System A with 50MW CYPL is 0.001998 yearly peaks/year, and LOLE=0.001998 as the chosen reliability level yields an IELCC of 2.32MW. Considering the interconnector capacity of 10MW, 2.32MW is fairly low. It is therefore important to point out that this is only an illustrative example. A CYPL-model is used, which can yield pessimistic results, as mentioned in Section 3.1.1. The initial IELCC-results, obtained in [7], were all based on a CYPL-model. This thesis improves on this, by expanding the framework DPL- and HPL-models for obtaining IELCC for larger test systems. These results are shown in Section 5.2.

4.2 Methodology for obtaining IELCC using EENS

The methodology for obtaining IELCC when using EENS as the guiding adequacy metric is very similar to the one explained in the previous section, where LOLE was used. The procedure for obtaining IELCC with EENS as the guiding metric is presented as follows:

Table 4.3: $COPT^U$ (a) and resulting LOLE for various peak loads (b) for the assisted system.

(a) $COPT^U$.

State j	Cap. out. x_j^U[MW]	Ind. prob $p(X = x_j^U)$	Cum. prob. $P(X \geq x_j^U)$
1	0	0.86609718	1.00000000
2	10	0.10812247	0.13390282
3	20	0.00562205	0.02578036
4	25	0.01767545	0.02015830
5	30	0.00015585	0.00248285
6	35	0.00220658	0.00232699
7	40	0.00000242	0.00012042
8	45	0.00011474	0.00011799
9	50	0.00000002	0.00000325
10	55	0.00000318	0.00000323
11	60	0.00000000	0.00000005
12	65	0.00000004	0.00000005
13	75	0.00000000	0.00000000
14	85	0.00000000	0.00000000

(b) $LOLE^U$ for different CYPLs.

CYPL [MW]	Reserve R^U[MW]	LOLE yearly peaks/year
25	60	0.00000005
30	55	0.00000005
35	50	0.00000323
40	45	0.00000325
45	40	0.00011799
50	35	0.00012042
55	30	0.00232699
60	25	0.00248285
65	20	0.02015830
70	15	0.02578036
75	10	0.02578036
80	5	0.13390282
85	0	0.13390282
90	-5	1.00000000

Step 1: Use the direct CEAU approach that was explained in Section 3.3.1.1 to obtain EENS for the system receiving assistance through the interconnector.

a) Obtain COPT of System A and System B, $COPT^A$ and $COPT^B$, respectively.

b) For time increment, t:

i) Merge $COPT^B$ and the interconnector model to get $COPT_t^{CEAU}$.

ii) Add $COPT_t^{CEAU}$ to $COPT^A$ as a multi-state unit to get $COPT_t^U$.

iii) Use $COPT_t^U$ and the load-model for System A to compute $EENS_t^U$.

c) Repeat steps a) and b) for all time increments in the load model for System A to calculate $EENS^U$ when assisted by System B through the interconnector.

Step 2: Plot the peak load vs. EENS curves for both the original isolated System A and for the assisted System A to calculate the ELCC as described in Section 3.2.1.

a) Create time/load-series for System A, represented by its peak load, by scaling the original time/load-series.

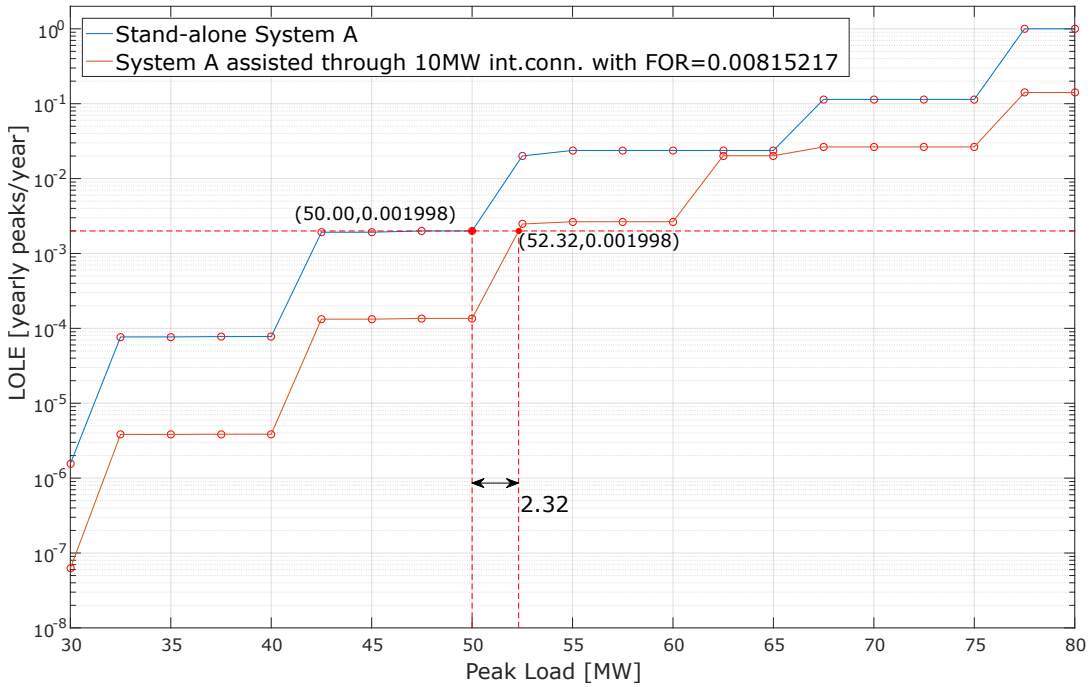

Figure 4.1: $IELCC_{LOLE}$-plot for the two bus system, using a 50MW CYPL-model.

b) Calculate EENS-values for the stand-alone system for the time/load-series, and plot the peak load vs. $EENS^A$ curve showing the relation between the peak load in the time/load-series and EENS values.

c) Repeat entire Step 1 for each time/load-series and plot the peak load vs. $EENS^U$ curve showing the relation between the peak load in the series and EENS values for the assisted System A.

d) Obtain ELCC for the chosen reliability level. As reliability standards for EENS are not as common as for LOLE, the reliability level used is the EENS level as it was in the original System A, before scaling of loads or interconnection. The ELCC is obtained as the horizontal distance between the two intersections of the chosen reliability level and the peak load vs. EENS curves. This horizontal distance is the IELCC, and serves as the de-rated capacity of the interconnector.

4.3 MATLAB-scripts

For the purpose of testing the methodology for systems of larger scale than in [7], scripts were implemented in MATLAB [50]. The scripts take load-, generation and interconnector data as input and are able to output LOLE, EENS and IELCC for both stand-alone and interconnected systems. These scripts have been released for further internal use and research in the Department of Electric Power Engineering. Pseudocode for the scripts is shown in Appendix C.

Chapter 5

Case study: Utilizing the IELCC-methodology for test systems

5.1 Case study data: Test systems

The main analysis in this chapter is done on the Roy Billinton Test System (RBTS). Some results based on the two-bus test-system presented in Tables 3.4-3.5, as well as on the IEEE-RTS are also included, but the main emphasis is on the RBTS.

5.1.1 RBTS

The RBTS stems from the reliability education programs conducted by the Power Systems Research Group at the University of Saskatchewan. It provides the basic system data needed to conduct adequacy studies at generation level (HLI), and at generation and transmission system level (HLII) [51]. RBTS offers an alternative to the IEEE Reliability Test System (RTS) which is about 15 times larger [52]. The main objective of the RBTS is [51] *"to make it sufficiently small to permit the conduct of a large number of reliability studies with reasonable solution time but sufficiently detailed to reflect the actual complexities involved in*

a practical reliability analysis." This is also the rationale behind choosing this as the test system for case studies, e.g., over the IEEE-RTS. If scripts that should be able to handle the IEEE-RTS with reasonable solution times were to be produced as part of the thesis work, this task would have become the main focus of the thesis work, and not the interconnector de-rating methodology. The RBTS is believed to be sufficiently detailed to showcase IELCC's performance for a realistic system.

The RBTS is a 6 Bus system with 9 transmission lines, a generating capacity of 240MW and a peak load of 185MW. Since the system is also designed for HL2-studies and cost/reliability-studies, it includes outage- and impedance data for the transmission lines as well as fuel-, operation- and capital costs for the generators. Since the studies in this thesis are concerned with evaluating generation adequacy, only the load data and generation data will be utilized.

Generation data

The generation fleet in the RBTS consists of 11 generating units, ranging from 5MW to 40MW. Generation unit data is shown in Table 5.1. Compared to the availability/DRFs in Tables 2.1-2.3, the generators in the RBTS have a high availability.

Table 5.1: Generator data for the RBTS generation fleet.

Unit size [MW]	Number of units	Forced outage rate	Availability %
5	2	0.010	99.0
10	1	0.020	98.0
20	4	0.015	98.5
20	1	0.025	97.5
40	1	0.020	98.0
40	2	0.030	97.0

The resulting COPT for the RBTS can be seen in Table 5.2a. Figure 5.2b shows an alternative representation of the generation probability, illustrating that the probability is clearly largest for having 240MW of generation at a given instance.

Load data

Several load-models can be constructed from the load-data in the RBTS. The base case yearly peak load is 185MW, weekly peak load is given in percentage of yearly peak load, daily peak load is given in percentage of the weekly peak load and hourly peak load is given in percentage of the daily peak load. These percentage values are the same as for the IEEE-RTS [52]. The full load data is included in Tables A1-A3 in Appendix A. Hourly load, HPL, for a specific hour, h, of a specific day, d, of a specific week, w, can be found by multiplying percentage values, l, and base case yearly peak load as in Equation (5.1). A DPL-model can be obtained the same way, by not multiplying with the hourly percentage values. The HPL-model for a year will have 8736 hourly load levels (52 weeks/year $\times$ 7 days/week $\times$ 24 hours/day) and the DPL-model will have 364 daily load levels (52 weeks/year $\times$ 7 days/week). Details regarding how these load levels are obtained are not given in [52], but it is a forecast based on previous experience that tries to predict typical yearly and daily load patterns.

$$HPL_{h,d,w} = l_h \cdot l_d \cdot l_w \cdot YPL \tag{5.1}$$

Table 5.2: Table and figures illustrating generation data (a)-(b) and load data (c)-(d).

State j	Cap. out x_j [MW]	Ind. prob. $p(X = x_j)$	Cum. prob. $P(X \geq x_j)$
1	0	0.81285961	1.00000000
2	5	0.01642141	0.18714039
3	10	0.01667191	0.17071898
4	15	0.00033513	0.15404707
5	20	0.07035854	0.15371194
6	25	0.00142135	0.08335340
7	30	0.00144303	0.08193205
8	35	0.00002901	0.08048902
9	40	0.06926973	0.08046001
10	45	0.00139939	0.01119028
11	50	0.00142073	0.00979090
12	55	0.00002856	0.00837017
13	60	0.00582845	0.00834161
14	65	0.00011774	0.00251316
15	70	0.00011954	0.00239541
16	75	0.00000240	0.00227587
17	80	0.00200148	0.00227347
18	85	0.00004043	0.00027199
19	90	0.00004105	0.00023155
20	95	0.00000083	0.00019050
21	100	0.00015945	0.00018968
22	105	0.00000322	0.00003023
23	110	0.00000327	0.00002701
24	115	0.00000007	0.00002374
25	120	0.00002122	0.00002367
26	125	0.00000043	0.00000245
27	130	0.00000044	0.00000202
28	135	0.00000000	0.00000158
29	140	0.00000146	0.00000157
30	145	0.00000003	0.00000011
31	150	0.00000003	0.00000008
.	.	.	.
.	.	.	.
.	.	.	.
47	230	0.00000000	0.00000000
48	235	0.00000000	0.00000000
49	240	0.00000000	0.00000000

(a) COPT for the RBTS.

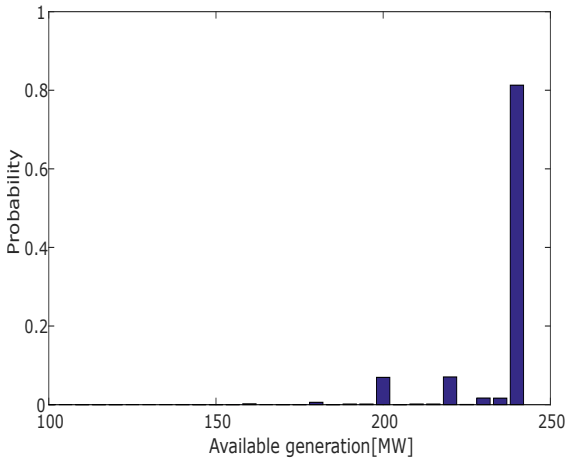

(b) Plot of available generation probability for the RBTS.

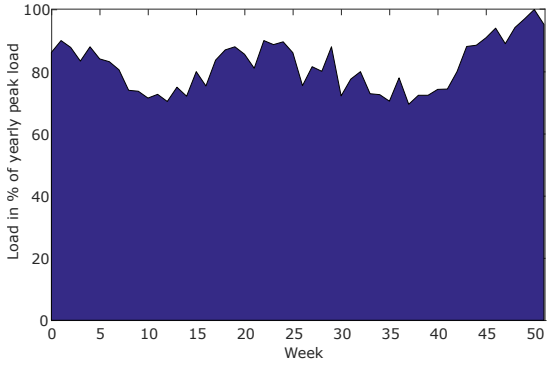

(c) Weekly peak loads in percent of the yearly peak load.

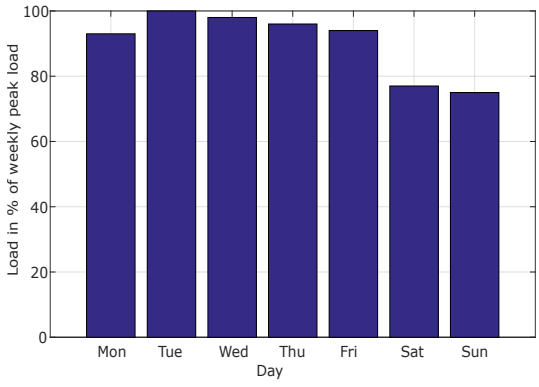

(d) Daily peak loads in percent of the weekly peak load.

5.1.2 RTS data

Since the RBTS is designed the same way as the RTS, only smaller, the RTS contains data for the same kinds of studies as the RBTS. Except the fact that the base case peak load is 2850MW, the load data is exactly the same as for the RBTS, as both systems utilize the same weekly-, daily- and hourly load percentage values. The generation fleet is more than ten times larger, with 3405MW of installed capacity. RTS-generators are shown in Table 5.3a and available generation capacity probabilities are illustrated in Figure 5.3b.

Table 5.3: RTS generator data.

Unit size [MW]	Number of units	Forced outage rate	Availability %
12	5	0.02	98.0
20	4	0.10	90.0
50	6	0.01	99.0
76	4	0.02	98.0
100	3	0.04	96.0
155	4	0.04	96.0
197	3	0.05	95.0
350	1	0.08	92.0
400	2	0.12	88.0

(a) RTS generator fleet data.

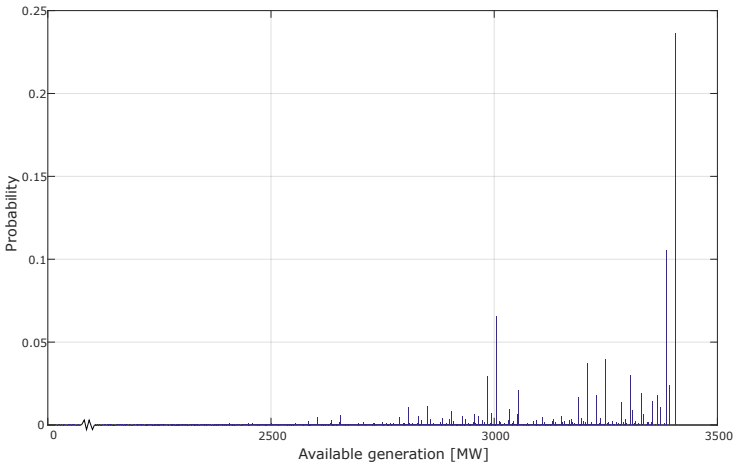

(b) Available generation probabilities for the RTS.

5.2 Case study results

This section shows IELCC-results for the different test systems, obtained by using the scripts produced in MATLAB. Results are shown both for the usage of LOLE ($IELCC_{LOLE}$) and EENS ($IELCC_{EENS}$) as the guiding reliability index. $IELCC_{LOLE}$ is shown for various load models, while $IELCC_{EENS}$ is only calculated for the HPL-model. The direct CEAU approach is used for all the results in this section.

The purpose of the case studies is to utilize the IELCC-methodology for larger test systems than what was done in the initial work [7], and to highlight subtleties in the procedure, thereby making it more transparent and comprehensible. The test systems used are described in Section 5.1, and there are a number of papers that present benchmark values for various indices, including [27, 28]. These references include benchmark-results for LOLE, LOLP', EENS and EDNS for stand-alone and/or interconnected systems, as shown in Tables 5.4-5.5. Using the same set-ups as in these references, allows for showing IELCC results for larger test systems, while simultaneously verifying the scripts' ability to calculate the various indices.

Table 5.4 shows LOLE, LOLP', EENS and EDNS for both the RBTS and RTS using an HPL-model, while Table 5.5 shows the same when using a CYPL-model. It can be seen that there is very little difference, represented in percent by ϵ, between benchmark results and the results obtained in this thesis. Further, the relation between LOLE and LOLP' is shown, the latter resulting from dividing the former by the toal number of time units considered (the same is true for the relation between EENS and EDNS). Following this, ϵ for LOLE and EENS should be equal to ϵ for LOLP' and EDNS, respectively. As can be seen in Table 5.4, this is not the case. The explanation to this is most likely that 8760 hours/year has been used as the total number of time units in the benchmark result, while the load model used in the thesis work only has 8736 hours/year.

Because LOLP' and EDNS are mere scaled versions of LOLE and EENS, respectively, only the two latter are used as reliability indices in the IELCC-plots in Sections 5.2.1-5.2.4. However, the user of the procedure is able to choose the reliability index most relevant for the system

under consideration, as it does not impose any major alterations to the procedure.

Table 5.4: Benchmark results vs. script-results for the HPL-model.

(a) LOLE and LOLP'.

	LOLE [hours/year]			LOLP'		
System	Benchmark	Script	$\|\epsilon\|$ [%]	Benchmark	Script	$\|\epsilon\|$ [%]
RBTS[28]	1.0919	1.0914	0.046	N/A	0.000125	N/A
RTS [27]	9.36881	9.39389	0.268	0.001069	0.001075	0.561

(b) EENS and EDNS.

	EENS [MWh/year]			EDNS [MW/year]		
System	Benchmark	Script	$\|\epsilon\|$ [%]	Benchmark	Script	$\|\epsilon\|$ [%]
RBTS[28]	9.8613	9.8603	0.010	N/A	0.00112869	N/A
RTS [27]	1181.195	1176.278	0.416	0.1348396	0.13464710	0.143

Table 5.5: Benchmark results vs. script-results for the CYPL-model.

(a) LOLE and LOLP'.

	LOLE [hours/year]			LOLP'		
System	Benchmark	Script	$\|\epsilon\|$ [%]	Benchmark	Script	$\|\epsilon\|$ [%]
RBTS[28]	73.0728	72.8722	0.275	N/A	0.00834	N/A
RTS	N/A	738.874	N/A	N/A	0.08458	N/A

(b) EENS and EDNS.

	EENS [MWh/year]			EDNS [MW/year]		
System	Benchmark	Script	$\|\epsilon\|$ [%]	Benchmark	Script	$\|\epsilon\|$ [%]
RBTS[28]	823.2555	821.0000	0.274	N/A	0.093979	N/A
RTS	N/A	128,364.0	N/A	N/A	14.69368	N/A

5.2.1 Two bus test system

CYPL-model

The IELCC-plot for a CYPL, originally shown in Figure 4.1, is also shown in Figure 5.1a. CYPLs of 50MW and 40MW are used in Systems A and B, respectively. The LOLE of the stand-alone System A with 50MW CYPL is 0.001998 yearly peaks/year, and LOLE=0.001998 as the chosen reliability level yields an IELCC of 2.32MW, which is fairly low for a 10MW interconnector. It has been mentioned earlier that using a CYPL-model can yield pessimistic results, as it assumes that the worst case load lasts the entire year, as shown in Figure 3.2a. However, it is debatable if it is the usage of the worst case load that gives pessimistic IELCC-results here. Both curves utilize the worst case load, and since the IELCC is the horizontal difference between the two curves, it can be argued that the IELCC shouldn't be too much affected by using worst case load. Nonetheless, there are also other aspects with the CYPL-model that influence the results. It can be seen that for a hypothetical case with a predefined LOLE-level of 0.003 yearly peaks/year as the reliability level, the resulting IELCC would be close to 10MW. This seemingly arbitrary increase of IELCC is mainly a result of using CYPL as the load model. Using a CYPL-model essentially limits the number of possible LOLE-levels to the ones found in $COPT^U$ and thereby also limits the possible LOLE-levels plotted in the curve.

The fact that possible LOLE-levels are limited, causes the configuration and unit sizes of the generators to also become significant factors as they decide the number of states in $COPT^A/COPT^U$ and the distance between each state in terms of Watts. For example it can be observed that for the peak loads between 32.5MW and 40MW in Figure 5.1a, the LOLE for the stand-alone system is almost constant. The explanation for this can be found by examining $COPT^A$ in Table 3.6. The LOLP (which is also LOLE in this case, since a CYPL-model is used) only changes for each 5MW increase in load. Both a peak load of 32.5MW and 35MW requires an outage of $x^A_{j=8}$ =45MW for a loss-of-load situation to occur, with $P(X \geq x^A_{j=8})$ =0.00007686. For peak loads of 37.5MW and 40MW, a loss-of-load situation occurs for $x^A_{j=7} = 40MW$, and $P(X \geq x^A_{j=7}) = 0.00007763$. These cumulative

probability values represent the resulting LOLE-values, and the difference between the two values are negligible, rendering the peak load vs. LOLE curve almost flat for a large peak load interval. Using DPL- or HPL-models reduces this effect, as shown by comparing Figures 5.1a and 5.2.

Figure 5.1b shows the IELCC-plot for the two bus test system when a DPL-model is used, where all daily peaks are equal to the CYPL. Comparison of Figures 5.1a and 5.1b therefore illustrates the concept of LOLE calculated with a CYPL-model being equal to LOLE calculated with a DPL-model for the unrealistic condition of having all daily loads through a year equal to the CYPL. The LOLE-level of 0.001998 yearly peaks/year in Figure 5.1a can be converted to the LOLE-level of 0.72715 days/year in Figure 5.1b by multiplication with 365 daily peaks/yearly peaks, since all daily loads in the latter case are equal to the single constant load in the first case.

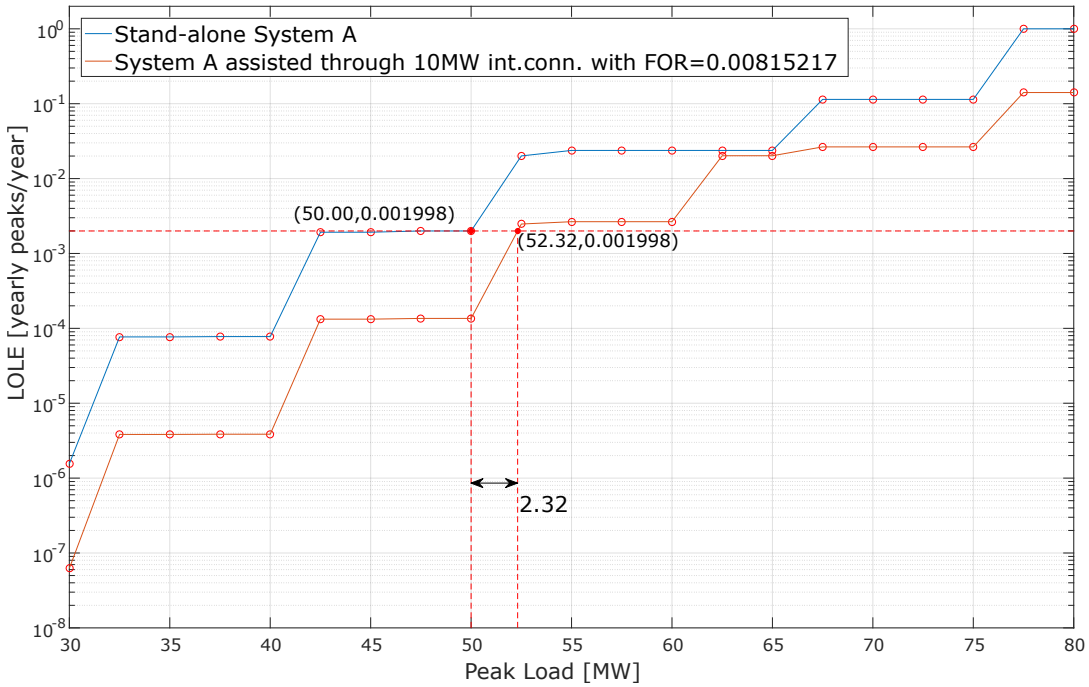

(a) $IELCC_{LOLE}$-plot for the two bus system, using CYPL-model of 50MW in System A, and 40 MW in System B.

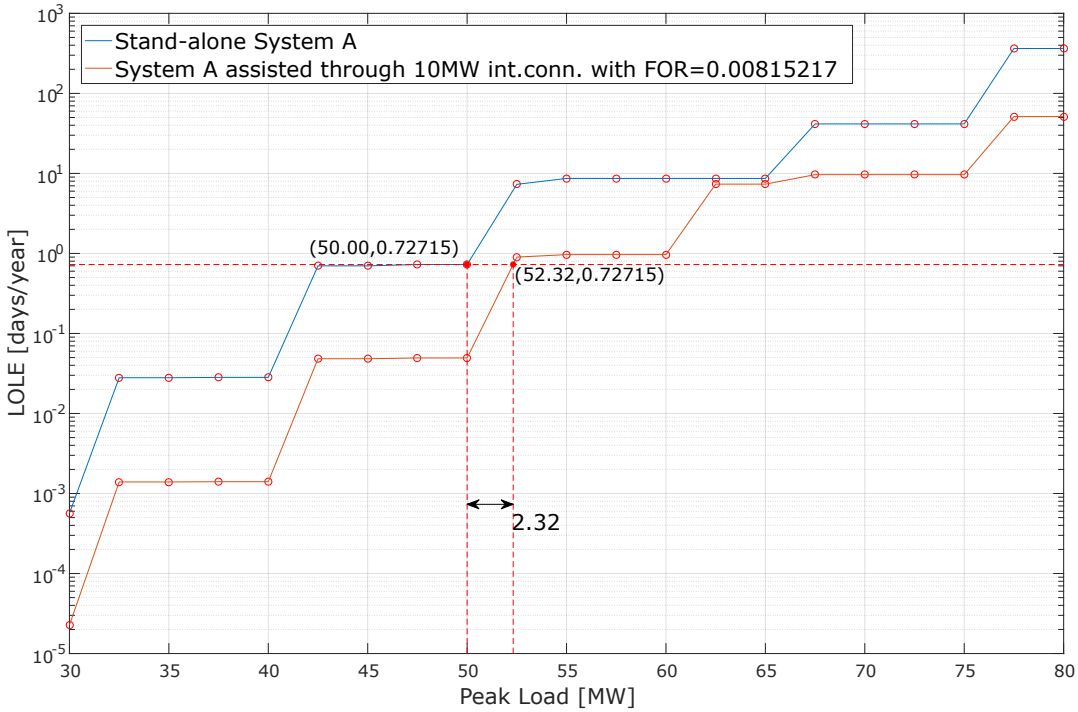

(b) $IELCC_{LOLE}$-plot for the example, using a DPL-model with all daily loads equal to 50MW (40MW CYPL in System B).

Figure 5.1: $IELCC_{LOLE}$-plots for the two bus system.

DPL-model

In Figure 5.2, a DPL-model is used, yielding more possible LOLE-levels and a less step-wise curve. The reliability standard is chosen to be 0.2463 days/year since this is the LOLE of the stand-alone system with base case peak load. The resulting IELCC is 11.20MW, meaning that the 10MW interconnector to System B improves the reliability of System A to the extent that System A can serve 11.20MW additional peak load, while still maintaining the chosen LOLE standard. This is an increase of approximately 20% from the original peak load of 50MW. It might seem non-intuitive that the IELCC can be larger than the nameplate capacity of the interconnector; however, as mentioned in Section 3.2.1, such results can be found for ELCC in literature [45]. Explanations to these results have not been found either in [45] or in other literature, but they are further examined in Section 5.3.

Further comparison of the curves in Figure 5.2 and Figure 5.1a shows that even though moving from a CYPL-model to a DPL-model increases the number of possible LOLE-levels, the effect the generation configuration has on the curve is still visible. For the peak load interval of 35MW-40MW, the LOLE-curves are more flat than they are immediately to the left or to the right of this interval. Although less obvious for the DPL-model, this is a similar pattern to that pointed out for the CYPL-model. This effect is also reduced when larger systems are evaluated, as more generators usually yield more possible outage levels in the COPT, with smaller distances between each state in terms of Watts[1].

[1]For large systems, it is common to round and lump outage states together, with a defined distance between each state in terms of Watts. This is to limit the size of the COPT for computational efficiency. This technique is not treated or utilized in this thesis work.

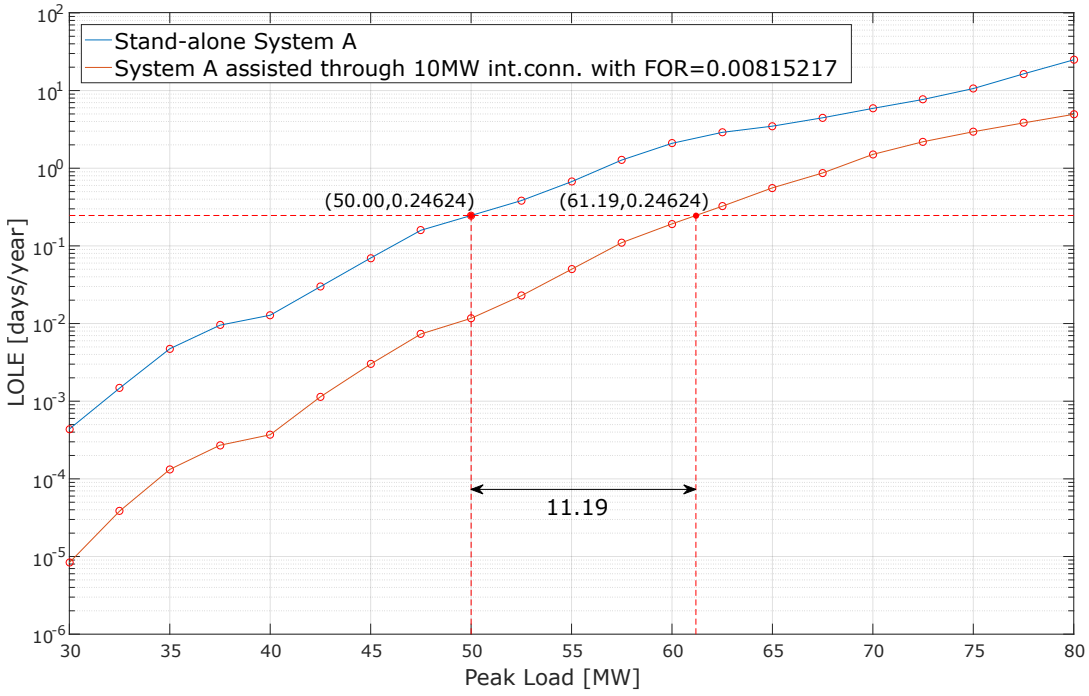

Figure 5.2: $IELCC_{LOLE}$-plot for the two bus system, using the DPL-model.

HPL-model

Moving on to an HPL-model, where 8736 hourly load points are used, results in the $IELCC_{LOLE}$- and $IELCC_{EENS}$-plots shown in Figures 5.3a and 5.3b, respectively. It can be observed that the overall shape of the peak load vs. LOLE curves is fairly similar for both the HPL- and DPL-cases, while $IELCC_{LOLE}$ increases by approximately 5%, from 11.19MW to 11.71MW. This is a much smaller increase than the one between CYPL- and DPL-model, as the shape of the curves for the DPL- and HPL-cases is more similar than for the CYPL- and DPL-cases.

When comparing Figures 5.3a and 5.3b, it can be seen that the $IELCC_{EENS}$-curves are smoother and closer to being parallel than for $IELCC_{LOLE}$. It can also be observed that $IELCC_{EENS}$ is slightly smaller than $IELCC_{LOLE}$, at 11.27MW, compared to 11.71MW. This difference, of about 4%, is not very large, but it is fully possible to have dissimilar results when different indices of reliability standards are used [45]. However, ELCC for LOLE and EENS have been showed to produce similar results [53].

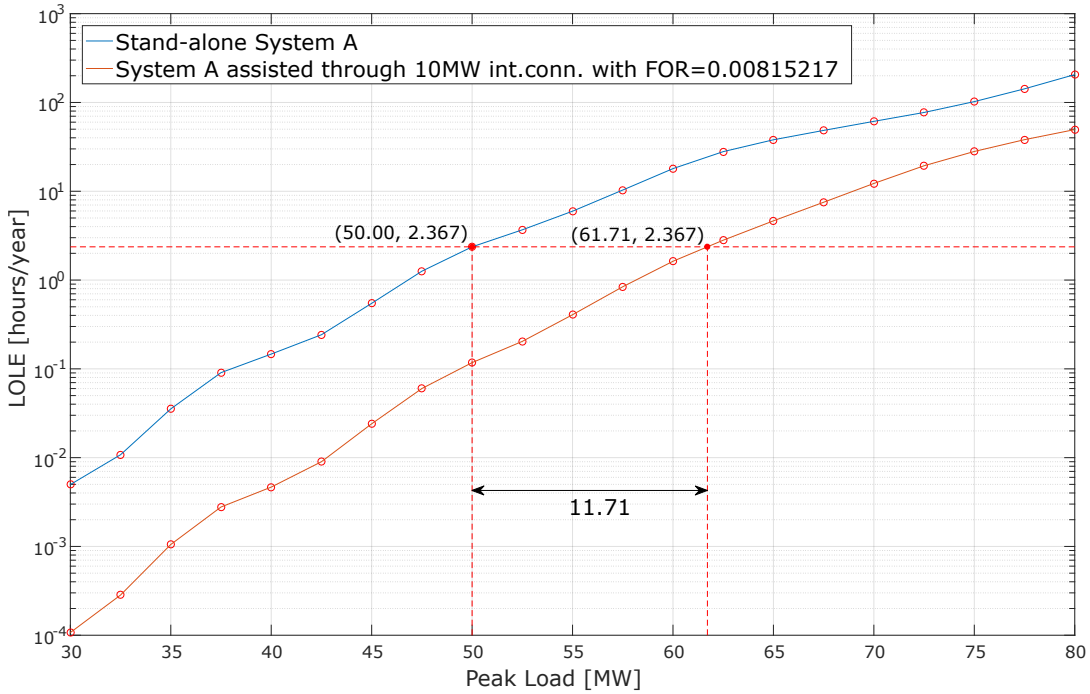

(a) $IELCC_{LOLE}$-plot for the two bus test system, using the HPL-model.

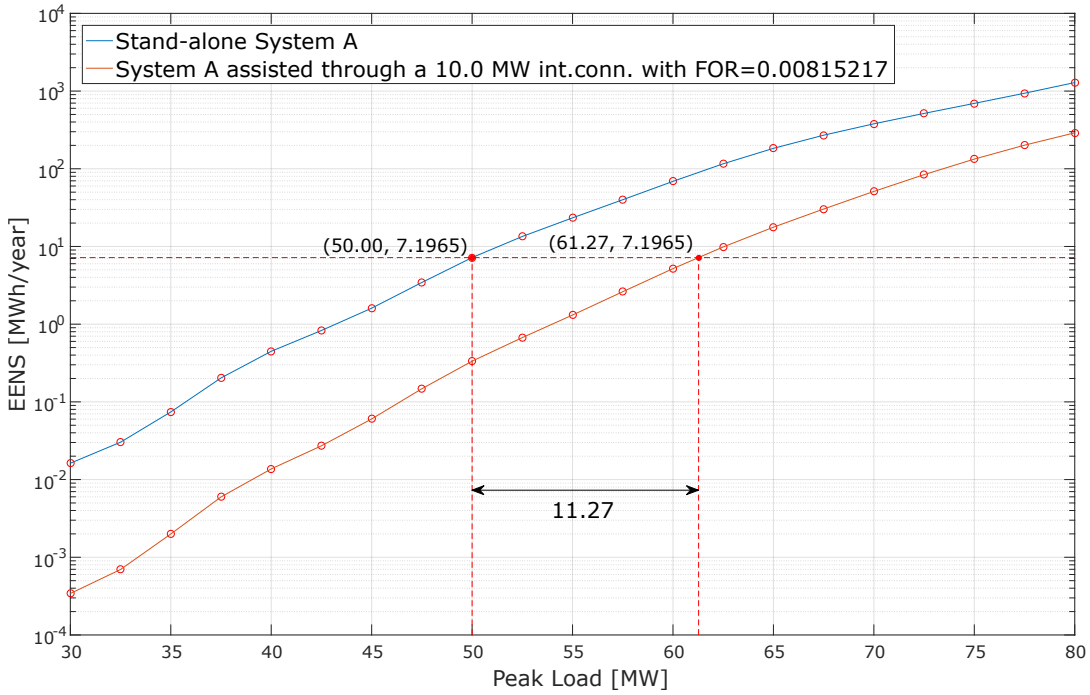

(b) $IELCC_{EENS}$-plot for the two bus test system, using the HPL-model.

Figure 5.3: $IELCC_{LOLE}$- (a) and $IELCC_{EENS}$-plots (b) for the two bus system, using the HPL-model.

5.2.2 RBTS

The results presented in this section are for the interconnected version of the RBTS, for two similar systems with 185MW as the base case peak load. The interconnector used is represented by a two-state model with a nameplate capacity of 30MW and FOR=0.001.

CYPL-model

Figure 5.4 shows the $IELCC_{LOLE}$-plot for the RBTS based on a CYPL-model. Compared to the CYPL-case for the two bus test system, the peak load vs. LOLE curves are smoother, as the RBTS will have more possible LOLE-values than the two bus system; however, the curves are still fairly step-wise. Comparing Figure 5.4 with the HPL-case for the RBTS in Figure 5.4 shows how moving to a load model with higher resolution makes the curves smoother. It also shows that the CYPL-model yields a lower $IELCC_{EENS}$ (29.31MW) than the HPL-model (33.84MW).

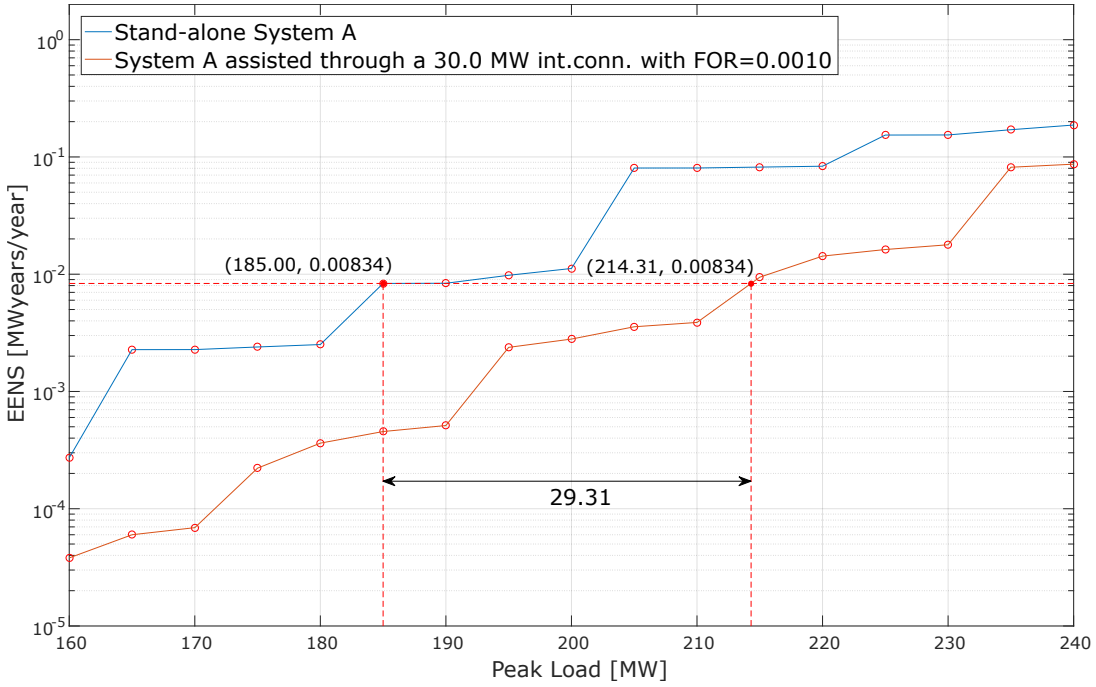

Figure 5.4: $IELCC_{LOLE}$-plot for the RBTS, using a 185MW CYPL-model.

HPL-model

Figures 5.5a and 5.5b show $IELCC_{LOLE}$- and $IELCC_{EENS}$-plots, respectively, for the two interconnected RBTS. Compared to the HPL-case for the two bus system, the curves are closer to being parallel both for LOLE and EENS as reliability index. It is reasonable to believe that this is a result of having a larger generation fleet with more and larger units, which can be seen by comparing Tables 3.6 and 5.2a. Further, it can be observed that the $IELCC_{LOLE}$- and $IELCC_{EENS}$-plots are very similar, with an almost identical IELCC. The $IELCC_{LOLE}$ of 33.84MW is approximately 113% of the interconnector's nameplate capacity. It is important to emphasize that this does not indicate that the interconnector will be able to supply a capacity to System A that is larger than its nameplate capacity. What it means is that System A, when assisted, will be able to supply an equally shaped, but scaled up by 18.3%[2], yearly load profile, while keeping System A at the same level of reliability.

[2]The percentage value comes from: $\frac{33.84MW \times 100\%}{185MW} = 18.3\%$.

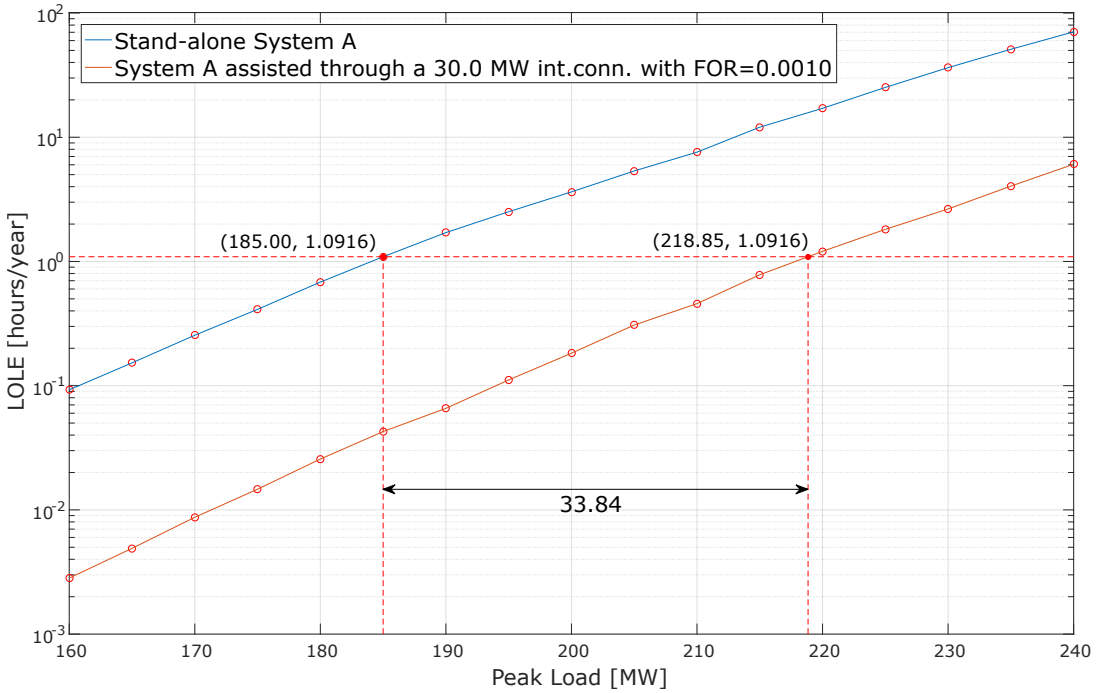

(a) $IELCC_{LOLE}$-plot for RBTS, using the HPL-model.

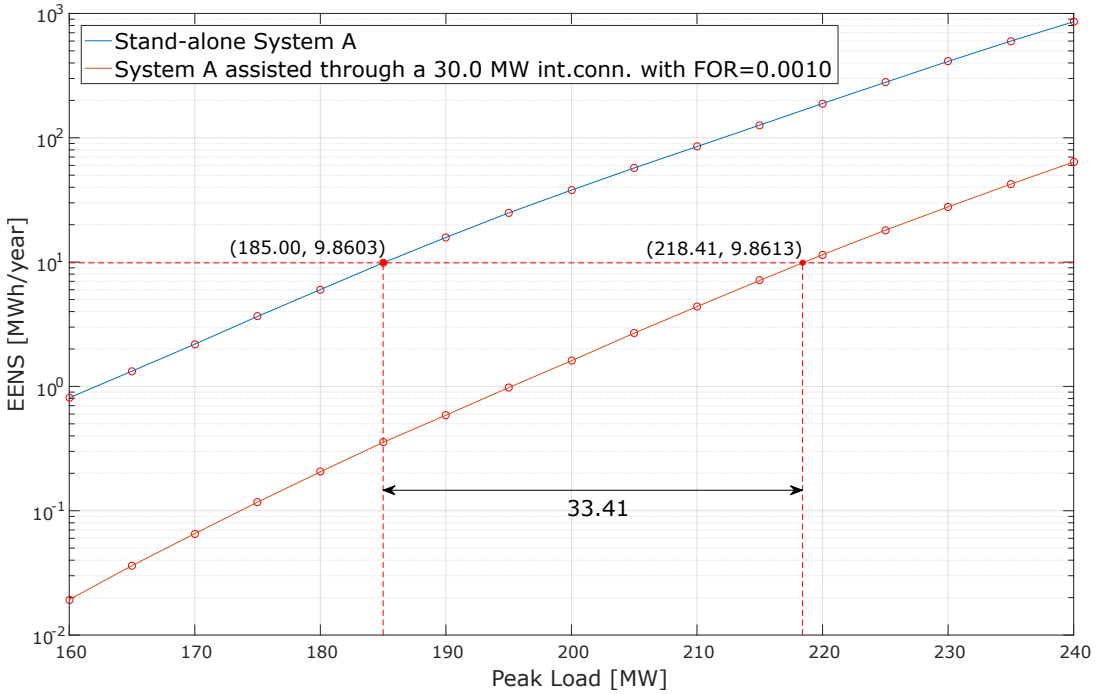

(b) $IELCC_{EENS}$-plot for RBTS, using the HPL-model.

Figure 5.5: $IELCC_{LOLE}$- (a) and $IELCC_{EENS}$-plots (b) for the RBTS, using the HPL-model.

The large IELCC for the case in Figure 5.5, can be explained by looking at the Constrained Equivalent Assisting Unit that is added to System A. The EAU-method adds an assisting unit, which is the equivalent of System B assisting through the interconnector, to System A. As explained in Section 3.3.1, this unit can be viewed as a multi-state generator with associated capacity states and probabilities. IELCC, whether it is based on LOLE or EENS, is to a large extent dependent on this multi-state unit. From a high-level perspective, there are three main factors that influence the properties of this unit: (1) The interconnector capacity (2), the reserve in System B, and (3), the unavailability/FOR of the interconnector. For the case evaluated in Figure 5.5, these three factors are elaborated in the following:

1. The interconnector capacity is often the constraining factor that decides the maximum possible assistance from System B. This is also true in the case evaluated here, and the maximum capacity of the multi-state CEAU is restricted to 30MW.

2. The reserve in the assisting system can also restrict the maximum assistance capacity, but following the case here, the worst case reserve (55MW) is almost double the interconnector capacity. Further, it can be gathered from Tables A1-A3 that the reserve is only as low as 55MW for two hours out of the year (hours 18 and 19 of day 2 in week 51). The median load for the year is 113MW, meaning that the reserve will be 127MW or larger for 50% of the time. The influence of the System B reserve on the CEAU for this case, and other interconnector constrained cases, is that a large median reserve causes the individual probability of the maximum CEAU capacity state to be very high. Essentially, this leads to adding a very reliable 30MW generator to System A. The CEAU in this case, for $L^B_{t=8430}$=111MW, is described by its assistance probability table in Table 5.6[3]. The resulting CEAU delivers 30MW with a certainty of 98.881051%, facilitated by the large System B reserve.

3. The last factor that can have a large influence on the CEAU, is the availability of the interconnector. Whether it is a two-state or multi-state interconnector, the probabilities of the capacity states affect the state probabilities of the CEAU. For the example

[3]The direct CEAU approach is utilized here to obtain a single CEAU-model for this time increment.

here, the interconnector has two states, with FOR=0.001. The probability of having zero assistance, $p(X = a^{CEAU}_{t=8430,j=8} = 0)$, consists almost solely of the probability of the interconnector being down. In this example, the FOR is fairly low. For HVDC-interconnectors this value can often be higher, which can cause lower probabilities of maximum capacity states in the CEAU, and thereby lower IELCC.

Table 5.6: CEAU assistance probability table for t=8430 for the case evaluated in Figure 5.5.

State j	Assistance $a^{CEAU}_{t=8430,j}$[MW]	Ind. prob. $p(X = a^{CEAU}_{t=8430,j})$
1	30	0.99881051
2	29	0.00015929
3	24	0.00000321
4	19	0.00000326
5	14	0.00000006
6	9	0.00002120
7	4	0.00000042
8	0	0.00100201

5.2.3 RTS

The results presented in this section are for the interconnected version of the RTS, for two similar systems with 2850MW as the base case peak load. The interconnector used is represented by a two-state model with a nameplate capacity of 600MW and FOR=0.00130873. The IEEE-RTS is more than ten times the size of the RBTS, with 3405MW installed capacity, increasing computation time vastly. Therefore the results shown for RTS are based on an HPL-model for System A, while System B has a CYPL of 2850MW.

HPL-model

Figures 5.6a and 5.6b show $IELCC_{LOLE}$- and $IELCC_{EENS}$-plots, respectively, for the interconnected version of the RTS. While IELCC for the HPL-cases were larger than the interconnector capacity for both the two bus system and the RBTS, it is here less than 50%

of the nameplate capacity of 600MW. $IELCC_{LOLE}$ is 260.63MW (43% of interconnector capacity), while $IELCC_{EENS}$ is slightly lower at 245.08MW (41% of interconnector capacity). As the FOR is low (FOR=0.0013), the explanation as to why the IELCC is low compared to nameplate capacity can be found by looking at the reserve. With a CYPL of 2850MW in System B, the reserve is constant at 555MW, rendering the maximum capacity level of the CEAU to be lower than the interconnector capacity. In addition, since any generator capacity outage in System B would further decrease the assistance capacity of the CEAU, probabilities of the capacity states near the maximum capacity are much lower than in the case evaluated in Table 5.6. In Table 5.7a, an excerpt of the assistance probability table is shown for the resulting CEAU for the case in Figure 5.6[4]. The median load in System B is 1735MW, and the resulting CEAU assistance probability table is shown in Table 5.7b. It can be seen from that table that besides increasing the maximum assistance capacity to 600MW (since the interconnector capacity is now the constraining factor) the probabilities of capacity states near the maximum capacity are much higher than those for the case with CYPL=2850MW. IELCC-plots for CYPL=1735MW are not shown here, but the resulting $IELCC_{LOLE}$ is 677.52MW.

Table 5.7: CEAU assistance probability table for the case evaluated in Figure 5.6.

(a) CYPL=2850MW.

State j	Assistance a_j^{CEAU}[MW]	Ind. prob. $p(X = a_j^{CEAU})$
1	555	0.23608574
2	543	0.02409038
3	535	0.10492700
4	531	0.00098328
5	523	0.01070684
:	:	:
441	2	0.00000058
442	1	0.00000031
443	0	0.09671499

(b) CYPL=1735MW.

State j	Assistance a_j^{CEAU}[MW]	Ind. prob. $p(X = a_j^{CEAU})$
1	600	0.99599928
2	599	0.00000548
3	598	0.00000671
4	597	0.00006113
5	596	0.00000112
:	:	:
599	2	0.00000001
600	1	0.00000007
601	0	0.00131160

[4]Since a CYPL-model is used for System B, the same CEAU will be added to $COPT^A$ for all time increments.

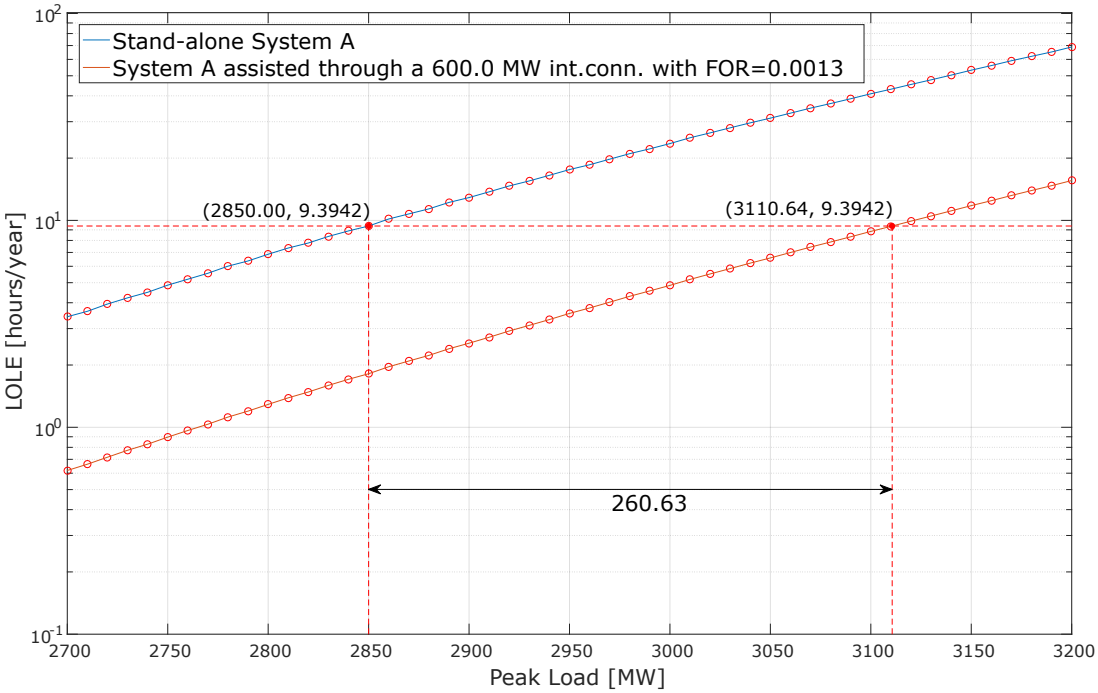

(a) $IELCC_{LOLE}$-plot for RTS, using the HPL-model.

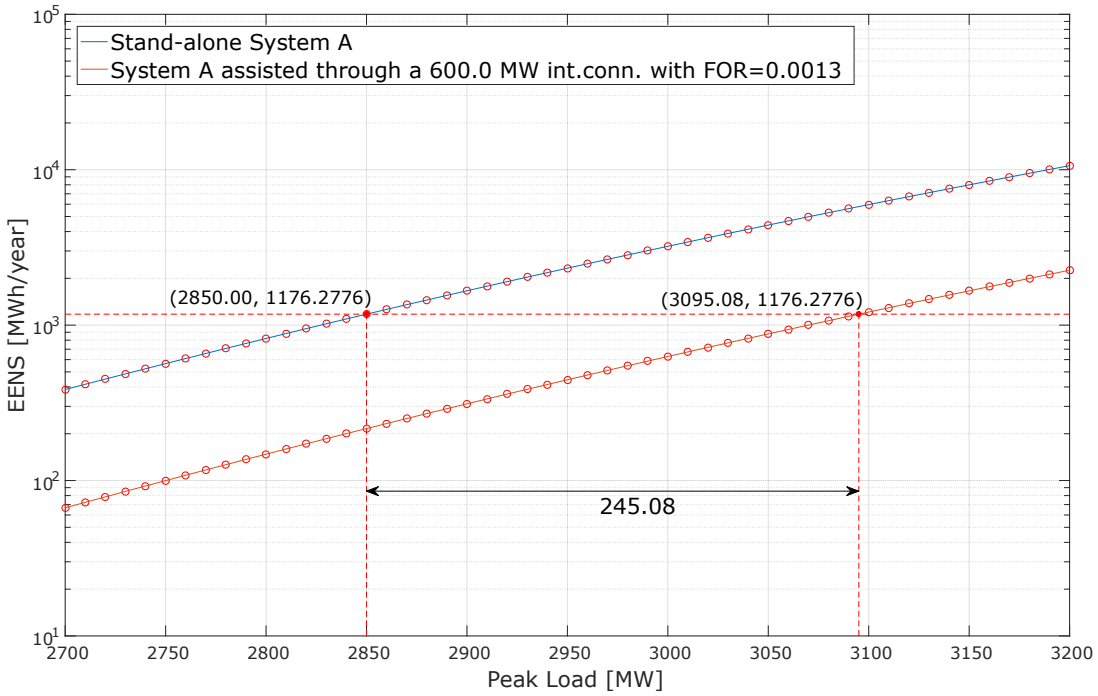

(b) $IELCC_{EENS}$-plot for RTS, using the HPL-model.

Figure 5.6: $IELCC_{LOLE}$- (a) and $IELCC_{EENS}$-plots (b) for the RTS, using the HPL-model.

Figure 5.7 shows the $IELCC_{LOLE}$- and $IELCC_{EENS}$-results for the RBTS (a) and RTS (b), highlighting the large difference in relative IELCC, i.e., IELCC in percent of interconnector capacity, for the cases evaluated in Figures 5.5 and 5.6.

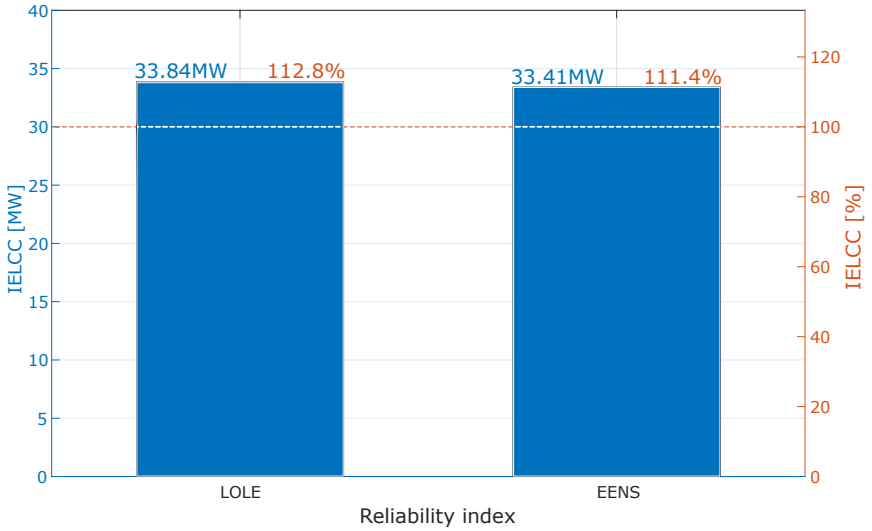

(a) Summary of IELCC-results for RBTS.

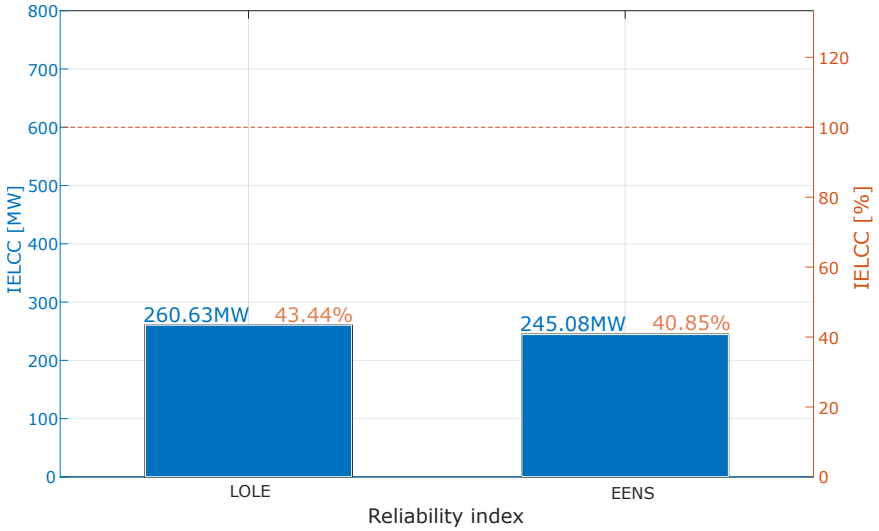

(b) Summary of IELCC-results for RTS.

Figure 5.7: $IELCC_{LOLE}$- and $IELCC_{EENS}$-results for the RBTS (a) and RTS (b).

5.2.4 IELCC for different specified LOLE-levels

Figure 5.8 shows the same case as was evaluated in Figure 5.5a, RBTS with an HPL-model. However, the specified LOLE-level that decides the intersection with the peak load vs. LOLE curves, and thereby the IELLC, is changed. In Figure 5.5a, the LOLE for the stand-alone system with base case peak load of 185MW (LOLE=1.0916 hours/year) was used as the desired LOLE-level in the plot. Using the pre-existing LOLE, from before changes are made to the system, is a common practice. However, as mentioned in Section 3.2.1, a predetermined LOLE can also be used as the desired LOLE-level. The predetermined LOLE is often the desired reliability level for the system, e.g., a reliability standard of LOLE=3 hours/year. Predetermined reliability levels can also be used when EENS is used as the guiding reliability index.

$IELCC_{LOLE}$ is plotted in Figure 5.8 both for (i) the predefined LOLE-standard of 3 hours/year, which is a more lenient standard than the LOLE-level used in Figure 5.5a, and for (ii) a stricter LOLE-level of 0.0427 hours/year. The latter LOLE-level is the resulting LOLE for the base case of System A when assisted by System B through the interconnector. This fact is evident from observing that the point (185.00, 0.0427) is on the blue curve, i.e., the peak load vs. LOLE curve belonging to the interconnected System A. The resulting IELCCs, $IELCC_{LOLE_{(i)}}$=34.25MW and $IELCC_{LOLE_{(ii)}}$=33.33MW, are very similar (approximately 1.5% difference) to the original value of $IELCC_{LOLE_{(i)}}$=33.84MW obtained in Figure 5.5a. This small difference could be expected from just inspecting the peak load vs. LOLE curves in Figure 5.5a as they are very parallel. A trend in the cases evaluated this far has been that the peak load vs. LOLE curves for stand-alone and interconnected systems have become closer to being parallel when moving towards larger generation systems and/or more load points in the load model. If this trend is assumed to be a universal one for IELCC, small variations in the desired LOLE-level, i.e., 1-2 orders of magnitude, should not affect the IELCC to a large extent.

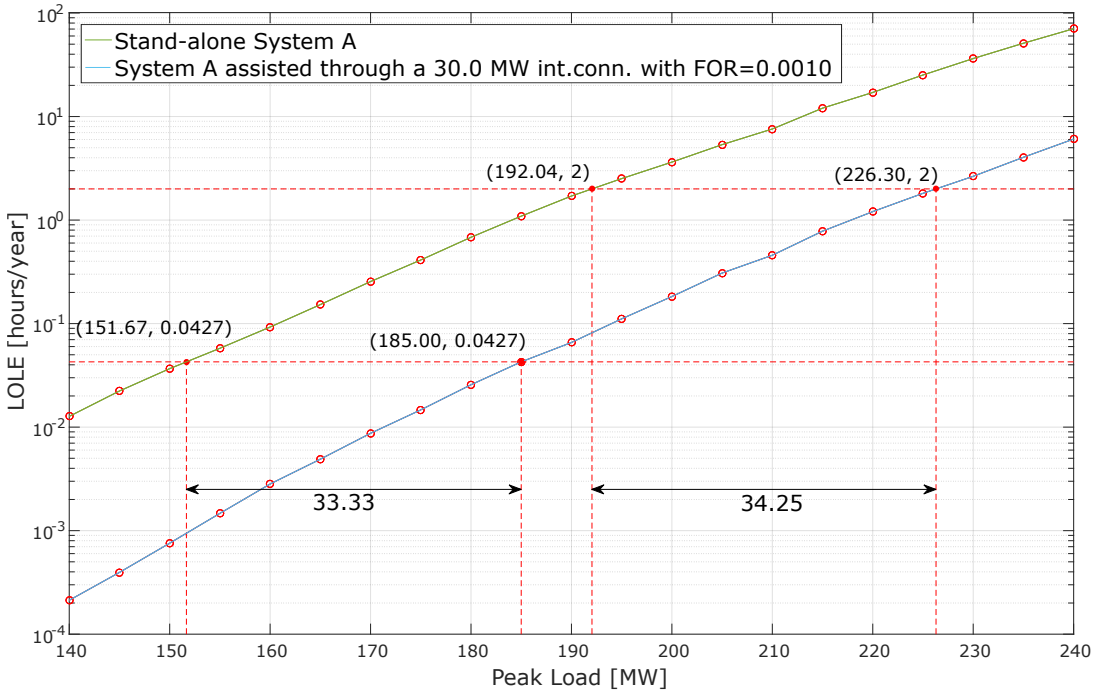

Figure 5.8: $IELCC_{LOLE}$-plot for the RBTS showing IELCC for different defined LOLE-levels.

5.3 Sensitivity analysis

5.3.1 IELCC higher than interconnector capacity

One facet of the counter-intuitive results of having IELCC larger than 100% of interconnector capacity was examined in Table 5.6. Having a highly reliable CEAU with maximum capacity equal to the interconnector capacity, points toward how the IELCC can get close to the interconnector capacity; however, it does not provide any obvious causality to how the IELCC can surpass the capacity of the interconnector. In Table 5.8 it is investigated how the addition of an extra unit in itself influences the reliability, and thereby also the IELCC. This is done by evaluating the ELCC for a stand-alone, base case RBTS, when one or more of its generating units are each split into two units, with half the capacity and the same FOR. This way, the installed capacity in the system will be unaltered, but the number of generators will increase. For each row in Table 5.8, a generator from Table 5.1 is split, starting from the largest units

(i.e., 12 units are obtained by splitting one of the 40MW units of FOR=0.030 into two units of 20MW and FOR=0.030, 13 units are obtained by splitting the second of the 40MW units with FOR=0.030, and so on). As this analysis does not consider any interconnections, ELCC is being evaluated here instead of IELCC.

Table 5.8: Variation of ELCC when splitting generators.

Number of generators	Cap. of previously split gen. [MW]	FOR of previously split gen.	Installed capacity [MW]	$ELCC_{LOLE}$ [MW]	$ELCC_{EENS}$ [MW]
11	N/A	N/A	240	0	0
12	40	0.03	240	7.60	7.98
13	40	0.03	240	16.05	17.20
14	40	0.02	240	25.28	27.01
15	20	0.025	240	26.36	28.28
16	20	0.015	240	27.05	29.11
17	20	0.015	240	27.75	29.96
18	20	0.015	240	28.45	30.88
19	20	0.015	240	29.15	31.84
20	10	0.02	240	29.30	32.00
21	5	0.01	240	29.31	32.01
22	5	0.01	240	29.31	32.03

As can be seen from Table 5.8, the reliability of the RBTS increases when generators are split into several units. This is evident from the increasing ELCC, depicting that the same amount of installed capacity is able to supply a larger amount of load, while the reliability of the system is kept at the same level. The results also indicate that the effect that splitting generators have on the reliability diminishes as the number of units in the system increases and/or that the increase in reliability is dependent on the size of the generator that is split. Further investigation is not made to verify or isolate the effect these two factors have on the reliability when splitting generators, as the results in Table 5.8 contribute to a plausible explanation as to how IELCC can be larger than the interconnector capacity. A combination of a very reliable CEAU, with maximum capacity equal to the interconnector capacity, and the fact that an additional generation unit added to the system in itself leads to a reliability improvement, can give IELCCs larger than 100% of interconnector capacity.

5.3.2 Saturation of IELCC

Deciding upon the capacity of the interconnector is a key question when planning major interconnection projects. From a reliability point of view, it seems intuitive that larger interconnector capacity will yield larger returns in terms of improved reliability. This is also the case, but only to some extent. As shown in Section 5.2, there are three main factors that influence the IELCC (i.e., that influence reliability), and interconnector capacity is only one of those. The effect of increasing the capacity of the interconnector diminishes as the capacity gets closer to the value of the reserve in the assisting system. This can be seen in Table 5.9, which shows that the IELCC saturates as the interconnector capacity increases beyond the reserve in the assisting system. For the base case RBTS, which is evaluated here, the reserve is 55MW. The same trend is illustrated in Figure 5.9.

Table 5.9: $IELCC_{LOLE}$ for the RBTS, when increasing interconnector capacity.

Interconnector capacity [MW]	$IELCC_{LOLE}$ [MW]
5	5.91
10	11.53
20	23.14
30	33.97
40	43.78
50	51.50
60	56.71
70	58.68
80	59.06
90	59.10
100	59.12

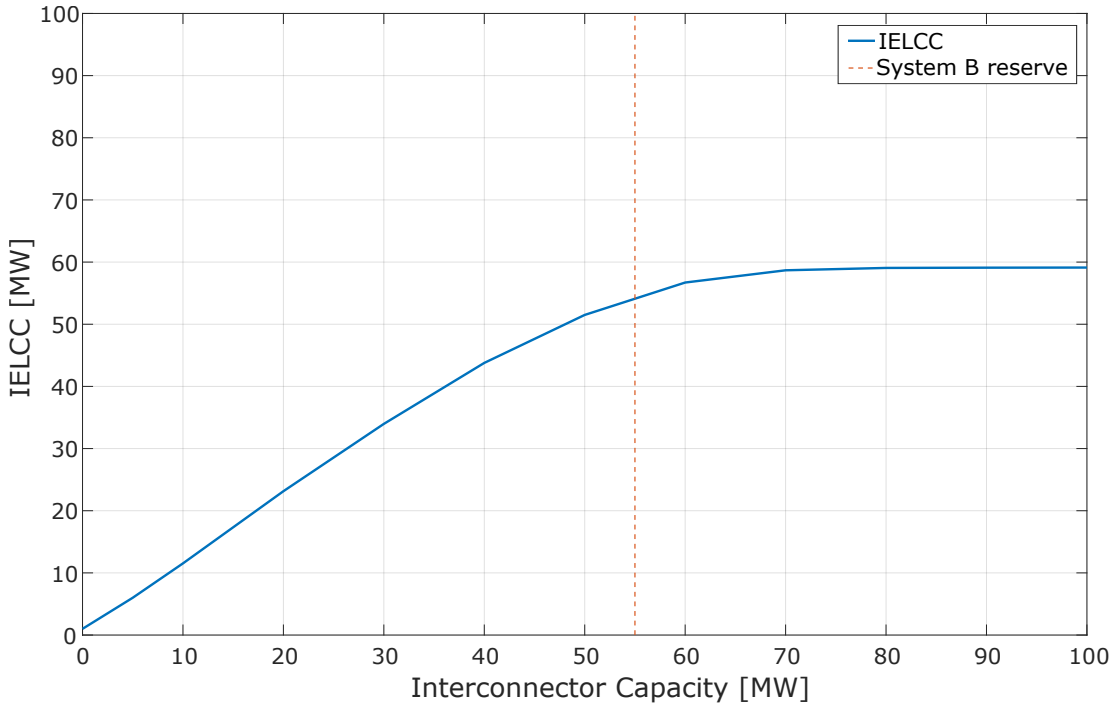

Figure 5.9: Plot of $IELCC_{LOLE}$ vs. interconnector capacity for the RBTS.

Chapter 6

Conclusions and future work

6.1 Discussion and Conclusions

This thesis examined and elaborated on a recently proposed approach, IELCC, for the derating of interconnectors seeking to participate in capacity mechanisms. A major part of the rationale for introducing capacity mechanisms is to ensure the reliability of the power system. It is well established that interconnectors can bring reliability benefits, and a well designed methodology is needed to ensure their participation in the capacity auctions without distorting the market. The examined methodology addresses this need by combining acknowledged concepts from Power System Reliability, such as LOLE and ELCC, and by utilizing them for interconnectors. The thesis sought to present the underlying concepts in a detailed manner to make it transparent and open for further scrutiny. As a part of this, a great deal of effort had to be put into understanding and clearly highlighting the distinctions between some of the numerous reliability indices (e.g., LOLP, LOLE, LOLP', EENS, EDNS) that can be used in the IELCC-procedure. A lot of ambiguities and confusion surrounds these concepts when they are presented in literature, and clear, unison definitions are not necessarily easy to come by. For individuals lacking experience in the field of PSR, it might be difficult to see how each one of these finely nuanced metrics can serve their own practical application, besides being a cause of confusion.

Further, this thesis added to the procedure by proposing the use of different reliability indices in stead of LOLE. LOLE was chosen as the reliability index in the original work, as that is most common for ELCC. However, one of the strengths of IELCC is that different indices can be used depending on what is most relevant for the system being evaluated. EENS was chosen in this thesis to demonstrate this since it considers the severity of outages, as opposed to LOLE. The thesis work also included construction of scripts in MATLAB that are able to evaluate the IELLC for larger systems than were originally analysed in [7]. These scripts were utilized for different case studies. The purpose of the case studies was to demonstrate the usage of the methodology, and to illuminate and discuss different aspects that influence its results.

The methodology was used to calculate the IELCC, i.e., the de-rated capacity of different interconnectors between various test systems. Three different test-system configurations were evaluated, investigating the effect on IELCC of factors including generation system size, resolution of load model and reserve of assisting system. It could be observed that the resolution of the load model greatly influenced the results, showcased both for the two bus system and the RBTS. In both cases the CYPL-model produced more pessimistic results than the HPL-model. It was not further investigated if this holds true for all cases, but as the HPL-model is a more accurate representation of actual conditions, it is either way the recommended model to use, as long as the solution time constraints allow it. The HPL-model is also an alternative, as it is a more accurate model than the CYPL-model, but not as computationally intensive as the HPL-model.

The results also showed that resolution and configuration of the generators/COPT influence the IELCC by making the peak load vs. LOLE curves very discontinuous, highlighted by analysing the shape of the curves for the two bus system, especially Figures 5.1 and 5.2. It was further observed that the resolution and configuration of the generators affected the IELCC to a smaller degree when larger resolution load models and/or larger generation systems were evaluated. As a result, resolution and configuration of generators/COPT should not influence the IELCC of large, real-life systems to a large extent.

Further, the results showed that interconnectors can bring reliability benefits large enough for the IELCC to become larger than the transmission capacity of the interconnector, i.e., the resulting de-rated capacity of the interconnector can be larger than 100%. Such results have been briefly presented for ELCC of conventional generators in other research, and were also shown here for interconnectors. These seemingly non-intuitive results were investigated by the means of a sensitivity analysis. The analysis showed that there is a reliability benefit in having a larger number of generators in itself, without increasing the installed capacity. E.g., splitting up a generator into two equal ones with capacity equal to half of that of the original, was shown to improve the reliability. This effect, in combination with an assisting system with a large reserve in relation to the interconnector capacity, indicates that it is plausible to have a de-rated capacity of more than 100% for an interconnector, when using the reliability benefits as a basis for the de-rating. Without undermining this observation, it should be mentioned that the results obtained are for very reliable interconnectors. Real life interconnectors, e.g., HVDC-interconnectors are expected to have slightly larger outage rates, which make them less likely to have IELCC larger than their nameplate capacities.

In Figure 5.7 it was indicated that the approach produces similar IELCC-results for both LOLE and EENS as the reliability index, with $IELCC_{LOLE}$ approximately 1.5-2.5% larger than $IELCC_{EENS}$ for both RBTS and RTS. The specific trend of $IELCC_{EENS}$ being lower than $IELCC_{LOLE}$ was not investigated further. As such, conclusions are not made to whether this trend is specific to the cases analysed here, or if it is a universal one. Either way, having the ability to use different reliability indices as the measure of reliability is a strength of this procedure, as it leaves the user able to choose which index is most compliant with the reliability standard in the system that is evaluated. If using EENS consistently produce more conservative results, an average or weighting between the two could be used to produces the final IELCC, to reduce the possibility of choosing the one producing the most beneficial results for the user. However, as mentioned in Section 3.1, EENS is in many cases a more realistic measure of reliability as it encompasses the serverity of loss-of-load situations. This is especially important as there is an increasing number of energy limited occasions in the power system, caused by the larger penetration of wind and solar. For systems where such

large penetration is the case, EENS would be the preferred reliability index.

Compared to the interconnector de-rating methodologies summarized in Section 2.2, the IELCC-procedure as presented in this thesis is not as extensive, in the sense that it does not consider several scenarios for future load demand and generation, nor does it include any modelling of the actual power flow through the interconnector. However, it must be emphasized that the IELCC-method presented in this thesis serves as a foundation that can be further extended to analyse real life systems and cases. There are no difficulties in expanding on the input data used, e.g., to utilize data resulting from best practices for load- and generation forecasting.

Compared to the GB method of de-rating summarized in 2.2, the IELCC-procedure is vastly more reliability-oriented. From what can be gathered from the available literature on the GB method, it is completely based on simulation and modelling of market-related quantities such as generation costs and price differentials. However, it is stated by National Grid that this procedure is an interim solution, and that ideally, interconnector flows and demand across Europe would be stochastically modelled to provide information such as LOLE, but that a suitable model or sufficient data is not available yet. Since the main motivation for CMs is to ensure reliability, it is logical that a de-rating approach should be based on, and provide information on, reliability inherent in the system. These features are extensively covered by the IELCC-procedure.

Several similarities can be found between the IELCC-procedure, and the de-rating procedure proposed for the Integrated — Single Electricity Market (I-SEM). Most notably, the latter procedure also makes use of a technique very similar to ELCC (illustrated in Figure 2.1); however, it is only utilized for obtaining a technical De-Rating Factor (DRF), while for IELCC, both technical- and simultaneous scarcity-contributions to the DRF are handled by the ELCC-methodology. Simultaneous scarcity's influence on the DRF is handled in I-SEM's procedure by probabilistic evaluations very similar to LOLE.

6.2 Limitations

Although being rooted in the reliability point of view, the IELCC-procedure does not explicitly handle the issue of simultaneous scarcity, nor does it incorporate how actual interconnector flows can turn out, or how this can influence the results. Regarding the first issue, it can be argued that the EAU-approach incorporates simultaneous scarcity implicitly through two details of the approach: The assisting system only contributes positively to the reliability of the assisted system as long as it has a positive reserve; and even though a positive reserve is forecasted in the assisting system, the procedure also considers probabilities of capacity outages that affect the ability to assist, by constructing the constrained equivalent assisting unit. However, further inspection of the procedure is needed to verify that it in fact covers simultaneous scarcity in an adequate manner.

Regardless of its ability to handle simultaneous scarcity, the IELCC-procedure should be coupled to appropriate market models to be applicable for real life purposes. Actual power flows are subject to complex interactions of generation and load across Europe, and on a day-day basis, they are governed by market coupling. As it is now, the IELCC-approach does not consider these issues. Some of the complexities can potentially be considered by means of the input data to the procedure; however, more work must be done to understand the mechanisms that determine the power flows, and how the potential effects they might have on the resulting de-rated capacity can be considered. This might be achieved through an extension of the approach, or more likely, through combination with market models.

For the results obtained in the case studies, there are some elements in the input data that could be altered to potentially yield more realistic results. For the RBTS and two bus test system, the same load percentage data is used to create the load models both for the assisting and assisted system. As a consequence, the variability of load in both systems is 100% correlated. Although neighbouring systems might have a large degree of correlation of peak load, they will not have completely equal loads for all time increments, as was the case for the interconnected RBTS case study. It has not been investigated how altering the load

in one of the systems would influence the IELCC for the interconnected version of RBTS. Also, it has not been explicitly tested through the case studies how the IELCC for the case studies would turn out when using interconnectors with larger FOR and/or multiple states, i.e., closer to a representation of a HVDC interconnector.

6.3 Suggestions for future work

There are several aspects of the IELCC-procedure that could benefit from further research. As earlier mentioned, it should be investigated how the procedure could be coupled to suitable market models, in an attempt to model the effects of actual power flows. Further testing and scrutinizing should also be conducted to verify that the procedure adequately considers simultaneous scarcity.

Furthermore, a natural step could be to utilize Monte Carlo Simulation in the procedure, in stead of basing it solely on analytical methods. MCS is favoured for many applications in reliability studies, and it could be used to assess LOLE and EENS. This can yield distributions of LOLE and EENS instead of just point values, which could prove useful for the obtainment of IELCC. Also, MCS is better able to handle correlation between loads in the assisting and assisted systems.

MCS can also be used for the creation of load- and generation input data as is done in the I-SEM de-rating methodology. Methods for obtaining accurate input data have not been treated in the original proposed methodology, nor in this thesis, as the IELCC-procedure this far only has been applied on test systems. If it is going to be used for real life systems, methods for securing precise input data must be implemented.

As this thesis has only evaluated the concept of interconnector de-rating from the perspective of generation adequacy, a reasonable extension would be to consider transmission facilities within the interconnected areas as well (i.e., HLII-studies). Taking the North-Sea Link as an example, it is obvious that transmission facilities within the Norway and GB systems

include constraints that are of influence to a de-rating methodology. Other areas that are connected to any of the two systems in question, will also have an influence, creating the need for evaluating adequacy of multi-area interconnected systems from the perspective of IELCC.

A natural extension of the work done in this thesis would be to investigate the algorithmic efficiency of the Probability Array Method (whose overview is given in Section 3.3.2) in obtaining $IELCC_{LOLE}$ and $IELCC_{EENS}$ metrics.

Both the Equivalent Assisting Unit Approach and the Probability Array Method can be suitably extended to obtain Frequency and Duration (F&D) based reliability indices, viz., Loss of Load Frequency (LOLF) and Loss of Load Duration (LOLD), for interconnected systems. Subsequently, $IELCC_{LOLF}$ and $IELCC_{LOLD}$ metrics can be computed, using the interconnector de-rating methodology posited in this thesis.

Though LOLE and EENS are the two most popularly used adequacy metrics in power system reliability studies, a plethora of indices such as EDNS, LOEP, System Minutes, Expected Loss of Load (XLOL), LOLF and LOLD are also available for use. Clear guidelines/interpretations are amiss on how these probabilistic indices with their many subtleties can distinctly aid in decision making in planning and operational horizons, from a reliability perspective. The situation is even more complicated when numerical values of one compound metric (such as IELCC as devised in this thesis) are quite different when using each of the aforementioned adequacy metrics as the underlying basis; there is a possibility for conflicting reliability management decision alternatives. Picking one metric over the other to serve as a definitive guiding adequacy metric seems to be quite subjective. More research on investigation into this issue is warranted.

Bibliography

[1] European Environmental Agency, "Renewable Energy in Europe 2016 - Recent Growth and Knock-on Effects," Tech. Rep., Jun. 2016. [Online]. Available: https://www.eea.europa.eu/publications/renewable-energy-in-europe-2016/at_download/file

[2] European Commission, "Energy Strategy," 2017. [Online]. Available: https://ec.europa.eu/energy/en/topics/energy-strategy

[3] CIGRE Working Group C5.17, "Capacity Mechanisms: Needs, Solutions and State of Affairs," CIGRE Technical Brochure TB 647, Mar. 2016.

[4] European Commission, "Guidelines on State aid for environmental protection and energy 2014-2020," Tech. Rep., Jun. 2014. [Online]. Available: http://eur-lex.europa.eu/legal-content/EN/TXT/PDF/?uri=CELEX:52014XC0628(01)&from=EN

[5] Council of European Energy Regulators, "Treatment of Interconnectors and Neighbouring Resources in CRMs," Tech. Rep., Jun. 2016. [Online]. Available: http://www.ceer.eu/portal/page/portal/EER_HOME/EER_PUBLICATIONS/CEER_PAPERS/Electricity/2016/C15-ESS-06-03_Treatment%20of%20Interconnectors%20and%20Neighbouring%20Resources%20in%20Capacity%20Remuneration%20Mechanisms.pdf

[6] European Commission, "Commission staff working document accompanying the document 'Report from the Commission - Final Report of the Sector Inquiry on Capacity Mechanisms'," Tech. Rep., Nov.

2016. [Online]. Available: https://ec.europa.eu/energy/sites/ener/files/documents/swd_2016_385_f1_other_staff_working_paper_en_v3_p1_870001.pdf

[7] V. V. Vadlamudi and G. Doorman, "Interconnector participation in capacity mechanisms: A new de-rating approach," in *International Conference on the European Energy Market*, Dresden, Germany, Jun. 2017.

[8] National Grid, "National Grid EMR (Electricity Market Reform) Electricity Capacity Report," Tech. Rep., May 2016. [Online]. Available: https://www.emrdeliverybody.com/Lists/Latest%20News/Attachments/47/Electricity%20Capacity%20Report%202016_Final_080716.pdf

[9] Royal Academy of Engineering, "GB Electricity Capacity Margin," Tech. Rep., Oct. 2013. [Online]. Available: http://www.raeng.org.uk/publications/reports/gb-electricity-capacity-margin

[10] Monitoring Analytics LLC, "State of the Market Report for PJM, Volume 2: Detailed Analysis," Tech. Rep., Mar. 2017. [Online]. Available: http://www.monitoringanalytics.com/reports/PJM_State_of_the_Market/2016/2016-som-pjm-volume2.pdf

[11] G. M. Curley, "Reliability Analysis of Power Plant Unit Outage Problems," in *Symposium on Managing Fleet Assets and Performance Presentations*, 2013. [Online]. Available: http://famos.scientech.us/PDFs/2013_Symposium/Reliability_Analysis_of_Power_Plants_Curley.pdf

[12] SEM (Single Electricity Market) Committee, "Integrated Single Electricity Market (I-SEM) Capacity Requirement and De-Rating Factor Methodology - Detailed Design - Decision Paper SEM-16-082," Tech. Rep., Dec. 2016. [Online]. Available: https://www.semcommittee.com/sites/semcommittee.com/files/media-files/SEM-16-082%20CRM%20Capacity%20Requirement%20%20De-rating%20Methodology%20Decision%20Paper.pdf

[13] SEM Committee, "I-SEM Capacity Market: Methodology for the Calculation of the Capacity Requirement and De-rating Factors - SEM-16-082 Appendix

1," Tech. Rep., Dec. 2016. [Online]. Available: https://www.semcommittee.com/sites/semcommittee.com/files/media-files/SEM-16-082a%20Appendix%201%20TSOs%20Capacity%20Requirement%20and%20De-rating%20Factors%20Methodology.pdf

[14] DECC, "EMR Panel of Technical Experts' Final Report on National Grid's 2016 Electricity Capacity Report," Tech. Rep., Jun. 2016. [Online]. Available: https://www.gov.uk/government/uploads/system/uploads/attachment_data/file/536032/050716_PTE_2016_ECR_Report_FINAL_CLEAN.pdf

[15] National Grid, "Capacity Market Auction Guidelines," Tech. Rep., Jul. 2016. [Online]. Available: https://www.emrdeliverybody.com/Lists/LatestNews/Attachments/48/CMAuctionGuidelinesJuly2016Final.pdf

[16] ——, "National Grid EMR (Electricity Market Reform) Electricity Capacity Report," Tech. Rep., Jun. 2015. [Online]. Available: https://www.emrdeliverybody.com/CapacityMarketsDocumentLibrary/ElectricityCapacityReport2015.pdf

[17] EPEX SPOT *et al.*, "EUPHEMIA Public Description - PCR Market Coupling Algorithm," Tech. Rep., Dec. 2016. [Online]. Available: https://www.epexspot.com/document/36580/EuphemiaPublicDescription-December2016

[18] DECC, "EMR Panel of Technical Experts' Final Report on National Grid's 2015 Electricity Capacity Report," Tech. Rep., Jun. 2015. [Online]. Available: https://www.gov.uk/government/uploads/system/uploads/attachment_data/file/438714/PTE_2015_ECR_Report_final.pdf

[19] SEM (Single Electricity Market) Committee, "Integrated Single Electricity Market (I-SEM): Interconnector De-Rating Factor Methodology Decision - SEM-16-082b Appendix 2," Tech. Rep., Dec. 2016. [Online]. Available: https://www.semcommittee.com/sites/semcommittee.com/files/media-files/SEM-16-082bAppendix2RAsInterconnectorDeratingMethodology.pdf

[20] R. Billinton and R. N. Allan, *Reliability evaluation of power systems, 2nd Edition.* New York: Plenum Press, 1996.

[21] P. Kundur *et al.*, "Definition and classification of power system stability," *IEEE Transactions on Power Systems*, vol. 19, no. 3, pp. 1387–1401, Aug. 2004.

[22] Blanco, Marta Poncela *et al.*, "Identification of Appropriate Generation and System Adequacy Standards for the Internal Electricity Market," Tech. Rep., Sep. 2016. [Online]. Available: http://publications.jrc.ec.europa.eu/repository/bitstream/JRC101590/jrc101590_online_rev1_19sept2016.pdf

[23] E. Ibanez *et al.*, "Comparing resource adequacy metrics and their influence on capacity value," in *International Conference on Probabilistic Methods Applied to Power Systems*, Durham, UK, Jul. 2014, pp. 1–6.

[24] D. Morrow and L. Gan, "Comparison of methods for building a capacity model in generation capacity adequacy studies," in *Communications, Computers and Power in the Modern Environment*, Saskatchewan, Canada, May 1993, pp. 143–149.

[25] H. G. Stoll, *Least-Cost Electric Utility Planning*. New York: John Wiley & Sons, 1989.

[26] X. Wang and J. R. McDonald, *Modern power system planning*. Cambridge: McGraw-Hill International (UK) Limited, 1994.

[27] S. Sulaeman *et al.*, "A wind farm reliability model considering both wind variability and turbine forced outages," *IEEE Transactions on Sustainable Energy*, vol. 8, no. 2, pp. 629–637, Apr. 2017.

[28] R. Billinton and D. Huang, "Basic concepts in generating capacity adequacy evaluation," in *International Conference on Probabilistic Methods Applied to Power Systems*, Stockholm, Sweeden, Jun. 2006, pp. 1–6.

[29] M. Papic, "Generation Reliability Concepts - Presentation from RAWG Meeting on Generation Reliability Concepts," Salt Lake City, USA, Sep. 2014. [Online]. Available: https://www.wecc.biz/Administrative/20140909_RAWG_Item5A1_Probabilistic_MPapic.pdf

[30] International Energy Agency, "Re-powering Markets," Tech. Rep., Mar. 2016. [Online]. Available: https://www.iea.org/publications/freepublications/publication/REPOWERINGMARKETS.pdf

[31] L. Conde-López *et al.*, "Generating adequacy analysis of Mexico's national interconnected power system," *International Journal of Energy Sector Management*, vol. 10, no. 4, pp. 561–575, Nov. 2016.

[32] R. Earle *et al.*, "Measuring the capacity impacts of demand response," *The Electricity Journal*, vol. 22, no. 6, pp. 47–58, Jul. 2009.

[33] S. Sheehy *et al.*, "Impact of high wind penetration on variability of unserved energy in power system adequacy," in *International Conference on Probabilistic Methods Applied to Power Systems*, Beijing, China, Oct. 2016, pp. 1–6.

[34] M. Papic *et al.*, "Practical experience in evaluating adequacy of generating capacity in the Western interconnection," in *IEEE Power & Energy Society General Meeting*, Denver, USA, Jul. 2015, pp. 1–5.

[35] AEMC (Australian Energy Market Commission) Reliability Panel, "Reliability Standard and Reliability Settings Review," Tech. Rep., Jul. 2014. [Online]. Available: http://www.aemc.gov.au/getattachment/b982ba23-bd74-42b5-8d5f-0d84472060d7/Reliability-Panel's-Final-report.aspx

[36] A. K. Basu *et al.*, "Distributed energy resource capacity adequacy assessment for PQR enhancement of CHP micro-grid," in *IEEE Power and Energy Society General Meeting*, Providence, USA, Jul. 2010, pp. 1–5.

[37] S. Tindemans *et al.*, "Resilience Performance of Smart Distribution Networks," Tech. Rep., Dec. 2014. [Online]. Available: https://innovation.ukpowernetworks.co.uk/innovation/en/Projects/tier-2-projects/Low-Carbon-London-(LCL)/Project-Documents/LCLLearningReport-D4-Resilienceperformanceofsmartdistributionnetworks.pdf

[38] M. Amelin, "Comparison of capacity credit calculation methods for conventional power plants and wind power," *IEEE Transactions on Power Systems*, vol. 24, no. 2, pp. 685–691, May 2009.

[39] Y. Zhou *et al.*, "Framework for capacity credit assessment of electrical energy storage and demand response," *IET Generation, Transmission & Distribution*, vol. 10, no. 9, pp. 2267–2276, Jun. 2016.

[40] S. Nolan *et al.*, "A methodology for estimating the capacity value of demand response," in *IEEE Power and Energy Society General Meeting*, National Harbor, USA, Jul. 2014, pp. 1–5.

[41] L. Garver, "Effective Load Carrying Capability of generating units," *IEEE Transactions on Power Apparatus and System*, vol. PAS-85, no. 8, pp. 910–919, Aug. 1966.

[42] P. E. O. Aguirre *et al.*, "Realistic calculation of wind generation capacity credits," in *CIGRE/IEEE Joint Symposium on Integration of Wide-Scale Renewable Resources Into the Power Delivery System*, Calgary, Canada, Jul. 2009, pp. 1–8.

[43] C. D'Annunzio, "Generation adequacy assessment of power systems with significant wind generation: a system planning and operations perspective," Ph.D. dissertation, Dept. Elec. and Comp. Eng., Univ. of Texas, Austin, 2009.

[44] R. Sioshansi *et al.*, "A dynamic programming approach to estimate the capacity value of energy storage," *IEEE Transactions on Power Systems*, vol. 29, no. 1, pp. 395–403, Jan. 2014.

[45] W. Wangdee and R. Billinton, "Probing the intermittent energy resource contributions from generation adequacy and security perspectives," *IEEE Transactions on Power Systems*, vol. 27, no. 4, pp. 2306–2313, Nov. 2012.

[46] M. Milligan and K. Porter, "The capacity value of wind in the United States: Methods and implementation," *Electricity Journal*, vol. 19, no. 2, pp. 91–99, Mar. 2006.

[47] A. Keane *et al.*, "Capacity value of wind power," *IEEE Transactions on Power Systems*, vol. 26, no. 2, pp. 564–572, May 2011.

[48] L. Söder, "Wind Power Capacity Credit," Tech. Rep., May 2013. [Online]. Available: http://www.nepp.se/pdf/wind_power_capacity.pdf

[49] R. Billinton *et al.*, "Adequacy evaluation of interconnected systems with an AC/DC link using an equivalent approach," in *Canadian Conference on Electrical and Computer Engineering*, Halifax, Canada, May 2000, pp. 755–759.

[50] MATLAB version 9.0.0 (R2016a), The MathWorks Inc., Natick, Massachusetts, USA. [Computer software] .

[51] R. Billinton *et al.*, "A reliability test system for educational purposes - basic data," *IEEE Transactions on Power Systems*, vol. 4, no. 3, pp. 1238–1244, Aug. 1989.

[52] Task Force of the Application of Probability Methods Subcommittee, "IEEE Reliability Test System," *IEEE Transactions on Power Apparatus and Systems*, vol. PAS-98, no. 6, pp. 2047–2054, Nov. 1979.

[53] W. Wangdee and R. Billinton, "Considering load-carrying capability and wind speed correlation of WECS in generation adequacy assessment," *IEEE Transactions on Energy Conversion*, vol. 21, no. 3, pp. 734–741, Sep. 2006.

Appendix A

Load data used for the test systems

Table A1: Weekly load data.

Week w	WPL [% of YPL]	Week w	WPL [% of YPL]	Week w	WPL [% of YPL]	Week w	WPL [% of YPL]
1	86.2	14	75.0	27	75.5	40	72.4
2	90.0	15	72.1	28	81.6	41	74.3
3	87.8	16	80.0	29	80.1	42	74.4
4	83.4	17	75.4	30	88.0	43	80.0
5	88.0	18	83.7	31	72.2	44	88.1
6	84.1	19	87.0	32	77.6	45	88.5
7	83.2	20	88.0	33	80.0	46	90.9
8	80.6	21	85.6	34	72.9	47	94.0
9	74.0	22	81.1	35	72.6	48	89.0
10	73.7	23	90.0	36	70.5	49	94.2
11	71.5	24	88.7	37	78.0	50	97.0
12	72.7	25	89.6	38	69.5	51	100.0
13	70.4	26	86.1	39	72.4	52	95.2

Table A2: Daily load data.

Day d	DPL [% of WPL]
1	93
2	100
3	98
4	96
5	94
6	77
7	75

Table A3: Hourly load data.

	Winter weeks 1-8 & 44-52		Summer weeks 18-30		Spring/Fall weeks 9-17 & 31-43	
Hour h	Weekday [% of DPL]	Weekend [% of DPL]	Weekday [% of DPL]	Weekend [% of DPL]	Weekday [% of DPL]	Weekend [% of DPL]
1	67	78	64	74	63	75
2	63	72	60	70	62	73
3	60	68	58	66	60	69
4	59	66	56	65	58	66
5	59	64	56	64	59	65
6	60	65	58	62	65	65
7	74	66	64	62	72	68
8	86	70	76	66	83	74
9	95	80	87	81	95	83
10	96	88	95	86	99	89
11	96	90	99	91	100	92
12	95	91	100	93	99	94
13	95	90	99	93	93	91
14	95	88	100	92	92	90
15	93	87	100	91	90	90
16	94	87	97	91	88	86
17	99	91	96	92	90	85
18	100	100	96	94	92	88
19	100	99	93	95	96	92
20	96	97	92	95	98	100
21	91	94	92	100	96	97
22	83	92	93	93	90	95
23	73	87	87	88	80	90
24	63	81	72	80	70	85

Appendix B

Intermediate results from a complete IELCC-calculation

This appendix shows a set of tables containing intermediate results from various steps of the IELCC-methodology.

Table B1: Hourly load data for Systems A and B.

Hour t	Load [MW]	Hour t	Load [MW]	Hour t	Load [MW]	Hour t	Load [MW]
1	99.37	11	142.37	:	:	8727	114.92
2	93.43	12	140.89	8428	109.15	8728	114.92
3	88.98	13	140.89	8429	109.15	8729	120.20
4	87.50	14	140.89	8430	111	8730	132.09
5	87.50	15	137.93	8431	136.90	8731	130.77
6	88.98	16	139.41	8432	159.10	8732	128.13
7	109.75	17	146.82	:	:	8733	124.16
8	127.54	18	148.31	8724	120.20	8734	121.52
9	140.89	19	148.31	8725	118.88	8735	114.92
10	142.37	20	142.37	8726	116.23	8736	106.99

Table B2: Interconnector data.

State k	Interconnector cap. IC_k[MW]	Probability p_k
1	0	0.001
2	30	0.999

Table B3: EAU- and CEAU-assitance probability tables.

(a) Assitance probability table for the EAU.

State j	Assistance $a^{EAU}_{t=8430,j}$[MW]	Ind. prob. $p(X = a^{EAU}_{t=8430,j})$
1	30	0.99981032
2	29	0.00015945
3	24	0.00000322
4	19	0.00000327
5	14	0.00000007
6	9	0.00002122
7	4	0.00000043
8	0	0.00000202

(b) Assitance probability table for the CEAU.

State j	Assistance $a^{CEAU}_{t=8430,j}$[MW]	Ind. prob. $p(X = a^{CEAU}_{t=8430,j})$
1	30	0.99881051
2	29	0.00015929
3	24	0.00000321
4	19	0.00000326
5	14	0.00000006
6	9	0.00002120
7	4	0.00000042
8	0	0.00100201

Table B4: COPTs for System A, System B and $COPT^{U}_{t=8430}$.

(a) $COPT^{A}$ and $COPT^{B}$.

State j	Cap. out x_j [MW]	Ind. prob. $p(X = x_j)$	Cum. prob. $P(X \geq x_j)$
1	0	0.81285961	1.00000000
2	5	0.01642141	0.18714039
3	10	0.01667191	0.17071898
4	15	0.00033513	0.15404707
5	20	0.07035854	0.15371194
6	25	0.00142135	0.08335340
7	30	0.00144303	0.08193205
8	35	0.00002901	0.08048902
9	40	0.06926973	0.08046001
10	45	0.00139939	0.01119028
11	50	0.00142073	0.00979090
12	55	0.00002856	0.00837017
13	60	0.00582845	0.00834161
14	65	0.00011774	0.00251316
15	70	0.00011954	0.00239541
16	75	0.00000240	0.00227587
17	80	0.00200148	0.00227347
18	85	0.00004043	0.00027199
19	90	0.00004105	0.00023155
20	95	0.00000083	0.00019050
21	100	0.00015945	0.00018968
22	105	0.00000322	0.00003023
23	110	0.00000327	0.00002701
24	115	0.00000007	0.00002374
25	120	0.00002122	0.00002367
26	125	0.00000043	0.00000245
27	130	0.00000044	0.00000202
28	135	0.00000000	0.00000158
29	140	0.00000146	0.00000157
30	145	0.00000003	0.00000011
.	.	.	.
.	.	.	.
.	.	.	.
47	230	0.00000000	0.00000000
48	235	0.00000000	0.00000000
49	240	0.00000000	0.00000000

(b) $COPT^{U}_{t=8430}$.

State j	Cap. out x^U_j [MW]	Ind. prob. $p(X = x^U_j)$	Cum. prob. $P(X \geq x^U_j)$
1	0	0.81202221	1.00000000
2	5	0.01640187	0.18797779
3	6	0.00000523	0.17157592
4	10	0.01665208	0.17157069
5	11	0.00000536	0.15491861
6	15	0.00033473	0.15491324
7	16	0.00000021	0.15457851
8	20	0.07027485	0.15457830
9	21	0.00002850	0.08430345
10	25	0.00141966	0.08427495
11	26	0.00000115	0.08285529
12	30	0.00225581	0.08285414
13	31	0.00000082	0.08059833
14	35	0.00004543	0.08059750
15	36	0.00000003	0.08055208
16	40	0.06920404	0.08055204
17	41	0.00001253	0.01134800
18	45	0.00139806	0.01133547
19	46	0.00000051	0.00993742
20	50	0.00148954	0.00993691
21	51	0.00000049	0.00844737
22	55	0.00002995	0.00844688
23	56	0.00000002	0.00841693
24	60	0.00582296	0.00841691
25	61	0.00000240	0.00259395
26	65	0.00011763	0.00259154
27	66	0.00000010	0.00247391
28	70	0.00018881	0.00247381
29	71	0.00000007	0.00228501
30	75	0.00000380	0.00228494
.	.	.	.
.	.	.	.
.	.	.	.
106	265	0.00000000	0.00000000
107	266	0.00000000	0.00000000
108	270	0.00000000	0.00000000

Table B5: $LOLP_t^U$ for an excerpt of time increments.

Hour, t	LOLP	Hour, t	LOLP	Hour, t	LOLP	Hour, t	LOLP
1	0.00000000	11	0.00000229	:	:	8727	0.00000005
2	0.00000000	12	0.00000229	8428	0.00000000	8728	0.00000005
3	0.00000000	13	0.00000229	8429	0.00000000	8729	0.00000011
4	0.00000000	14	0.00000229	8430	0.00000005	8730	0.00000160
5	0.00000000	15	0.00000162	8431	0.00000162	8731	0.00000160
6	0.00000000	16	0.00000162	8432	0.00002463	8732	0.00000014
7	0.00000000	17	0.00000273	:	:	8733	0.00000011
8	0.00000014	18	0.00000275	8724	0.00000011	8734	0.00000011
9	0.00000229	19	0.00000275	8725	0.00000005	8735	0.00000005
10	0.00000229	20	0.00000229	8726	0.00000005	8736	0.00000000

Table B6: LOLE-values for the stand-alone- and interconnected systems.

Peak load [MW]	Stand-alone system LOLE [hours/year]	Interconnected system LOLE [hours/year]
160	0.09264189	0.00282307
165	0.15263652	0.00490212
170	0.25474697	0.00871761
175	0.41167928	0.01468111
180	0.68211267	0.02566529
185	1.09141791	0.04270443
190	1.70703008	0.06570963
195	2.51506747	0.11117800
200	3.63046000	0.18258691
205	5.35274708	0.30776547
210	7.58440461	0.45753983
215	12.05345797	0.78128931
218.85	15.53207073	1.10180921
220	17.09040181	1.20676375
225	25.19179297	1.81286302
230	36.32170774	2.64665717
235	51.06777775	4.04173034
240	70.54598282	6.06291089

Appendix C

Pseudocode for MATLAB-scripts

Algorithms 1-8 show pseudocode for the scripts used to obtain the results in Chapter 5.

Algorithm 1 Script to create the $COPT$ for a generating system.

Input: Generator data is read from an appropriate datafile, creating three arrays for the function to use: Generator number G, possible outages states, *outage*, and probability values for the outage states, *prob*. The function implements the recursive function in (3.4). *outage* stores g_i values, *prob* stores $p_i values$ and $COPT$ stores $P(X \geq x_j)$- and x_j-values.

1: **function** CREATECOPT(*G, outage, prob*)
2: **for** each generator in G **do**
3: Count the number of derated states for each generator and store in the array *deratedStates*
4: **end for**
5: Create an array, $COPT$ and add the first unit with its outage states and probabilities
6: **while** Current gen. being added to $COPT \leq$ tot. no. of gens. **do**
7: **for** all existing outage states in $COPT$ **do**
8: Find new cum. prob.(cumulative probability) of the state with:
$$P^{new}(X \geq x_j) = \sum_{i=1}^{n} p_i \cdot P^{old}(X \geq x_j - g_i)$$ ▷ Ref. Eq. (3.4)
9: **end for**
10: Each comb. (combination) of existing out. cap. and a cap. state of the gen. being added, can potentially create a new state, therefore:
11: **for** iterate through all existing out. st. (outage state) in $COPT$ **do**
12: **for** all derated st. of the current gen. **do**
13: Cap of potential new out. st., *newState* is equal to:
(out. cap. of curr. (current) $COPT$-state) + (out. cap. of curr. gen. (generator) state)
14: **if** There is an existing out. state cap. equal to *newState* **then**
15: Do nothing ▷ Cum. prob. of existing states are updated earlier
16: **else if** *newState* is larger than the current max.(maximum) out. st. **then**
17: Add *newState* on the end of $COPT$ with cum. prob. as in line 8
18: **else** A new out. st. must be added somewhere in the $COPT$
19: Add *newState* w/cum. prob. as in line 8 to correct row in $COPT$, making sure that out. states are still sorted in ascending order
20: **end if**
21: **end for**
22: **end for**
23: **end while**
24: **return** $COPT$
25: **end function**

Output: The function outputs a two-column array with as many rows as there are outage states. The first column contains outage capacities, x_j, in ascending order, and the second column contains cumulative probability values, $P(X \geq x_j)$, for each outage state.

Algorithm 2 Script to calculate LOLE for a stand-alone system.

Input: $COPT$ and a vector, *loadVec* containing load levels for each time increment in the load model. Installed cap. of the system, C, is found as the cap. of the largest outage state in the $COPT$.

```
1: function singleSysLOLE(COPT, loadVec)
2:     Create an array, LOLP, to store the LOLP-values, LOLP_t, for each time increment
3:     for All time increments, t, in loadVec do
4:         if Load level for the time increment is larger than C then
5:             LOLP_t=1
6:         else
7:             for iterate through outage states of the COPT and  do
8:                 if Out. cap. is larger than reserve then          ▷ Ref. Eq. (3.5)
9:                     LOLP_t is equal to the cum. prob. of the current outage state
10:                    break out of the inner for-loop
11:                end if
12:            end for
13:        end if
14:    end for
15:    LOLE=sum of all LOLP_t-values in LOLP
16:    return LOLE
17: end function
```

Output: A single LOLE-value for the stand-alone system evaluated.

Algorithm 3 Script to calculate EENS for a stand-alone system.

Input: $COPT$ and a vector, *loadVec* containing load levels for each time increment in the load model. Installed cap. of the system, C, is found as the cap. of the largest outage state in the $COPT$.

1: **function** SINGLESYSEENS($COPT$, loadVec)
2: Create an array, UE, to store the unserved energy, UE_t, from each time increment
3: **for** All time increments, t, in $loadVec$ **do**
4: Find the lowest outage state, j, in the $COPT$ that causes loss-of-load with the load level in time increment t
5: **for** All outage states $\geq j$ **do**
6: Add UE_t, which is the product of the cap. deficiency and the ind. prob. (individual probability) of the outage state, to UE ▷ Ref. Eq. (3.10)
7: **end for**
8: **end for**
9: $EENS$=sum of all UE_t-values in UE
10: **return** $EENS$
11: **end function**

Output: A single EENS-value for the stand-alone system evaluated.

Algorithm 4 Script that implements the EAU-procedure, creating a CEAU-model

Input: $COPT$ for the assisting system, a vector, a load level for the assisting system and an array containing capacity states and probabilities for the interconnector, $COPT^{IC}$. Installed cap. of the system, C, is found as the cap. of the largest outage state in the $COPT$.

1: **function** CREATECEAU($COPT^B$, $loadLevel^B$, $COPT^{IC}$)
2: Find the highest outage state, j, in $COPT^B$ with outage $\leq$ reserve in System B. Create an array $EAUass$ that has states with the capacity innages and ind. prob. of all $COPT^B$ out. st. $\leq j$. ▷ Cap. innage=C-cap. out.
3: Add a row to the end of $EAUass$ with zero assistance and ind. prob. equal to cum. prob. of out. st. $j+1$ in $COPT^B$.
4: Flip both columns of $EAUass$ so it shows ass. st. (assistance states) in ascending order
5: **if** max int.conn. cap. (interconnector capacity) $\geq$ max ass. from $EAUass$ **then**
6: the largest ass. st. in $EAUass$ decides the max. ass. st. from the CEAU, $CEAUmax$.
7: Merge all int.conn. states, k, in $COPT^{IC}$ with capacity $\geq CEAUmax$ into one cap. st. with cap. equal to $CEAUmax$ and ind. prob. equal to the sum of ind. prob. of the merged states
8: **else** the largest cap. st. in $COPT^{line}$ decides the max. ass. st. from the CEAU, $CEAUmax$.
9: Merge all ass. states, j, in $EAUass$ with capacity $\geq CEAUmax$ into one ass. st. with cap. equal to $CEAUmax$, and ind. prob. equal to the sum of ind. prob. of the merged states
10: **end if**
11: Create an array, $COPT^{CEAU}$ to store cap. levels and ind. prob. of the CEAU
12: Add the zero ass. state to the $COPT^{CEAU}$ with prob. equal to: (prob. of int.conn. being down) + ((prob. of zero ass. from $EAUass$)$\times$(int.conn. being down))
13: $currICst \leftarrow 2$
14: $currEAUst \leftarrow 2$
15: $currCEAUst \leftarrow 2$
16: **while** $currICst \leq$ no. of st. in $COPT^{line}$ **do**
17: **if** there are ass. states in $EAUass$ that fall between int.conn. states **then**
18: **for** all such $EAUass$-states **do**
19: in ascending order of these $EAUass$-states, append a row to the $COPT^{CEAU}$ with cap. equal to cap. of the $currEAUst$ and prob. equal to: (sum of probs. of cap. st. in $COPT^{line}$ larger than $currICst$)$\times$(prob. of $currEAUst$)
20: $currEAUst \leftarrow currEAUst+1$
21: $currCEAUst \leftarrow currCEAUst+1$
22: **end for**
23: **end if**

24: **if** Cap. of *currEAUst* = Cap. of *currICst* **then**
25: **if** Cap. of *currEAUst* = Max. cap. of $COPT^{line}$ **then**
26: Append a row with cap. equal to max. int.conn. cap. and prob. equal to: (prob. of being in *currICst*)×(prob. of being in *currEAUst*)
▷ This will be the last state of the $COPT^{CEAU}$
27: **return** $COPT^{CEAU}$ ▷ Last state is added, so the function returns
28: **else**
29: Append row to $COPT^{CEAU}$ with cap. of *currICst* and prob. equal to: (sum of probs. of cap. st. in $COPT^{line}$ larger than *currICst*)×(prob. of *currEAUst*) + (prob. of *currICst*)×(sum of probs. of cap. st. in *EAUass* larger than *currEAUst*)
30: *currEAUst* ← *currEAUst*+1
31: *currCEAUst* ← *currCEAUst*+1
32: *currICst* ← *currICst*+1
33: **end if**
34: **else** Cap. of *currICst* ≠ cap. of *currEAUst*
35: Append row to $COPT^{CEAU}$ with cap. of *currICst* and prob. equal to: (Prob. of *currICst*)×(sum of probs. of cap. st. in *EAUass* larger than *currEAUst*)
36: *currICst* ← *currICst*+1
37: **end if**
38: **end while**
39: **end function**

Output: A multi-state representation of the CEAU.

Algorithm 5 Script to add multi-state unit to existing COPT.

Input: $COPT$ and an array containing a multi-state unit, *msu* with *outage*- and *prob*-data as in Algorithm 1. This function is almost identical to *createCOPT*, except for the fact that a COPT already exists, and only one unit is added.

1: **function** ADDUNIT($COPT$, *msu*)
2: **for** all existing outage states in $COPT$ **do**
3: Find new cum. prob. of the state by using:
$$P^{new}(X \geq x_j) = \sum_{i=1}^{n} p_i \cdot P^{old}(X \geq x_j - g_i)$$ ▷ Ref. Eq. (3.4)
4: **end for**
5: Each comb. of existing out. cap. and a cap. state of the gen. being added, can pot. create a new state, therefore:
6: **for** iterate through all existing out. st. in $COPT$ **do**
7: **for** all derated st. of the current gen. **do**
8: Cap of pot. new out. st., *newState* is equal to:
(out. cap. of curr. $COPT$-state) + (out. cap. of curr. gen. state)
9: **if** There is an existing out. state cap. equal to *newState* **then**
10: Do nothing ▷ Cum. prob. of existing states are updated earlier
11: **else if** *newState* is larger than the current max. out. st. **then**
12: Add *newState* on the end of $COPT$ with cum. prob. as in line 3
13: **else** A new out. st. must be added somewhere in the $COPT$
14: Add *newState* w/cum. prob. as in line 3 to correct row in $COPT$
15: **end if**
16: **end for**
17: **end for**
18: **return** $COPT^{new}$
19: **end function**

Output: $COPT^{new}$ for the system the *msu* is added to.

Algorithm 6 Script to calculate LOLE for an interconnected system.

Input: $COPT^A$, $COPT^B$ vectors $loadVec^A$ and $loadVec^B$ containing load levels for each time increment in the load model for both systems and $COPT^{line}$.

1: **function** INTCONNLOLE($COPT^A$, $COPT^B$, $loadVec^A$ $loadVec^B$, $COPT^{line}$)
2: Create an array, $LOLP$, to store the LOLP-values, $LOLP_t$, for each time increment
3: **for** All time increments, t, in $loadVec^A$ **do**
4: **Call** *createCEAU* to get $COPT^{CEAU}$:
$COPT^{CEAU} \leftarrow$ CRATECEAU($COPT^B$, $loadLevel_t^B$, $COPT^{IC}$) ▷ Ref. Alg. 4
5: Here it is assumed that there are a equal number of time increments in $loadVec^A$ and $loadVec^B$
6: **Call** *addUnit* to get $COPT^U$:
$COPT^U \leftarrow$ ADDUNIT($COPT^A$, $COPT^{CEAU}$)
7: **if** Load level for the time increment is larger than max. innage of $COPT^U$ **then**
8: $LOLP_t$=1
9: **else**
10: **for** iterate through outage states of the $COPT^U$ and **do**
11: **if** Out. cap. is larger than reserve **then** ▷ Ref. Eq. (3.5)
12: $LOLP_t$ is equal to the cum. prob. of the current outage state
13: **break** out of the inner for-loop
14: **end if**
15: **end for**
16: **end if**
17: **end for**
18: $LOLE$=sum of all $LOLP_t$-values in $LOLP$
19: **return** $LOLE$
20: **end function**

Output: A single LOLE-value for the interconnected system evaluated.

Algorithm 7 Script to calculate EENS for an interconnected system.

Input: $COPT^A$, $COPT^B$ vectors $loadVec^A$ and $loadVec^B$ containing load levels for each time increment in the load model for both systems and $COPT^{line}$.

1: **function** INTCONNEENS($COPT^A$, $COPT^B$, $loadVec^A$ $loadVec^B$, $COPT^{line}$)
2: Create an array, UE, to store the unserved energy, UE_t, from each time increment
3: **for** All time increments, t, in $loadVec^A$ **do**
4: **Call** *createCEAU* to get $COPT^{CEAU}$:
$COPT^{CEAU} \leftarrow$ CRATECEAU($COPT^B$, $loadLevel_t^B$, $COPT^{IC}$) ▷ Ref. Alg. 4
5: Here it is assumed that there are a equal number of time increments in $loadVec^A$ and $loadVec^B$
6: **Call** *addUnit* to get $COPT^U$:
$COPT^U \leftarrow$ ADDUNIT($COPT^A$, $COPT^{CEAU}$)
7: Find the lowest outage state, j, in $COPT^U$ that causes loss-of-load with the load level in system A for time increment t
8: **for** All outage states $\geq j$ **do**
9: Add UE_t, which is the product of the cap. deficiency and the ind. prob. of the outage state, to UE ▷ Ref. Eq. (3.10)
10: **end for**
11: **end for**
12: $EENS$=sum of all UE_t-values in UE
13: **return** $EENS$
14: **end function**

Output: A single EENS-value for the interconnected system evaluated.

Algorithm 8 Script to plot peak load vs. LOLE-/EENS-curves and calculate $IELCC_{LOLE}$/ $IELCC_{EENS}$ for an interconnected system. This script is almost identical whether LOLE or EENS is used as reliability index. Everywhere the algorithm has a index-specific step, LOLE/EENS is used in the pseudocode.

Input: Generator- and load data for systems A and B, as well as interconnector data.

1: **function** IELCC(G^A, $outage^A$, $prob^A$, $loadVec^A$, G^B, $outage^B$, $prob^B$, $loadVec^B$, $COPT^{IC}$)
2: **Call** *createCOPT* to get $COPT^A$ and $COPT^B$:
3: $COPT^A \leftarrow$ createCOPT(G^A, $outage^A$, $prob^A$) and
4: $COPT^B \leftarrow$ createCOPT(G^B, $outage^B$, $prob^B$)
5: Define the LOLE-level the IELCC will be calculated for.
6: Create a peak load vector, *pLoadVec*, that defines the interval on the x-axis that will be considered. Peak load vs. LOLE/EENS curves must intersect the defined LOLE/EENS-level in this interval.
7: Create two vectors, *LOLEvec/EENSvec* and *LOLEvecInt/EENSvecInt*, for the stand-alone and interconnected system, respectively, that will store LOLE/EENS values for each peak load in the *pLoadVec.*
8: **for** each peak load, *pl*, in *pLoadVec* **do** ▷ Each peak load repr. a full load model
9: Create a scaled loadvector for sys. A, $scaledLoad^A$, by scaling $loadVec^A$ by $\frac{pl}{loadVec^A_{max}}$
10: **Call** *singleSysLOLE/singleSysEENS* to get $LOLE_{pl}/EENS_{pl}$:
$LOLEvec(pl) \leftarrow$ singleSysLOLE($COPT^A$, $scaledLoad^A$)/
$EENSvec(pl) \leftarrow$ singleSysEENS($COPT^A$, $scaledLoad^A$)
11: **Call** *intconnLOLE/intconnEENS* to get $LOLEint_{pl}/EENSint_{pl}$:
$LOLEvecInt(pl) \leftarrow$ intconnLOLE($COPT^A$, $scaledLoad^A$, $COPT^B$, $loadVec^B$, $COPT^{IC}$)/
$EENSvecInt(pl) \leftarrow$ intconnEENS($COPT^A$, $scaledLoad^A$, $COPT^B$, $loadVec^B$, $COPT^{IC}$)
12: **end for**
13: Plot peak load vs. LOLE/EENS on a semi-logarithmic scale (log. on y-axis) for both LOLE-/EENS-vectors, $LOLEvec/EENSvec$ and $LOLEvecInt/EENSvecInt$. Find the horizontal distance in MW between the points where the curves and the defined LOLE-/EENS-level intersect.
14: **return** $IELCC_{LOLE}/IELCC_{EENS}$
15: **end function**

Output: An $IELCC_{LOLE}/IELCC_{EENS}$-value and plot of peak load vs. LOLE/EENS is produced for the interconnected system.